

SHEAR CONNECTED CAVITY WALLS UNDER VERTICAL LOADS

Ajay Goyal
Michael A. Hatzinikolas
Joseph Warwaruk

ABSTRACT

Traditionally brick veneer is connected to concrete block walls by non-structural wire ties. In this report, shear connectors consisting of a 14 gage metal plate and a metal rod tie were used. Seven cavity walls, four with plain block wythes and three with reinforced block wythes, were subjected to vertical eccentric loads. The results obtained are compared with those obtained from testing similar single wythe walls ($h/t=27.9$).

A review of published data indicates a scarcity of information regarding the influence of veneer wythes on the strength and stability of backup wythes under axial loads. Effect of the position of eccentricity with respect to the position of the brick veneer, effect of increase in cavity width and effect of reinforcement, on the behaviour of cavity walls were evaluated. An increase in the stiffness, ultimate load carrying capacity of wall assembly and a decrease in deflection, was observed. The shear connector was found to be more effective with an increase in eccentricity of the load. In addition to the collection, analysis and presentation of test results, an equation is proposed for the calculation of effective flexural rigidity of cavity walls.

ACKNOWLEDGEMENTS

This investigation was made possible by financial assistance and material donations provided by the Natural Sciences and Engineering Research Council of Canada, Prairie Masonry Research Institute, Edmonton, Edcon and I.X.L Industries Ltd. Also the financial support to the author by the Department of Civil Engineering and by Harry Edward Sim Memorial Scholarship is gratefully acknowledged.

The authors appreciate the assistance from laboratory technicians L. Burden, R. Helfrich and S. Undershute in testing the specimens.

This report was prepared as a Master's thesis under the supervision of Dr. M. Hatzinikolas and Prof. J. Warwaruk.

TABLE OF CONTENTS

Chapter	Page
ABSTRACT	
ACKNOWLEDGEMENT	
TABLE OF CONTENTS	
LIST OF FIGURES	
LIST OF TABLES	
LIST OF PLATES	
1. INTRODUCTION	1
1.1 General remarks	1
1.2 Objectives	2
1.3 Scope	3
2. LITERATURE REVIEW	4
2.1 General Remarks	4
2.2 Current Design Procedures	4
2.3 Previous Investigations on Cavity Walls Subjected to Vertical Loads and Lateral Loads	5
2.3.1 Traditional Cavity walls	5
2.3.2 Shear Connected Cavity Walls	8
3. EXPERIMENTAL PROGRAM	14
3.1 Materials	14
3.1.1 Concrete Masonry Units	14
3.1.2 Burnt Clay Units	15

3.1.3 Mortar	15
3.1.4 Grout	16
3.1.5 Reinforcement	16
3.1.6 Shear Connector	17
3.2 Fabrication of Test Specimens	18
3.2.1 Prisms	18
3.2.1.1 Block Prisms	18
3.2.1.2 Brick Prisms	19
3.2.2 Full Scale Walls	19
3.3 Instrumentation	21
3.3.1 Single Wythe Walls	21
3.3.2 Cavity Walls	22
3.4 Test Procedure	23
3.4.1 Prisms	23
3.4.2 Full Scale Walls	24
4. TEST RESULTS	41
4.1 General Remarks	41
4.2 Concrete Block Units	41
4.3 Burnt Clay Units	42
4.4 Block Prisms	42
4.5 Brick Prisms	42
4.6 Flexural Bond of Brick Masonry	43
4.7 Full Scale Walls	43
4.7.1 Plain Single and Cavity Walls	43
4.7.1.1 Single Wythe Wall S1, $e=0.0$	44

4.7.1.2	Single Wythe Wall S2, $e=t/6$	44
4.7.1.3	Single Wythe Wall S3, $e=t/3$	45
4.7.1.4	Cavity Wall C7, $c=75\text{mm}$, $e=0.0$	45
4.7.1.5	Cavity wall C1, $c=75\text{mm}$, $e=t/3$ towards brick veneer	46
4.7.1.6	Cavity Wall C2, $c=75\text{mm}$, $e=t/6$ Towards Brick Veneer	47
4.7.1.7	Cavity Wall C3, $c=75\text{mm}$, $e=t/6$ Away From Brick Veneer	48
4.7.2	Reinforced Single and Cavity Walls	48
4.7.2.1	Single Wythe Wall S4, $e=t/3$	49
4.7.2.2	Single Wythe Wall S5, $e=t/2.5$	49
4.7.2.3	Cavity Wall C4, $c=100\text{mm}$, $e=t/3$ Towards Brick Veneer	50
4.7.2.4	Cavity Wall C5, $c=75\text{mm}$, $e=t/3$ Towards Brick Veneer	51
4.7.2.5	Cavity Wall C6, $c=75\text{mm}$, $e=t/2.5$ Towards Brick Veneer	52
5.	DISCUSSION AND ANALYSIS OF TEST RESULTS	91
5.1	General remarks	91
5.2	Discussion of Test Results	91
5.2.1	Behaviour of Axially Loaded Walls	91
5.2.2	Influence of Direction of Eccentricity With Respect to Brick Veneer on the Ability of the Backup Wythe to Carry Vertical Load	93

5.2.3	Influence of Cavity width	94
5.2.4	Comparison Between Eccentrically Loaded Single And Cavity Wall ($c=75\text{mm}$, Eccentricity Towards Brick Veneer).	95
5.2.4.1	Comparison Between Single Wall S2 And Cavity Walls C2, $e=t/6$.	95
5.2.4.2	Comparison Between Single Wall S3 And Cavity Walls C1, $e=t/3$.	96
5.2.4.3	Comparison Between Single Wall S4 And Cavity Walls C5, $e=t/3$.	97
5.2.4.4	Comparison Between Single Wall S5 And Cavity Walls C6, $e=t/2.5$.	98
5.3	Flexural Rigidity of Walls	99
6.	SUMMARY, CONCLUSIONS AND RECOMMENDATIONS	120
6.1	Summary	120
6.2	Conclusions	120
6.3	Recommendations	121
7.	REFERENCES	123

LIST OF FIGURES

Figures		Page
Figure 2.1	Mullins and O' Connor's Shear Connector Shear	11
Figure 2.2	Connector Developed By Pacholok et al Shear	12
Figure 2.3	Connector Developed By Papanikolas et al	13
Figure 3.1	Dimensions of 200 mm Concrete Block Units	30
Figure 3.2	Dimensions of 8 inch Concrete Block Units	31
Figure 3.3	Dimensions of Clay Burnt Unit	32
Figure 3.4	Ladder Type Horizontal Reinforcement	32
Figure 3.5	Loading Frame	33
Figure 3.6	Calibration of the Shelf Angle	34
Figure 3.7	Shear Connector Arrangement	35
Figure 3.8	Position Of Reinforcement	36
Figure 4.1	Unreinforced Single Wall S1, $e=0.0$	58
Figure 4.2	Deflected Shape of Unreinforced Single Wall S1, $e= 0.0$	59
Figure 4.3	Unreinforced Single Wall S2, $e=t/6$	60
Figure 4.4	Deflected Shape of Unreinforced Single Wall S2, $e=t/6$	61
Figure 4.5	Unreinforced Single Wall S3, $e=t/3$	62
Figure 4.6	Deflected Shape of Unreinforced Single Wall S3, $e=t/3$	63
Figure 4.7	Cavity Wall C7, $e=0.0$	64
Figure 4.8	Deflected Shape of Cavity Wall C7, $e=0.0$	65
Figure 4.9	Cavity Wall C1, $e=t/3$	66

Figure 4.10	Deflected Shape of Cavity Wall C1, $e=t/3$	67
Figure 4.11	Cavity Wall C2, $e=t/6$ Towards Brick Veneer	68
Figure 4.12	Deflected Shape of Cavity Wall C2, $e=t/6$ Towards Brick Veneer	69
Figure 4.13	Cavity Wall C3, $e=t/6$ Away From Brick Veneer	70
Figure 4.14	Deflected Shape of Cavity Wall C3, $e=t/6$ Away From Brick Veneer	71
Figure 4.15	Reinforced Single Wall S4, $e=t/3$	72
Figure 4.16	Deflected Shape of Reinforced Single Wall S4, $e=t/3$	73
Figure 4.17	Reinforced Single Wall S5, $e=t/2.5$	74
Figure 4.18	Deflected Shape of Reinforced Single Wall S5, $e=t/2.5$	75
Figure 4.19	Cavity Wall C4, $e=t/3$, $c=100$ mm	76
Figure 4.20	Deflected Shape of Cavity Wall C4, $e=t/3$, $c=100$ mm	77
Figure 4.21	Cavity Wall C5, $e=t/3$, $c=75$ mm	78
Figure 4.22	Deflected Shape of Cavity Wall C5, $e=t/3$, $c=75$ mm	79
Figure 4.23	Cavity Wall C6, $e=t/2.5$	80
Figure 4.24	Deflected Shape of Cavity Wall C6, $e=t/2.5$	81
Figure 5.1	Rotation Versus Load on Shelf Angle Unreinforced Cavity Walls	105
Figure 5.2	Rotation Versus Load on Shelf Angle for Reinforced Cavity Walls	106
Figure 5.3	Single Wall S1 and Cavity Wall C7	107

Figure 5.4	Cavity Walls C2 and C3	108
Figure 5.5	Load Versus Rotation for Unreinforced Cavity Walls	109
Figure 5.6	Cavity Walls C4 and C5	110
Figure 5.7	Load Versus Rotation for Reinforced Cavity Walls	111
Figure 5.8	Single Wall S2 and Cavity Wall C2	112
Figure 5.9	Single Wall S3 and Cavity Wall C1	113
Figure 5.10	Single Wall S4 and Cavity Wall C5	114
Figure 5.11	Single Wall S5 and Cavity Wall C6	115
Figure 5.12	Flexural Rigidity of Unreinforced Walls S2, C2 and C3	116
Figure 5.13	Flexural Rigidity of Unreinforced Walls S1 and C3	117
Figure 5.14	Flexural Rigidity of Reinforced Walls S4, C4, C5	118
Figure 5.15	Flexural Rigidity of Reinforced Walls S5 and C6	119

LIST OF TABLES

Tables	Page
Table 3.1 Physical Properties of Concrete Block Units	26
Table 3.2 Physical Properties of Clay Burnt Brick Units	27
Table 3.3 Mortar Cube Test Results for Type S Mortar	28
Table 3.4 Grout Strength Tests	29
Table 4.1 Compressive Strength Of 200 mm Concrete Block Units	53
Table 4.2 Compressive Strength Of 8 inch Concrete Block Units	53
Table 4.3 Compressive Strength Of Clay Burnt Units	54
Table 4.4 Compressive Strength Of Concrete Block Prisms	54
Table 4.5 Compressive Strength Of Clay Burnt Unit Prisms	55
Table 4.6 Flexural Bond Strength Of Brick Masonry	55
Table 4.7 Experimental Results of Plain Single And Cavity Walls	56
Table 4.8 Experimental Results of Single And Cavity Reinforced Walls	57
Table 5.1 Comparision of Experimental And Theoretical EI values	104

LIST OF PLATES

Plate	Page
Plate 3.1 Flexural Test on Brick Prism	37
Plate 3.2 Lifting Mechanism of Single Wall	38
Plate 3.3 Lifting Mechanism of Cavity Walls	39
Plate 3.4 Moment Arm Loading Frame	40
Plate 4.1 Typical Failure Pattern of Concrete Block Prism	82
Plate 4.2 Wall S1 in the Testing Machine	83
Plate 4.3 Wall S2 During Failure	84
Plate 4.4 Wall C7 After Failure	85
Plate 4.5 Wall C1 After Failure	86
Plate 4.6 Wall C2 After Failure	87
Plate 4.7 Wall C3 After Failure	88
Plate 4.8 Crack in the Wall C5	89
Plate 4.9 Topmost Connector in Wall C6	90

CHAPTER 1

INTRODUCTION

1.1 General remarks

Masonry cavity walls are frequently used for the exterior walls of buildings in order to achieve higher degree of weather protection and thermal insulation. A cavity wall consists of an exterior wythe, a cavity consisting of air space, insulation, air vapour barrier and an interior backup wythe. Cavity widths usually range from 25 mm to 100 mm depending on the thickness of insulation and the air cavity. The two wythes are tied together by one of a variety of available types of ties. The exterior wythe is usually constructed with burned clay or concrete masonry units and is referred to as a masonry veneer. The interior or backup wythe is usually constructed using concrete masonry units.

The current Canadian design code for Masonry Buildings, CAN3-S304-M84¹ considers the exterior wythe to be a weathering surface and an aesthetic covering of the building. No consideration is given to the structural strength of the veneer. All the loads acting on the assembly are assumed to be applied to, and carried by the backup wythe.

Recently researchers (1988, 1990) especially at the University of Alberta, Edmonton have shown that the brick veneer, when

connected to the backup wall by specially designed shear connectors, increases the stiffness of the wall. The connector has shear transfer capabilities. Tests carried out on laterally loaded cavity walls constructed by using shear connectors and subjected to lateral loads have demonstrated the feasibility of shear connecting the two wythes. This project examines, in a preliminary manner the contribution of a masonry veneer to the ability of the back-up wythe to carry load when the two wythes are connected by ties capable of transferring shear.

1.2 Objectives

The main objectives of the present program are:

1. To design and construct a testing frame to test a number of cavity walls under vertical eccentric loads, such that actual field conditions are simulated.
2. To carry out a preliminary experimental study of the shear connected cavity walls subjected to vertical loads by which future research can be expanded.
3. To determine experimentally the benefits of connecting a brick veneer to a backup wall subjected to axial and vertical eccentric loads.
4. To study experimentally the behaviour of cavity walls subjected to different eccentricities.

5. To study experimentally the behaviour of cavity wall loaded with eccentricities towards and away from the brick veneer.
6. To study experimentally the influence of certain geometric parameters such as cavity width and reinforcement.
7. To establish some guide-lines on evaluating the rigidity of shear connected cavity walls.

1.3 Scope

A total of 5 single and 7 cavity wall specimens were tested at the I.F. Morrison Structural Engineering Laboratory of the University of Alberta. The walls were 24 block courses high, had both ends hinged and were loaded under vertical eccentric loads subjected to single curvature bending. Parameters studied include the effect of direction of eccentricity of load with respect to the position of the veneer, effect of cavity width, vertical reinforcement and eccentricity of load. Auxiliary tests consisted of prism and unit tests to determine material properties. The walls were instrumented and monitored during testing in order to evaluate changes in the rigidity, crack propagation, modes of failure and load distribution. From the experimental data, the behaviour of the cavity wall is analyzed and conclusions are drawn.

CHAPTER 2

LITERATURE REVIEW

2.1 General Remarks

This chapter provides a review of previous research work related to shear connected cavity walls and on cavity walls subjected to axial and eccentric loads. In addition, the design criteria for cavity walls as specified by CSA-S304-M84¹, the current Canadian masonry design code, are examined.

2.2 Current Design Procedures

In the present design code, CAN3-S304-M84¹, the veneer is considered to be a non-structural component and the backup wythe is the structural component. The veneer is usually designed to support its own weight, and be able to span between the ties without cracking. Lateral loads acting on the veneer are transferred to the backup wythe through a grid of connectors. Veneers built 11 m above the foundation should not span greater than 3.6 m and shall bear on masonry or concrete or non-combustible supports. The backup wythe is designed to resist all loads acting on the veneer.

The ability of cavity walls to carry load in composite action is recognized by the above noted standard. The standard defines the cavity wall as construction of masonry laid up with a cavity between the wythes, which are tied together with metal ties or bonding units, and where the wythes are relied upon to act together in resisting lateral and vertical loads. Ref. 1 recognizes the structural effects of differential movements between the wythes of a cavity wall due to deflection, creep, shrinkage, moisture changes and temperature changes. The effect of long term differential movement in cavity walls due to wythes made of different materials is also recognized. It limits the width of the cavity in a cavity wall to 150 mm and provides some guide-lines for the design of these walls.

2.3 Previous Investigations on Cavity Walls Subjected to Vertical Loads and Lateral Loads

2.3.1 Traditional Cavity walls

Traditionally cavity walls consist of two wythes separated by 25 to 100 mm cavity. The cavity consists of airspace and insulation. The two wythes are tied together by one of the different available types of connectors. Usually connectors made of steel wire or brick units are used and no consideration is given to the design of the connectors. The brick ties are header brick units spanning across the cavity and the steel ties are usually made of steel wire of less than 5

mm diameter. Previous tests done by researchers on these walls are presented in this section.

Yokel et al (1971) tested hollow concrete block-block and brick-block cavity walls subjected to combined axial vertical and lateral loads. Both the block and the brick wythe were four inches thick and were separated by a two_ inch cavity. Steel rod rectangle ties were used to connect the wythes. The bottom end for the cavity wall was partially fixed and the top end was hinged. The vertical load was applied in the centre of both the wythes such that the vertical load was carried by both the wythes. When the test results of brick-block cavity walls were compared with those of a single wythe brick wall, it was found that the cavity walls had less axial load capacity and almost the same moment capacity. It was concluded that the cavity wall will develop greater axial load capacity and moment capacity of the same order, if the entire vertical load is applied on the burnt clay part of the assembly, instead of resting on both wall components.

Kumar and de Vekey (1982) tested seven cavity walls. The cavity walls consisted of brick wythe and block wythe connected by butterfly galvanized steel wire ties. The brick and the block wythes were 100 mm thick and were separated by a cavity of 50 mm. The backup wythe was loaded with an eccentricity of 0 and $t/4$ (t is the thickness of the block wythe). Both wythes were fixed on the base. The top end of the block wythe was hinged while the brick wythe

was free. No considerable contribution of the brick wythe towards the increase in the capacity of the backup wall was found.

Neis et al. (1991) conducted full scale tests on six plain block-brick cavity walls built using ladder type wire ties, subjected to eccentric vertical loads on the block wythe. The thickness of the block and the brick wythes were 140 mm and 90 mm respectively. Both wythes were resting on hinges fixed to the floor. The top end of the block wythe was hinged and that of brick wythe was free. On comparing the cavity wall containing wire ties at every second course with cavity walls containing ties at every course, no significant increase in the ultimate load carrying capacity was found. The direction of eccentricity with respect to the veneer had significant effects on the capacity of the cavity wall.

Alani, et al. (1990) tested nine full scale brick-brick cavity walls under vertical eccentric loads. Both the brick wythes were 120 mm thick, separated by a cavity of 50 mm. Cavity walls with two types of ties (brick ties and steel wire ties) were tested. The load was applied to both the wythes and the eccentricity was measured with respect to the centre of the cavity wall. The bottom end for the cavity wall was partially fixed and the top end was hinged. The walls with brick ties had slightly better performance in terms of ultimate load carrying capacities, lateral deflection and the slippage when compared to walls built with steel wire ties.

2.3.2 Shear Connected Cavity Walls

The performance of a cavity wall under lateral loads depends on the ability of the connection of the veneer to transfer load to the backup wythe. Failure in traditional cavity walls is usually in the ties. The ties either fail in buckling, punch-out or pullout from the mortar beds in which they are placed. Sometimes the ties fail in shear. Because in such cavity walls excessive deflection is considered the limit state, investigators developed stiffer connectors with less rotational restraint, increased shear strength and grip (with mortar joints).

Mullins and O' Conner (1987) developed a shear connector for the cavity walls, as shown in Fig. 2.1. It consists of a sheet of metal frame placed between the wythes along the height, perpendicular to the two wythes. The wythes are then connected to metal frame by tabs extending into the head joints at every course. A comparison of cavity wall made using this shear connector with that of using traditional steel rod connectors showed that the shear connector resulted in an improved performance of the cavity wall under lateral load. The limitation of the system requires that both the wythes are constructed of units of same width and height.

Pacholok et al (1988) developed the shear connector as shown in Fig. 2.2. It consisted of a plate, cross legs, bent rod and a device to

hold insulation. Five full scale shear connected cavity walls were tested under lateral loading. The use of shear connector as opposed to a conventional type of connector, in the wall system resulted in increased lateral load carrying capacity and decreased lateral deflection at comparable loads.

The connector developed in Ref. 8 was modified (shown in Fig. 2.3) by Papanikolas et al.(1990) to improve installation procedures and to minimize the material and environmental effects. Full scale shear connected cavity walls were tested under lateral loads. The load carrying capacity and the flexural strength of the cavity wall was found to increase with the increase in concrete block size, vertical reinforcement and cavity width when subjected to lateral load. A composite behaviour between the wythes was observed.

The literature review provided a minimum amount of information as it relates to the ability of cavity walls to carry vertical load and moment. Most of the work on shear connected cavity walls was at the University of Alberta and on walls subjected to lateral loading. No information is available on the behaviour of vertically loaded shear connected cavity walls.

In view of the findings from laterally loaded shear connected cavity walls, a experimental study was carried out to study the behaviour of these walls under vertical eccentric loads. The results

are reported herein. The shear connector developed in Ref. 9 was used.

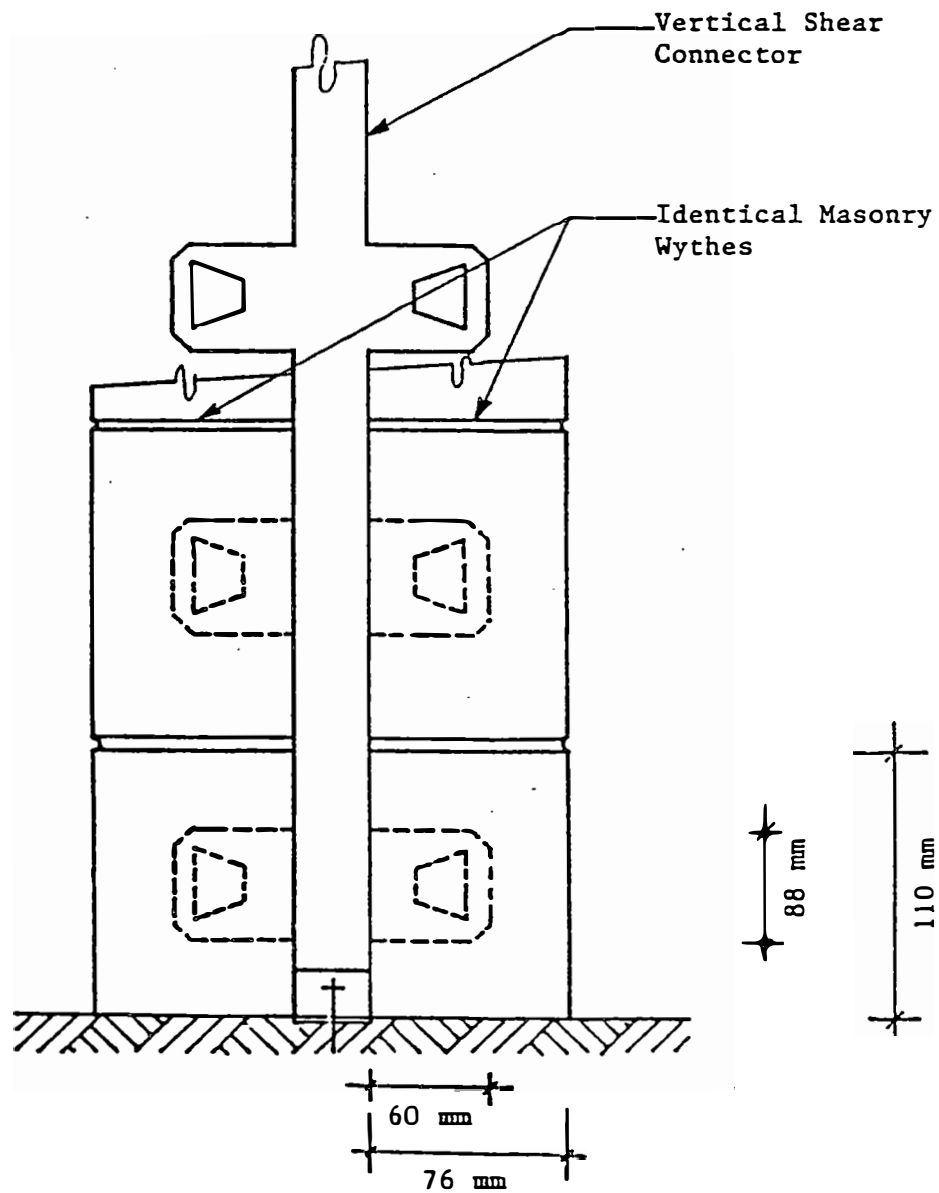


Figure 2.1 Mullins and O' Connor's Shear Connector
(Courtesy Ref. 8)

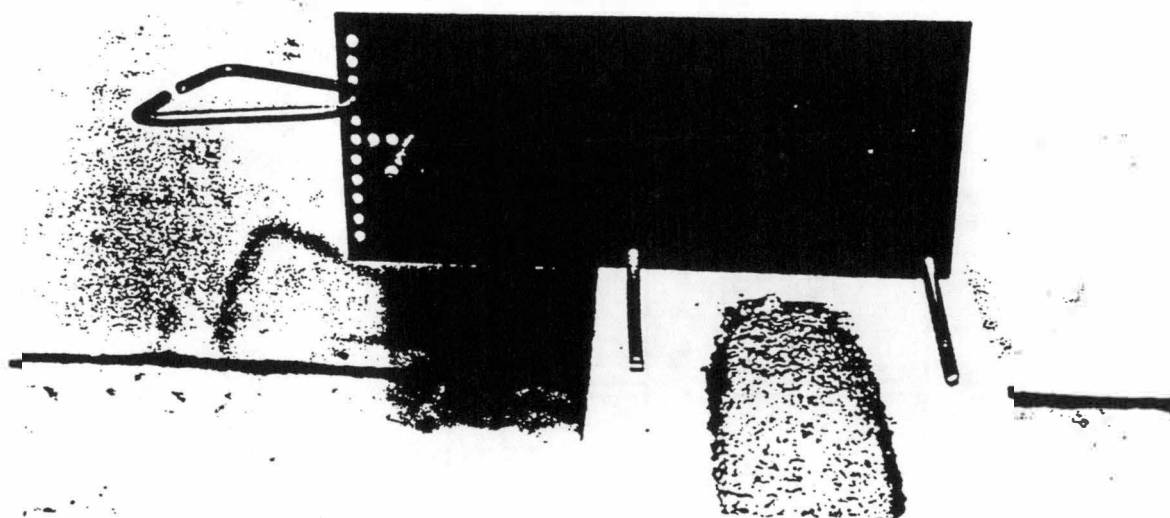


Figure 2.2 The Shear Connector Tested By Pacholok et al (1988)

(Courtesy Ref. 8)

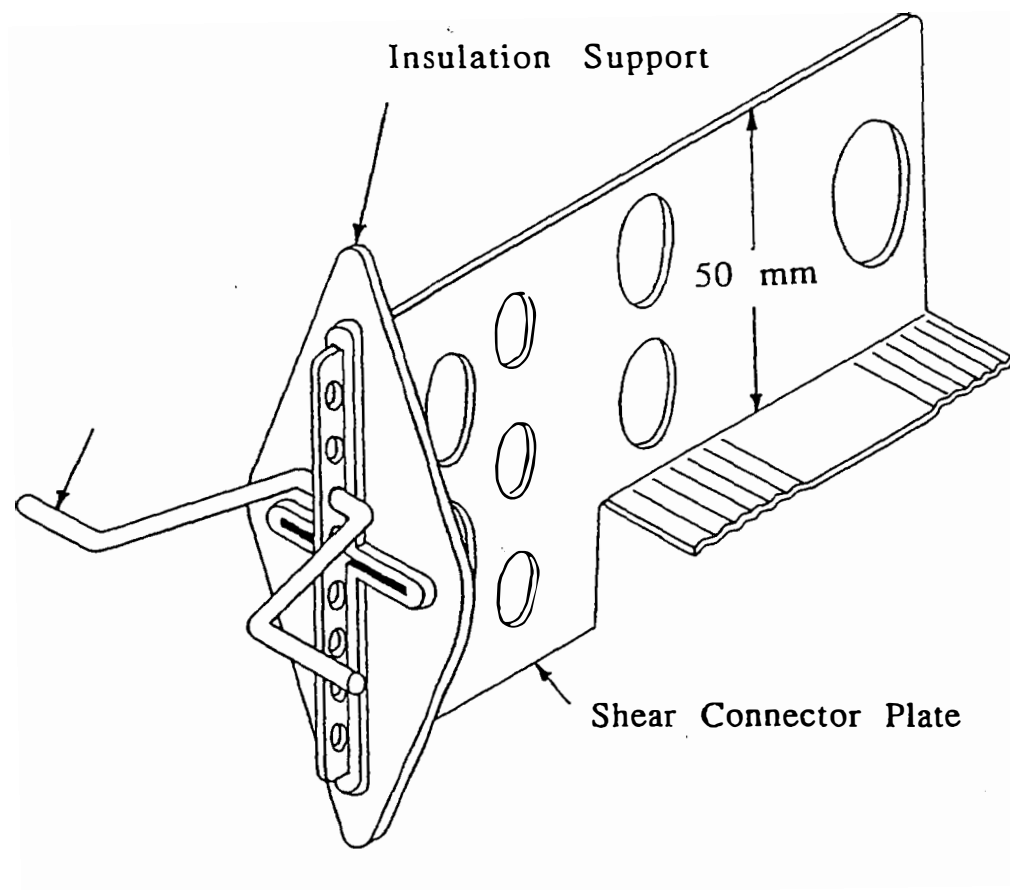


Figure 2.3 The Shear Connector Tested By Papanikolas et al (1990)

CHAPTER 3

EXPERIMENTAL PROGRAM

3.1 Materials

All materials used in constructing the test specimens were obtained from local suppliers and were representative of those commonly used in building construction in the Edmonton area.

3.1.1 Concrete Masonry Units

Two types of units were used in the testing program. All the concrete masonry prisms and the unreinforced masonry walls were constructed with H/15/C/O, 200 mm standard hollow concrete masonry units and all the reinforced masonry walls were constructed with H/15/C/O, 8 inch standard hollow concrete units, since at the time of construction of the reinforced walls, the 200 mm metric units were out of stock. All concrete units were supplied by the Edcon Block of Edmonton. The half units had only one core and a length of 200 mm or 4 inches.

The nominal dimensions of the 200 mm metric units are shown in Fig. 3.1 and those of the eight inch imperial units are shown in

Fig 3.2. The physical properties of the units tested in accordance with CSA standard CAN3-A165-M1985 (1985) are given in Table 3.1.

3.1.2 Burnt Clay Units

All the brick prisms and the veneer for all the cavity walls were constructed with burnt clay units. The bricks were supplied by I-XL Industries Ltd. Physical properties of the bricks tested in accordance with CAN3-A82.1-M1987 (1987) are presented in Table 3.2. The nominal dimensions of the brick units are shown in Fig 3.3.

3.1.3 Mortar

Type S premixed retarded mortar was used in the construction of all the test specimens. The mortar was supplied by Manstar Distributions of Edmonton. For each batch of mortar supplied six 50 x 50 x 50 mm cubes were cast. All mortar cubes were cured in saturated lime water and were tested after 28 days in accordance with CSA Standard A1 79-M1975 (1975), "Mortar and Grout for Unit Masonry". The strength of tested mortar cubes is summarized in Table 3.3.

3.1.4 Grout

The grout was mixed in the laboratory in a rotary type, upright, flat bottom mixer of nine cubic foot capacity. The grout contained 1 part of normal Portland cement, 2 1/2 parts of concrete sand and 2 parts of 10 mm pea gravel by weight. The water cement ratio was 1 by weight.

All grouted cores of the reinforced block wythes were filled in two stages of 12 courses each. Three samples of grout test specimens for each batch were tested in accordance with CSA Standard A179-M1975 (1975). The strength of the test samples is summarized in Table 3.4.

3.1.5 Reinforcement

Deformed metric 15M bars were used for the vertical reinforcement in the reinforced wythes. Their specified tensile yield strength was 300 MPa.

In the reinforced wythes, joint reinforcement was placed every third course in the horizontal mortar joints. The joint reinforcement was made of #9 gauge galvanized wire and consisted of two parallel longitudinal wires welded to perpendicular wires as shown in Fig 3.4.

3.1.6 Shear Connectors

The shear connector developed in Ref. 1 was used in all the cavity walls. Shear connectors were supplied by Fero Holdings Limited, Edmonton. A schematic diagram of the shear connector is shown in Fig 2.3. This shear connector consists of a V-Tie, shear connector plate and an optional insulation support.

The connector plate is made from 1.61 mm (16 gauge) sheet metal. The holes in the insulation thickness portion of the connector plate are provided to minimize the thermal bridging between the two wythes. The corrugations in the plate and the holes in the face shell region of the block are to provide better bonding between the mortar and the connector. The notch in the plate is for proper positioning of the shear connector plate in the assembly. The length of the plate varies depending on the block width, cavity width, insulation thickness and air space in the cavity wall. The series of eight 5.5 mm diameter holes in the plate are provided to connect the connector plate with the brick wythe by inserting the V-Tie in one of the holes such that the V-Tie is placed horizontally in the brick mortar joint.

The V-Tie is made of 4.76 mm diameter wue. The legs of the V-Tie are mortared into place at the centre line of the brick veneer. Its length varies depending on the veneer thickness. The insulation

support holds the insulation against the backup wall and is made of polyethylene.

Two lengths of connector plates were used to accommodate cavity widths of 75 mm and 100 mm. The V-ties were chosen to accommodate the 90 mm burned clay units used in the construction of the veneer part of the assembly and the 25 mm airspace. The length of the V-ties was 60 mm.

3.2 Fabrication of Test Specimens

A detail description of the masonry prisms and wall specimens and the method of fabrication of these specimens is presented in this section. All the prisms and wall panels were constructed by the same experienced masons using techniques representative of good workmanship.

3.2.1 Prisms

3.2.1.1 Block Prisms

Five 4-block high prisms were constructed to determine the compressive strength of block masonry. Standard 200 mm stretcher blocks were used. The first courses were laid directly on the floor

without mortar. The remaining three courses were laid on face shell bedded mortar joints.

3.2.1.2 Brick Prisms

Five 5-brick high prisms were constructed to determine the compressive strength of brick masonry. The first courses were laid directly on the floor without mortar. The remaining four courses were laid in stacked bond on fully bedded mortar joints.

Five 7-brick high prisms were constructed to determine the modulus of rupture of brick masonry. The first courses were laid directly on the floor without mortar. The remaining six courses were laid in stacked bond on fully bedded mortar joints. All the prisms were of one unit length.

3.2.2 Full Scale Walls

Seven block-brick cavity walls and five single walls were constructed. Of these seven cavity walls, four had plain block masonry back-up wythes and the rest had reinforced block masonry back-up wythes. Of the five single walls, three were of plain block masonry and two were reinforced.

The backup wythe of the cavity walls was made of block masonry and the veneer wythe was made of brick veneer. All the wall panels were constructed in running bond and were nominally 1.2m wide and 24 concrete block courses high. Only face shell bedded mortar joints were used for constructing the concrete block wythes and fully bedded mortar joints were used for constructing the brick masonry wythes. Both faces of the walls were tooled. All the cavity walls had a similar shear connector arrangement.

To facilitate moving and placement of test panels in the testing machine, the first course of block masonry of all the single walls was laid on a 1300 mm x 200 mm x 50 mm steel plate. The first course of the block masonry wythe of all the cavity walls was laid on a concrete pedestal along with the first course of the brick masonry wythe laid on an overhanging 50 mm x 150 mm x 20 mm shelf angle. The first courses of the block masonry and brick masonry were laid on a mortar bed. Details of the pedestal are shown in Fig 3.5. The walls were erected in a line between two steel columns to facilitate alignment of blocks. Horizontal joint reinforcement as shown in Fig 3.4 was placed every third courses in all the block wythes. No joint reinforcement was placed in unreinforced block wythes. The thickness of joints in the block and brick masonry was maintained at 10 mm. The shear connectors were placed as per the shear connector arrangement shown in Fig. 3.7. The arrangement was symmetrical about the centre of wall. The first connector was 200 mm from the ends and the next was at 400 mm. The connectors

between them had a spacing of 600 mm. The horizontal distance between the connectors was alternately 400 mm and 800 mm. The block wythes were braced during construction. Then at the specified cavity width away from the block wythe, the brick wythe was laid and V-Ties were placed in the respective mortar joints of the brick wythe.

Two deformed 15M bars were grouted in each of the reinforced block wythes. Location of the reinforcement is shown in Fig. 3.8. The grouting was done in two stages of 12 courses each. Six mortar cubes were made for each batch of mortar and three grout test specimens were made at the time of grouting.

3.3 Instrumentation Single

3.3.1 Wythe Walls

Vertical load applied on the block wall by the MTS testing machine, load applied to the moment arm, vertical shortening and lateral deflections of the wall were monitored and recorded automatically by a personal computer using a FLUKE data acquisition system.

The vertical load on the block wall was also measured by the MTS testing machine. A load cell was used to measure the load applied by using a hydraulic jack on the moment arm.

The lateral deflection of the walls was measured using nine LVDT's fixed to a independent column. To prevent damage of LVDT's during the failure, they were placed between the flanges of the column and thin wires were passed through the holes in the flange. These wires were glued to the wall at their corresponding elevations.

3.3.2 Cavity Walls

Besides the instruments used in single wall tests, twelve additional LVDT's were used during the testing of cavity walls. Vertical load applied by MTS testing machine, load applied on the moment arm, vertical shortening of the block wall, lateral deflection of both the brick and the block wythes, vertical movement of the brick wythe at the top end and the vertical deflection of the shelf angle were measured and recorded automatically by a computer, during the testing of the cavity walls.

To determine the change in the width of the cavity, lateral deflection of both the wythes was measured at similar elevations. The set-up of LVDT's used for single walls, was used to measure the lateral deflection of the brick wythe and lateral deflection of the block wythe was measured using another nine LVDT's fixed at corresponding elevations, to that for the brick wall, on another

independent steel column. The position of the LVDT's and the placing of the column is shown in Fig 3.5.

To measure the effect of rotation of the wall on the shelf angle, two LVDT's were clamped to the concrete pedestal under the shelf angle. They were calibrated by applying several levels of load on the shelf angle. Fig. 3.6 illustrates the calibration curve (load versus deflection curve of the shelf angle). This was obtained by loading the shelf angle with a known load and measuring the deflection of the shelf angle. The load was applied on a 800 mm high brick panel positioned at the location of brick veneer in a cavity wall and it was measured using a load cell.

3.4 Test Procedure

3.4.1 Prisms

Prisms were tested after 30 days of curing. The concrete masonry prisms were capped with test fiberboard while the brick masonry prisms were capped with Plaster of Paris and tested under concentric vertical load. The prisms were loaded at a constant rate of loading (30 kN/minute) until failure. Five 7-brick high prisms were tested under third point loading as shown in Plate 3.1. The specimen was loaded at a constant rate until failure.

3.4.2 Full Scale Walls

The walls were moved for testing in the 6600 kN MTS testing machine using a 10 tonne overhead crane. Plate 3.2 shows the lifting mechanism of the single walls and Plate 3.3 shows that for the cavity walls. Both the top and bottom ends of the walls were hinged.

The hinge consisted of a 50 mm diameter cold rolled steel bar resting among two 38 mm thick, 103 mm wide and 1265 mm long steel plates with circular groove all along the length of the two plates. The hinge was of the length of the wall.

At the top end of the wall, the moment was applied by shifting the position of the hinge. A piece of tentest board was kept on the top of the block wall and a built up channel section was placed on. top of it. The channel section was made of 50 mm thick, 243 mm wide, 1265 mm long plate (web) and 18 mm thick, 152 mm wide side plates (flanges). A hinge assembly was placed above the channel. It was positioned at the required eccentricity and was secured with a 3 mm thick steel plate bolted to both the plates, roller and channel. Then a bracing arm (65 mm x 40 mm x 6 mm) was connected to the centre of the hinge. The other end of the brace was connected to a independent column. It is shown schematically in Fig 3.5.

At the bottom end of the wall the hinge was placed under the concrete pedestal of the wall such that the centre line of the wall was

in line with the centre of the hinge. The moment was applied by an external moment arm, that was bolted to the pedestal of the wall as shown in the Fig 3.5. This method of applying moment at the lower end was used to counter-balance the moment created by the self weight of the overhanging brick veneer. Load on the moment arm was applied by a manually operated hydraulic ram. Plate 3.4 shows the moment arm loading device for single wythe walls and for cavity walls. The load was applied on the arm in such a way as to induce the same moment as that introduced by the eccentricity of the vertical load. The load applied to the moment arm was calculated by using simple statics and was applied continuously depending on the vertical load, until failure.

Table 3.1 Physical Properties of Concrete Block Units

Properties	200 mm Standard Block H/15/C/O	8 inch Standard Block H/15/C/O
Width	190 mm	7 5/8 in.
Length	390 mm	15 9/16 in.
Height	190 mm	7 5/8 in.
Minimum Face Shell thickness	32 mm	1 in.
Gross Area	74100 mm ²	119.15 in. ²
Net Area	41500 mm ²	64.88 in. ²
Unit Mass (Kg)	13.4	13.9
Moisture Content (%)	10.2	10.2
Absorption (%)	14.3	14.3
Compressive Strength based on Net area(MPa)	16.1	18.8

Table 3.2 Physical Properties of Clay Burnt Brick Units

CSA Specification	CAN3-A 82.1 M78
ASTM Specification	ASTM C 216-87
Length	190 mm
Width	90 mm
Height	62 mm
Volume of Voids	25 %
Fire rating	1 hour
(Clay brick is non-combustible)	
Thermal Resistance	$R=1.56$
Sound Trans. Class	46 db
Thermal Expansion Coeff.	3.6×10^{-6}
Weight of Wall./ Sq. M	140 kg
Weight per unit	1.6 kg

Table 3.3 Mortar Cube Test Results for Type S Mortar

Serial No.	Crushing Strength (MPa)
1	17.0
2	18.0
3	16.0
4	20.4
5	17.2
6	21.6
7	19.2
8	20.4
9	18.8
10	14.4
11	15.2
12	15.6
13	12.4
14	16.2
15	17.2
16	15.8
17	13.2
18	13.2
19	12.8
20	12.6
21	11.4
22	12.6
23	12.2
24	11.8
25	13.6
26	14.4
27	14.2
28	13.4

Mean Strength 15.3 MPa

Table 3.4 Grout Strength Tests

Serial No.	Compressive Strength (MPa)
1	19.8
2	21.5
3	20.7
4	19.5
5	22.0
6	21.4
7	20.9
8	21.3
9	20.6

Average Strength 20.8 MPa

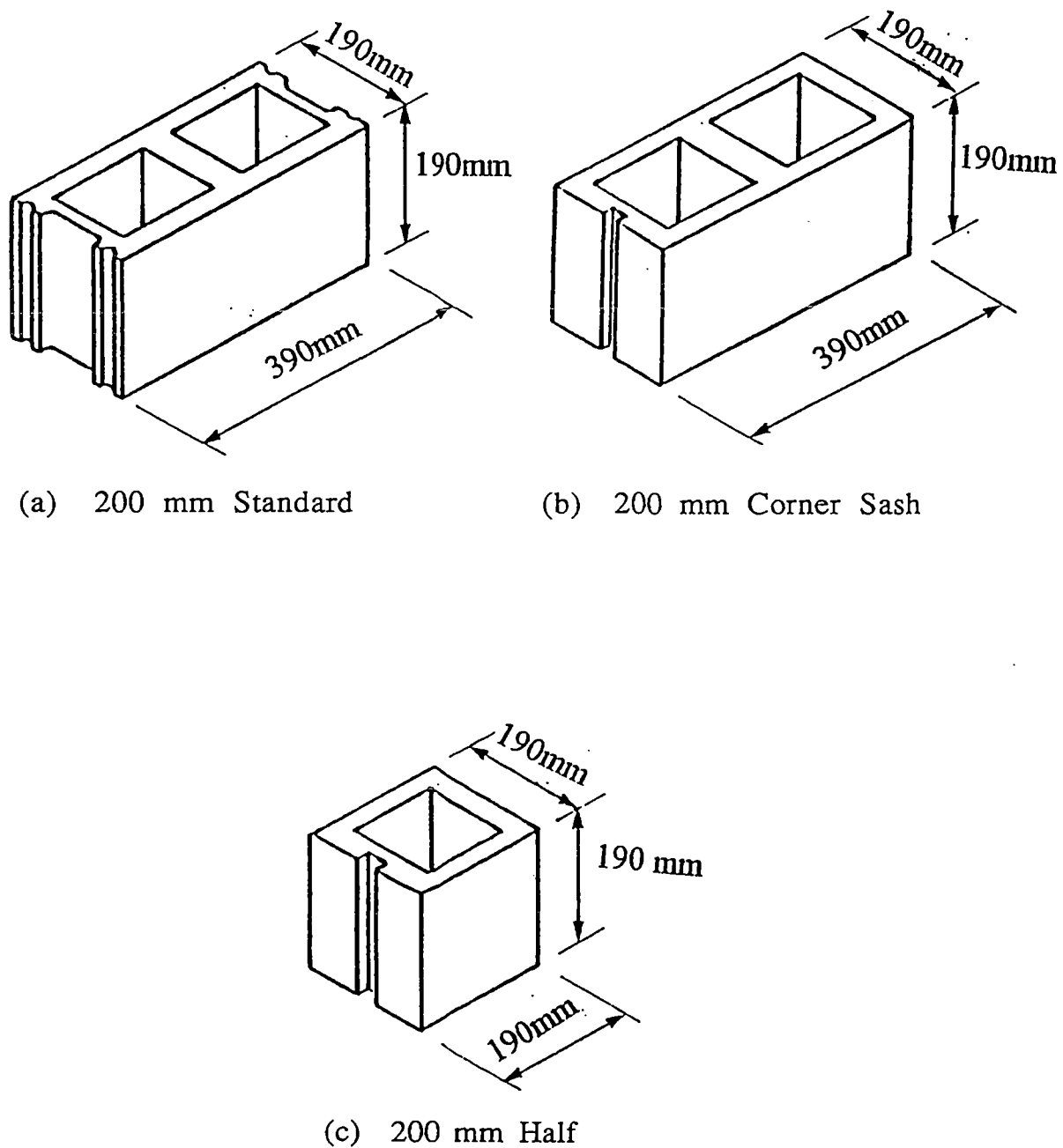
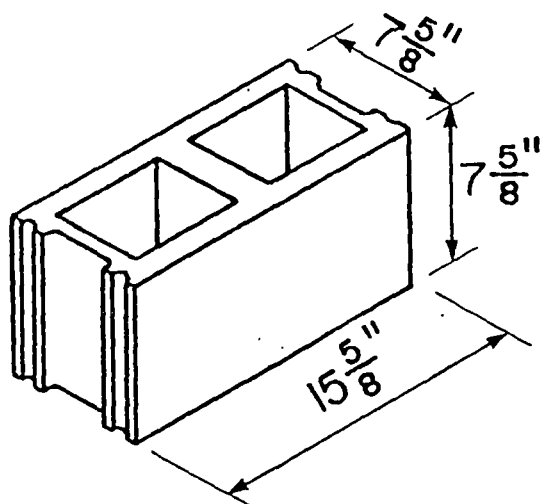
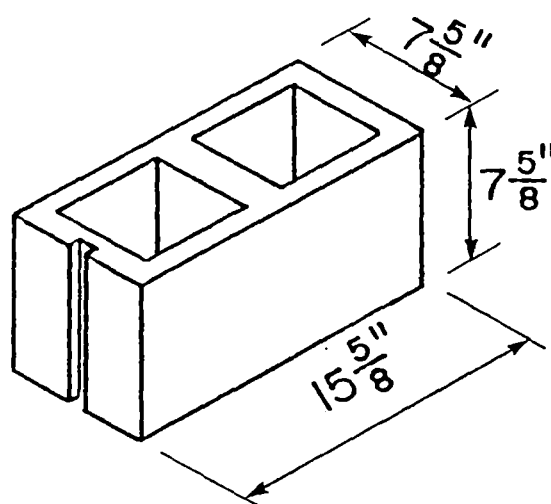


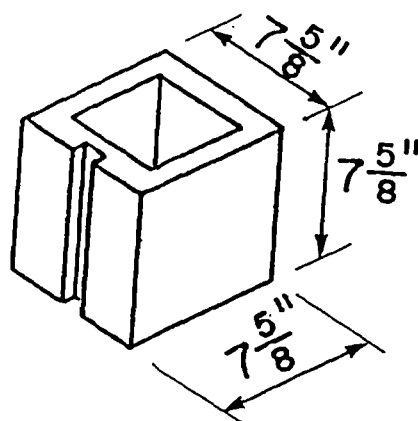
Figure 3.1 Dimensions of 200 mm Concrete Block Units



(a) 8 in. Standard



(b) 8 in. Corner Sash



(c) 8 in. Half

Figure 3.2 Dimensions of 8 inch Concrete Block Units

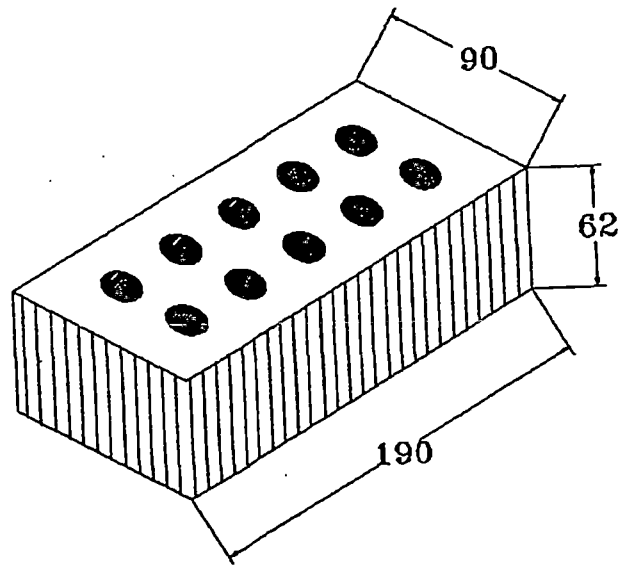


Figure 3.3 Dimensions of Clay Burnt Units



Figure 3.4 Ladder Type Horizontal Reinforcement

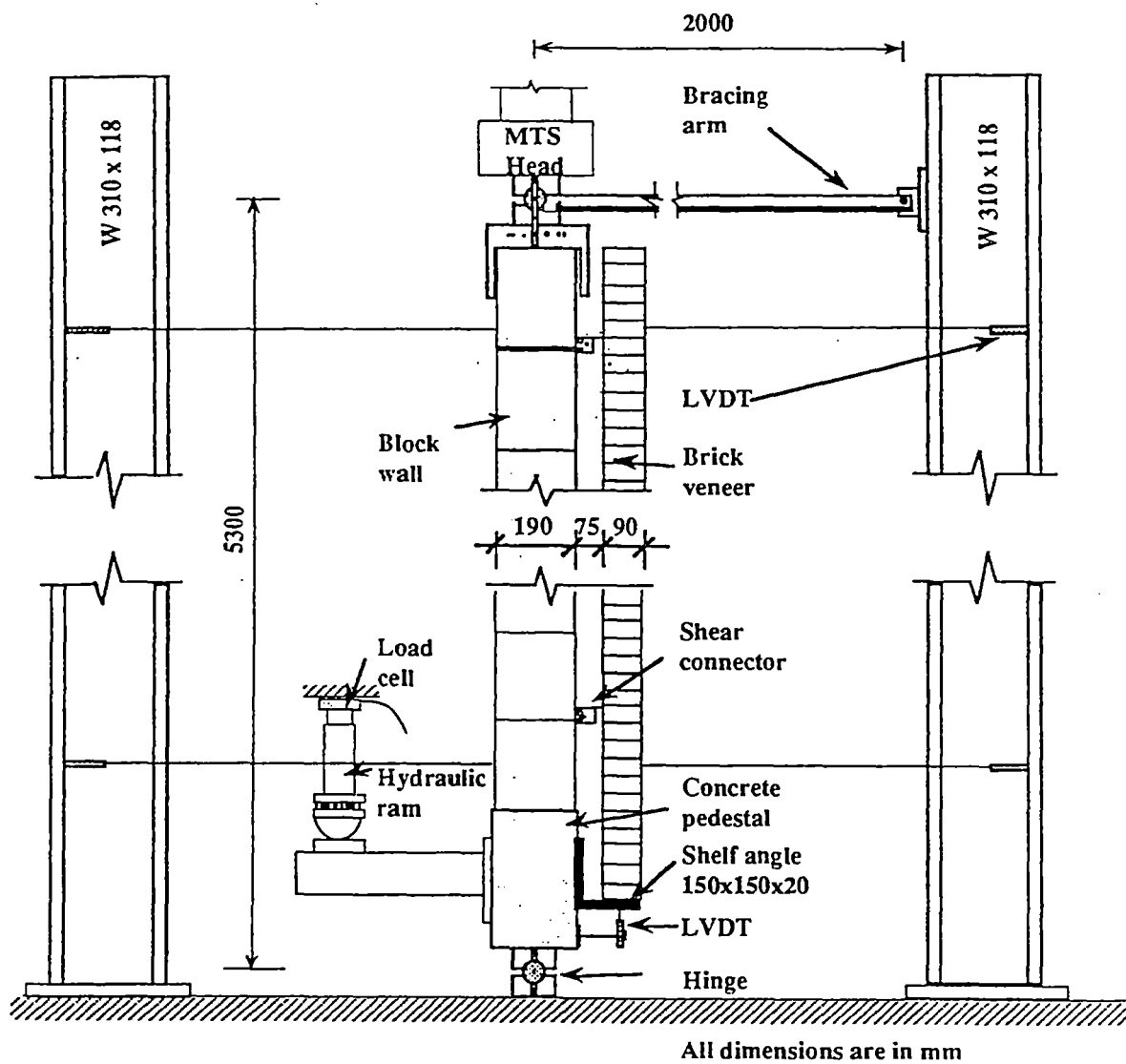


Figure 3.5 Loading Frame

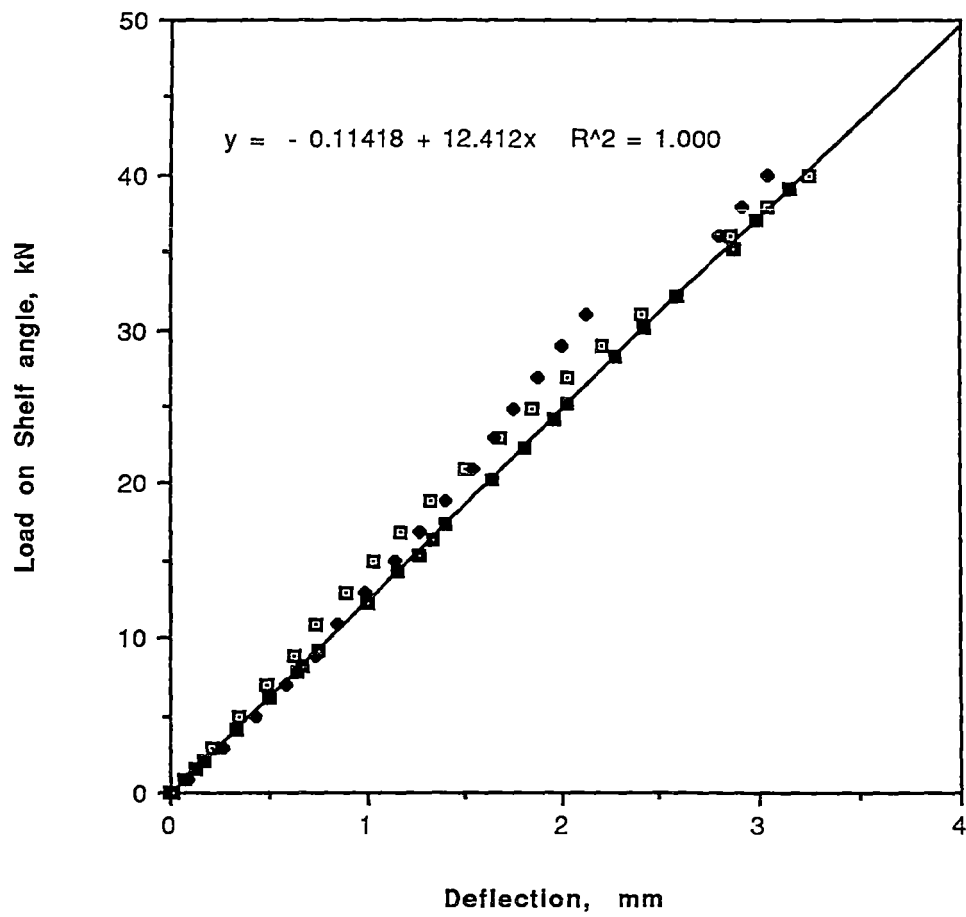


Figure 3.6 Calibration of the Shelf Angle

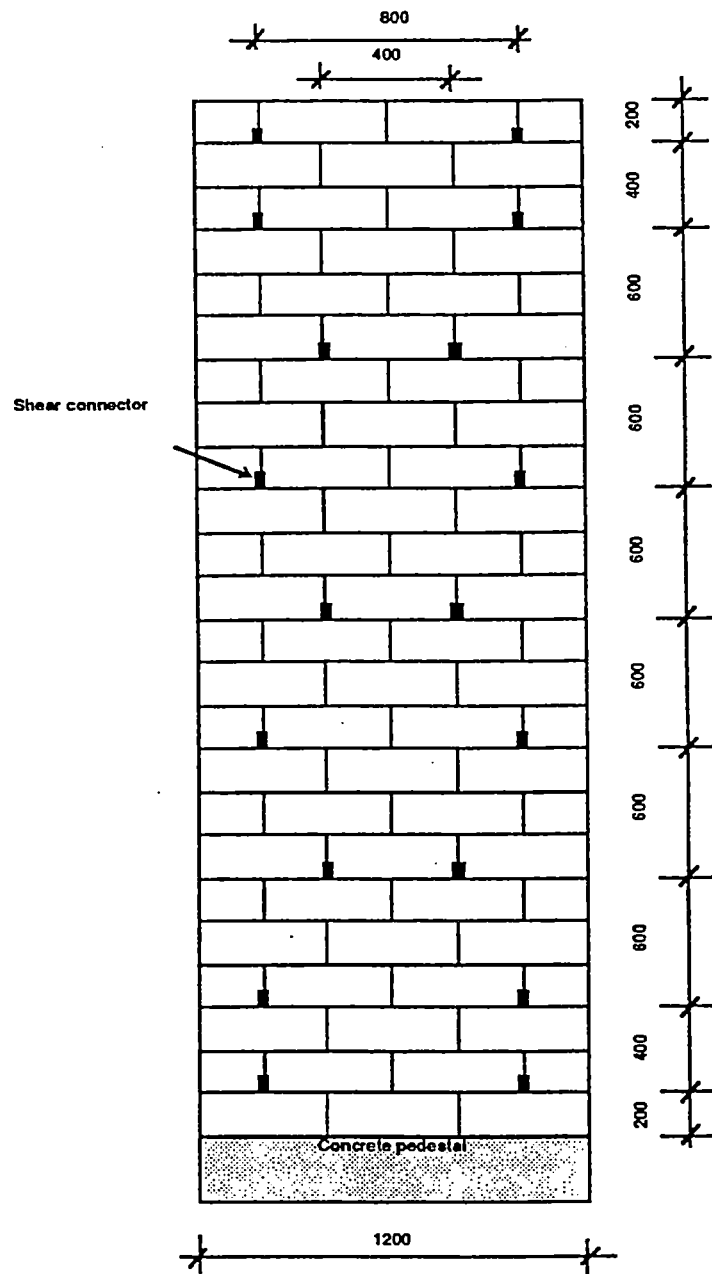


Figure 3.6 Shear Connector Arrangement

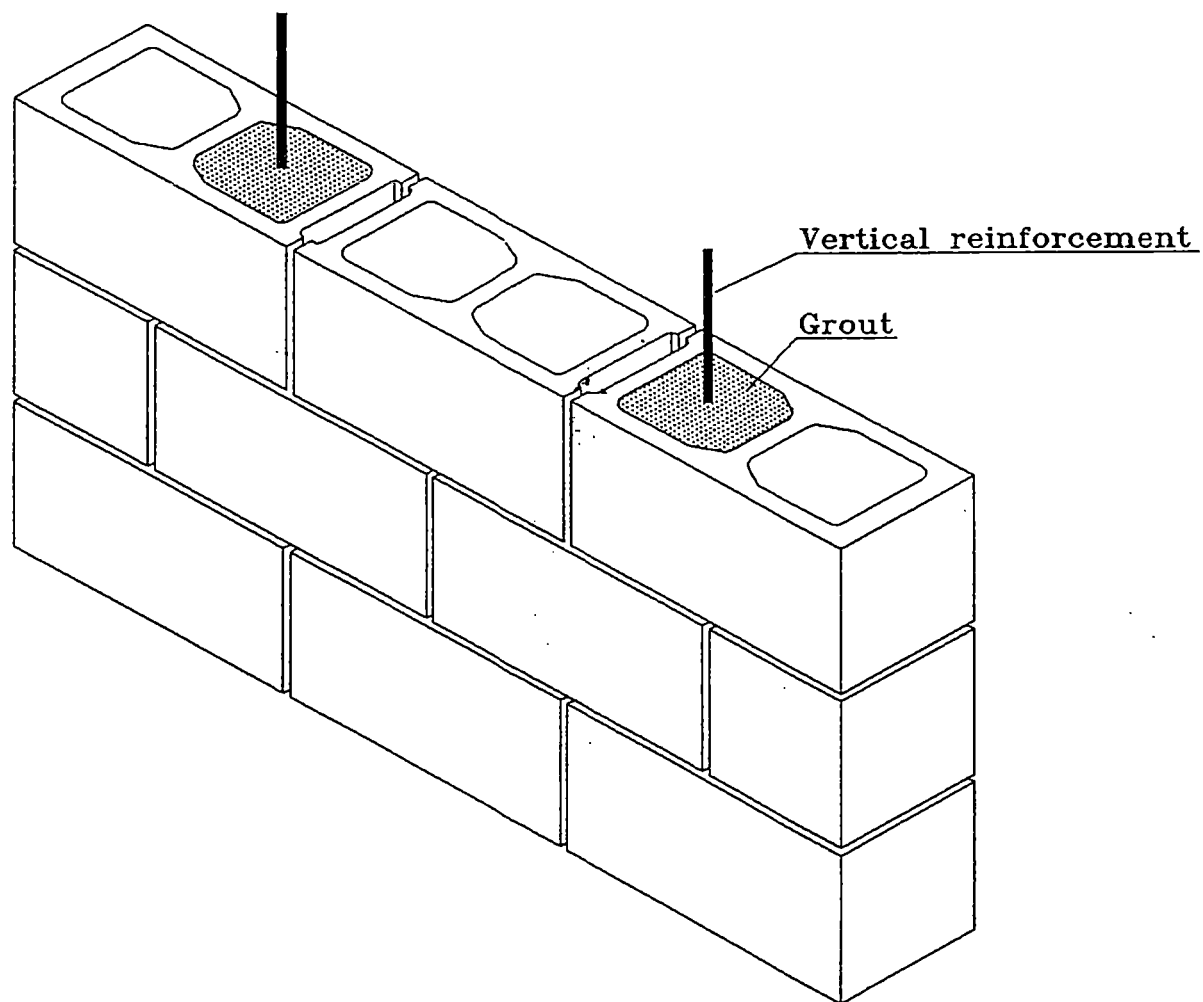


Figure 3.7 Position Of Reinforcement

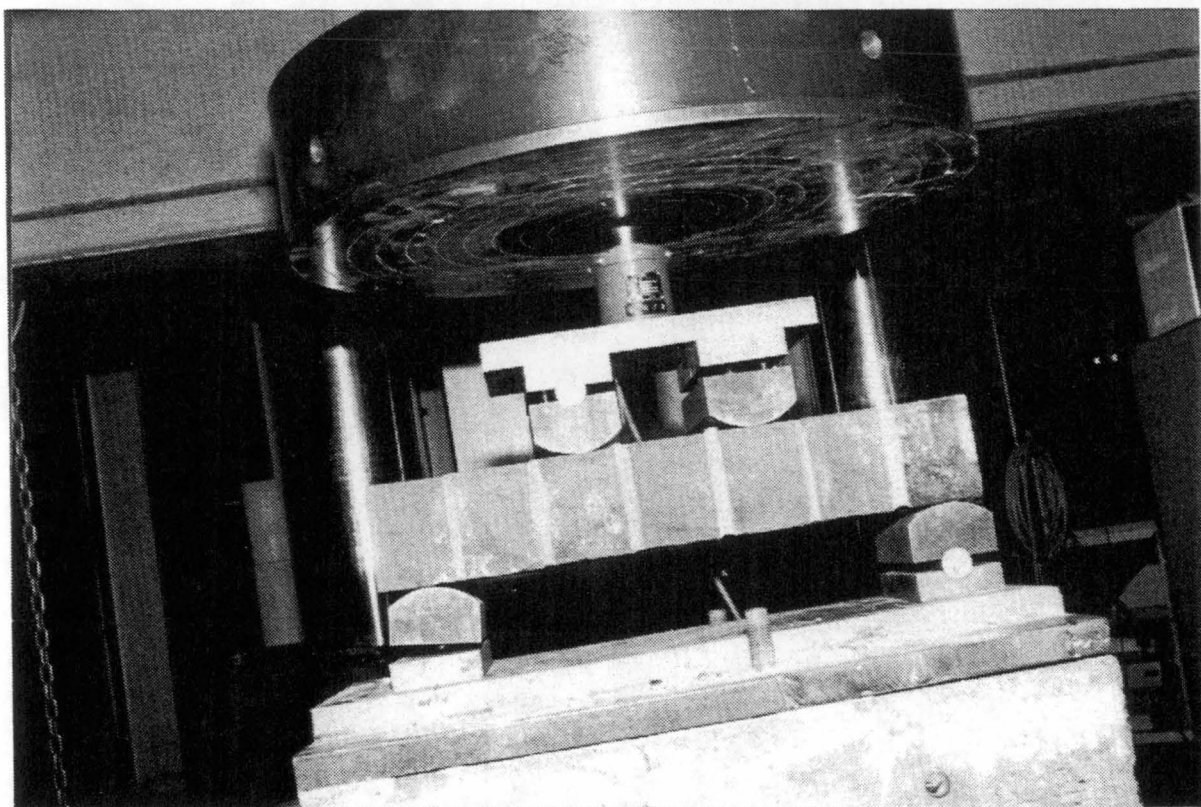


Plate 3.1 Flexural Test on Brick Prism

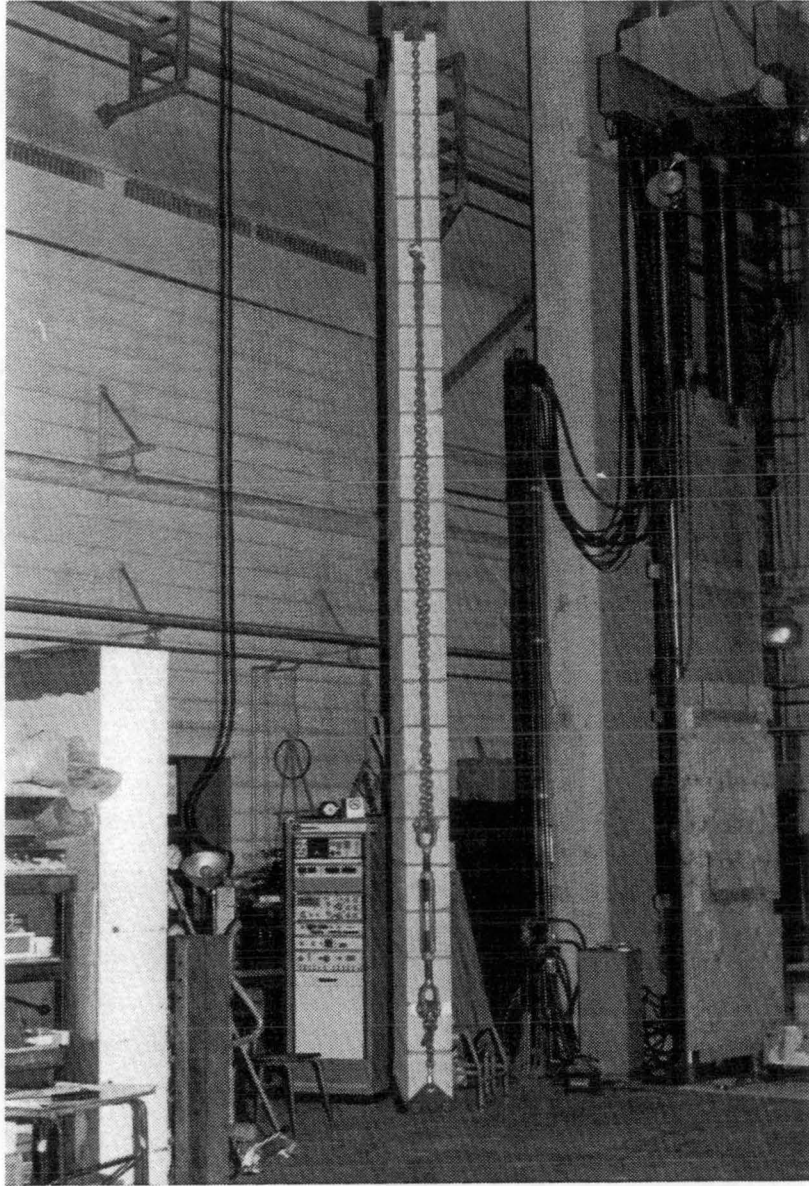


Plate 3.2 Lifting Mechanism of Single Wall

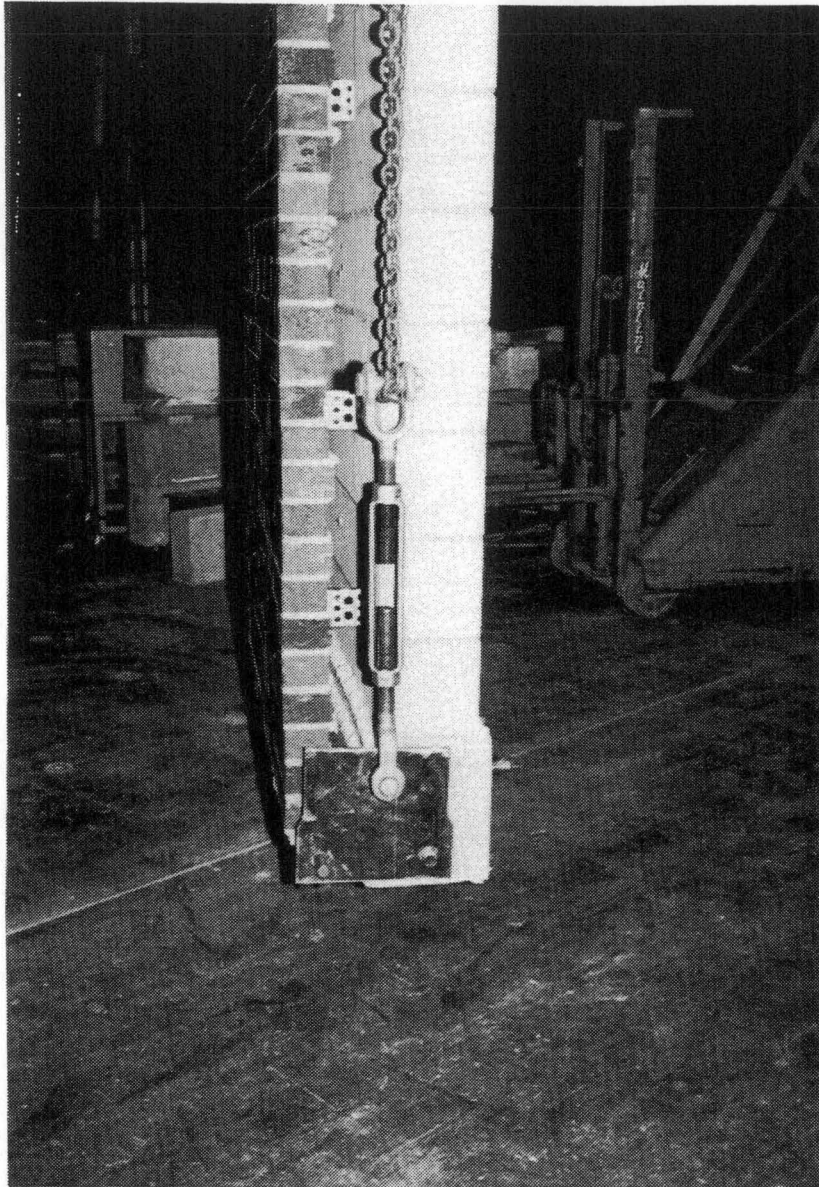


Plate 3.3 Lifting Mechanism of Cavity Walls

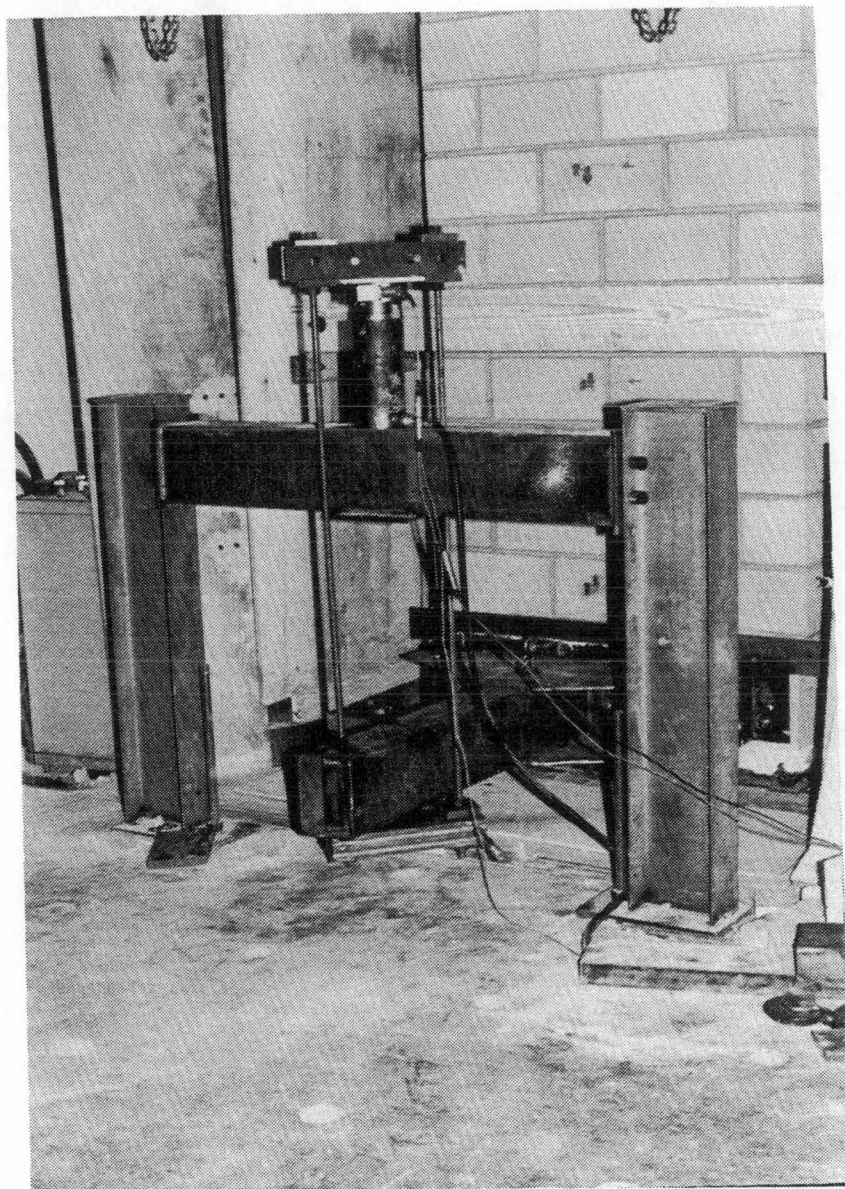


Plate 3.4 Moment Arm Loading Frame

CHAPTER 4

TEST RESULTS

4.1 General Remarks

The results of the tests on masonry units, prisms and full-scale wall specimens are summarized and presented in this chapter in tabular, graphic and photographic form.

4.2 Concrete Block Units

The compressive strength of five 200 mm concrete block units are recorded in Table 4.1. The maximum and minimum compressive strength based on the net area of 41500 mm² were 14.9 MPa and 17.4 MPa respectively with a mean of 16.1 MPa.

Table 4.2 summarizes the compressive strength of five 8 inch concrete blocks. The maximum and minimum compressive strengths based on the net area of 41870 mm² were 20.3 MPa and 17.3 MPa, with a mean of 18.8 MPa.

4.3 Burnt Clay Units

The ultimate loads and compressive strengths of ten burnt clay units, based on the gross area of 16530 mm^2 are shown in Table 4.3. The minimum and maximum values were 33.7 MPa and 47.3 MPa, with a mean of 39.6 MPa.

4.4 Block Prisms

The test results of four block high prisms made of 200 mm block tested under compression are presented on Table 4.4. The minimum and maximum ultimate strengths based on mortar bedded area of 29950 mm^2 are 10.9 MPa and 14.8 MPa, with a mean of 13.5 MPa. A typical failure pattern is shown in Plate 4.1

4.5 Brick Prisms

The ultimate load and ultimate strength of the five brick high prisms when tested in compression are presented in Table 4.5. Two prisms were damaged in the mortar joints while transporting them to the testing machine. They were tested and the results are reported in Table 4.5. The mean ultimate strength of the undamaged prisms based on the gross area of 16530 mm^2 is 18.3 MPa. All the prisms failed in splitting of bricks.

4.6 Flexural Bond of Brick Masonry

The ultimate loads carried by the 7 brick high prisms tested under third point loading are presented in Table 4.6. The mean flexural bond strength is 0.59 MPa. All the specimens failed in the constant moment region, that is middle third span.

4.7 Full Scale Walls

The ultimate loads and the corresponding deflection of the full scale plain walls and reinforced walls are summarised in Table 4.7 and Table 4.8.. The following subsections illustrate the observations made during the individual wall tests. It is noted that the ultimate load usually does not represent the failure load of the specimen. All the walls were loaded at a rate of 15-30 kN/minute.

4.7.1 Plain Single and Cavity Walls

The observations made during the testing of plain single and cavity walls are described in the following sections.

4.7.1.1 Single Wythe Wall S1, $e=0.0$

This wall was tested under axial vertical load. Splitting of webs occurred at a load of 750 kN. In order to observe the effect of loading a cracked wall, the load was removed. On unloading there was a permanent midheight deflection of 0.288 mm. The specimen was next reloaded until failure. The wall carried an ultimate load of 845.5 kN. It failed explosively by additional splitting and rupture of webs. Fig 4.1 shows the load versus the midheight deflection relationship. It also shows the unloading and reloading of the wall. The deflected shapes of the wall at various load levels are shown in Fig 4.2. Plate 4.2 shows the wall in the testing machine.

4.7.1.2 Single Wythe Wall S2, $e=t/6$

This specimen was loaded with a eccentricity of $t/6$ in single curvature bending. After 700 kN the rate of deflection per load increment increased due to formation of cracks at the horizontal mortar joints of the wall. The wall failed in splitting of webs. The upper 9 courses fell at the ultimate load of 735.4 kN and a midheight deflection of 24.38 mm. Fig 4.3 illustrates the load versus midheight relationship and Fig 4.4 shows the deflection of the wall at various load intervals. Plate 4.3 shows the wall during failure.

4.7.1.3 Single Wythe Wall S3, $e=t/3$

This single wythe wall was loaded with an eccentricity of $t/3$ at both ends under single curvature bending. After 230 kN of load the rate of deflection of the wall per load increment started increasing at a faster rate. This was because of the increase in cracks in the horizontal mortar joints of the wall. The specimen failed at a load of 248.0 kN at the fourth course from the top. Failure of the wall was due to tension failure of the joint between the fourth and fifth courses from top. Since the moment was applied manually by a hydraulic pump, the piston of the pump could not be pushed faster so as to counteract the rotation of the lower end of the wall. This led to a drop in moment at the bottom end and hence less rotation as compared to that of the top end of the wall. This can be observed in Fig 4.6 showing the unsymmetry about the midheight in the deflected shape at higher loads. The load versus midheight relationship is shown in Fig 4.5.

4.7.1.4 Cavity Wall C7, $c=75\text{mm}$, $e=0.0$

The wall was tested such that the centreline of the top and the bottom hinges passed through the centre of the concrete block wythe. The effect of selfweight of the overhanging brick veneer was neutralised by placing weights on the moment arm.

The wall deflected towards the concrete block wythe. The load versus midheight deflection relationship is illustrated in Fig 4.7 and the deflected shapes of the wall at various loads is shown in Fig 4.8.

Cracking of webs of the concrete blocks started at a load of 558 kN. It can be observed from the load versus midheight deflection curve that the rate of increase of deflection increased after this load. At a load of 700 kN, a vertical crack running all along the height was formed on the face of the block wythe. The location of the crack can be seen in Plate 4.4. Failure occurred at a load of 793.1 kN and a midheight deflection of 23.67 mm.

4.7.1.5 Cavity wall C1, $c=75\text{mm}$, $e=t/3$ towards brick veneer

Masonry cavity wall C1 was identical to wall C7. The hinge at the top end was placed such that it was at a distance of $t/3$ from the centre of concrete block wythe and measured towards the brick veneer. The same moment was applied at the lower end such that the wall was subjected to bending in single curvature.

The load versus midheight deflection curve is shown in Fig 4.9 and the deflected shapes at various loads is shown in Fig 4.10. The rate of deflection of the wall increased abruptly after 330 kN of load.

The wall failed by cracking of the joint between the 18th and 19th block course at a load of 340.0 kN and a midheight deflection of 16.81 mm. This was the location of a shear connector. The mortar joint in the brick veneer at the corresponding level also failed. Plate 4.5 shows the wall after failure.

4.7.1.6 Cavity Wall C2, $c=75\text{mm}$, $e=t/6$ Towards Brick Veneer

The block wythe of this cavity wall was loaded at an eccentricity of $t/6$ measured from the centre of the block wythe towards the brick veneer. Both ends had the same eccentricity of loading measured in the same direction, that is towards the brick veneer.

Splitting of webs occurred at a load of 640 kN. Complete failure occurred at a load of 798.0 kN at a midheight deflection of 43.53 mm. The blocks in the top half portion of the wall broke in splitting of webs. The mortar joint in the brick veneer at the level of mortar joint between the ninth and tenth block courses from top also failed.

The load versus midheight deflection relationship of the wall is shown in Fig 4.11 and the deflected shapes of the wall at various loads is presented in Fig 4.12. Plate 4.6 shows the wall after failure.

4.7.1.7 Cavity Wall C3, $c=75\text{mm}$, $e=t/6$ Away From Brick Veneer

This wall was similar to wall C2, except for the direction of eccentricity of loading. The eccentricity of $t/6$ was measured from the centre of the block wythe away from the brick veneer. At the lower end the moment was applied by the moment arm, to maintain equal end moments and single curvature bending.

At a load of 690 kN a crack formed on the face of the block wythe running all along the height. Plate 4.7 shows the crack in the wall. Failure occurred at a load of 745.0 kN by a sudden failure of blocks at the joint of sixth and seventh block from top; the mortar joint of brick veneer at that level failed in tension. The midheight deflection of the wall at failure was 28.82 mm. The relationship of load and midheight deflection is presented in Fig 4.13 and the deflected shapes of the wythes at various loads are shown in Fig 4.14.

4.7.2 Reinforced Single and Cavity Walls

The data collected and observations made during the test of the reinforced single and cavity walls are described in the following sections. Cavity wall C4, had a cavity width of 100 mm and cavity walls C5 and C6 had cavity widths of 75mm. The ultimate loads and

the corresponding midheight deflection of all the reinforced walls are presented in Table 4.8.

4.7.2.1 Single Wythe Wall S4, $e=t/3$

This single wythe wall was tested under an equal end eccentricity of $t/3$, in single curvature bending. After the load reached 130 kN, the rate of deflection increased, due to formation of cracks in the horizontal joints. Cracks were formed in all the horizontal joints of block wythe of the middle one-third region of the wall. Cracks were wider in the joints near the midheight than those towards the ends. The load started dropping after a ultimate load of 225.8 kN was reached, with a midheight deflection of 35.95 mm. Fig 4.15 shows the load versus midheight deflection relationship and Fig 4.16 shows the deflected shapes at various loads.

4.7.2.2 Single Wythe Wall SS, $e=t/2.5$

Wall S4 was tested with an eccentricity of $t/2.5$ at both ends under single curvature bending. After a load of 100 kN, the rate of deflection per load increment increased, due to loss of flexural rigidity caused by cracking in the horizontal mortar joints. Cracking was observed all along the height of the wall. The cracks were wider in the middle 1/3 region of the wall. The cracks were in almost all

the horizontal bed joints. The wall failed at a load of 197.1 kN and a midheight deflection of 41.28 mm. Fig 4.17 and Fig 4.18 illustrates the load versus midheight deflection relationship and the deflected shape at various loads respectively.

4.7.2.3 Cavity Wall C4, $c=100\text{mm}$, $e=t/3$ Towards Brick Veneer

This wall had a cavity of 100 mm, and it was tested to study the influence of change in cavity width on the behaviour of a cavity wall. The backup wythe of this wall was loaded with a eccentricity of $t/3$ towards the brick veneer at both ends.

The load versus midheight deflection of the block wythe and the deflected shapes of both wythes at various loads are given in Fig. 4.19 and Fig. 4.20 respectively. At a load of approximately 150 kN, a crack appeared in the horizontal joint of the block wythe at midheight. The corresponding midheight deflection was 6.6 mm. After this, the deflection started to increase at a faster rate and cracks began to develop all over the block wythe. After a load of 330.7 kN and a midheight deflection of 29.21 mm, the load started dropping. At the ultimate load the connector plates of the upper half of wall were buckled.

4.7.2.4 Cavity Wall CS, $c=75\text{mm}$, $e=t/3$ Towards Brick Veneer

This specimen was similar to C4 except for the cavity width. Cavity width was 75 mm instead of 100 mm. It was tested under a eccentricity of $t/3$ towards the brick veneer at both ends.

The load versus midheight deflection relationship for the block wythe and the deflected shapes of both wythes are shown in Fig. 4.21 and Fig. 4.22 respectively. When the vertical load reached 170 kN, a crack was observed in the horizontal joint at midheight of the block wythe. The corresponding deflection was 8.1 mm. After that, cracks started to develop along the height in horizontal joints of the block wythe. After a ultimate load of 325.5 kN and a midheight deflection of 34.98 mm the load started dropping. At ultimate load, all the V-ties in the upper half of the wall were bent downwards. At a midheight deflection of 64 mm the loading was stopped. None of the connector plates were buckled, but all the V-ties were bent downwards. Plate 4.8 shows the crack between the 12th and the 13th course of the block wythe.

4.7.2.5 Cavity Wall C6, $c=75\text{mm}$, $e=t/2.5$ Towards Brick Veneer

This wall had a cavity of 75 mm. The backup wythe was loaded with a eccentricity of $t/2.5$. The load versus midheight deflection of the block wythe and the deflected shapes of both the wythes at various loads are given in Fig. 4.23 and Fig. 4.24 respectively. The first crack was observed in a horizontal joint of the concrete block wythe at midheight, at a load of approximately 70 kN with a midheight deflection of 6.4 mm. After that, cracks were developed all over the entire height.

The wall carried an ultimate load of 280.2 kN at a midheight deflection of 53.57 mm. At the ultimate load, all the V-ties of the upper half of the wall were bent downwards. There was a drop in load after the ultimate load. The loading was stopped at a midheight deflection of 78 mm. All the V-ties were bent downwards and the connector plates on the top three levels were buckled. Plate 4.9 shows one of the connectors after failure.

Table 4.1 Compressive Strength Of 200 mm Concrete Block Units

Ultimate load, KN	Ultimate Strength, MPa
652.0	15.7
619.4	14.9
683.3	16.5
721.4	17.4
658.2	15.9

Average Compressive Strength 16.1 MPa
(based on net area of 41500 mm²)

Table 4.2 Compressive Strength Of 8 inch Concrete Block Units

Ultimate load, KN	Ultimate Strength, MPa
725.0	17.3
785.0	18.7
850.0	20.3
805.0	19.2
775.0	18.5

Average Compressive Strength 18.8 MPa
(based on net area of 41870 mm²)

Table 4.3 Compressive Strength Of Clay Burnt Units.

Ultimate load, KN	Ultimate Strength, MPa
655	39.6
560	33.9
557	33.7
580	35.1
720	43.6
705	42.6
722	43.7
782	47.3
625	37.8
645	39.0

Average Compressive Strength 39.6 MPa
(based on gross area of 16530 mm²)

Table 4.4 Compressive Strength Of Concrete Block Prisms

Ultimate load, KN	Ultimate Strength, MPa
406.3	13.6
328.1	10.9
444.4	14.8
417.7	13.9
434.3	14.5

Average Compressive Strength 13.5 MPa
(based on mortar bedded area of 29950 mm²)

Table 4.5 Compressive Strength Of Clay Burnt Unit Prisms.

Ultimate load, KN	Ultimate Strength, MPa
316	19.1
315	19.1
276	16.7
284 (Damaged)	17.2
240 (Damaged)	14.5

Average Compressive Strength
of undamaged prisms 18.3 MPa
(Based on Gross area of 16530 mm²)

Table 4.6 Flexural Bond Strength Of Brick Masonry

Ultimate load, P N	Modulus of Rupture $R = (P.L) / (b.d^2)$, MPa
1869.8	0.56
2232.2	0.67
1937.9	0.59
1830.0	0.55
1947.7	0.59

Average Modulus of Rupture 0.59 MPa

Table 4.7 : Experimental Results of Plain Single And Cavity Walls

Wall type (No.)	Eccentricity Top & Bottom	Ultimate load kN	Midheight deflection at Ultimate, m m
Single (S1)	0.0	845.5	4.15
Cavity (C7)	0.0	793.1	23.67
Single (S2)	$t/6$	735.4	24.38
Cavity (C2)	$t/6$ towards brick veneer	798.0	43.53
Cavity (C3)	$t/6$ away from brick veneer	745.0	28.82
Single (S3)	$t/3$	248.0	24.38
Cavity (C1)	$t/3$ towards brick veneer	340.0	16.81

- Eccentricity of load measured with respect to the centre of the block wythe.
- Actual h/t of all the walls was 27.7, where h is the centre to centre distance between the hinges was 5282 mm and t is the thickness of the block wythe.
- All the block walls were built of 200 mm size concrete blocks.
- All the cavity walls had cavity width of 75mm

Table 4.8 Experimental Results of Single And Cavity Reinforced Walls

Wall type (No.)	Cavity m m	Eccentricity top & bottom	Ultimate load, kN	Deflection at Ultimate load, mm
Single (S4)	----	$t/3$	225.8	35.95
Cavity (C4)	100	$t/3$ towards brick veneer	330.7	29.21
Cavity (C5)	75	$t/3$ towards brick veneer	325.5	34.98
Single (S5)	----	$t/2.5$	197.1	41.28
Cavity (C6)	75	$t/2.5$ towards brick veneer	280.2	53.57

- Eccentricity of load measured with respect to the centre of the block wythe.
- Actual h/t of all the block walls was 27.7, where h , the centre to centre distance between the top and the bottom hinges of the walls was 5360 mm and t , the thickness of the block wythe.
- All the block walls were built of 8 inches size concrete blocks
- All the block walls were reinforced with 2-#15 M bars in cores as shown in fig. 3.8

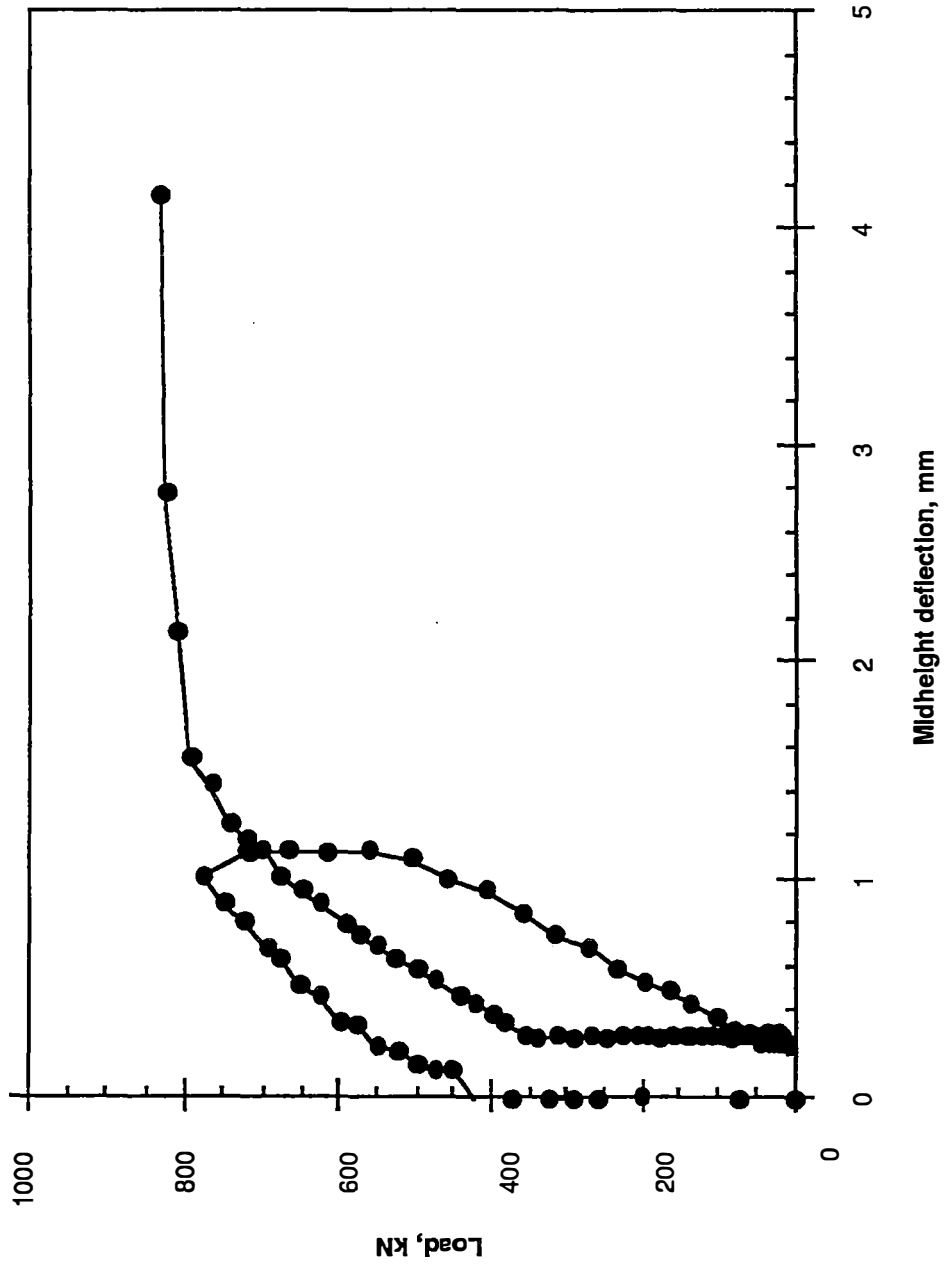


Figure 4.1 Unreinforced Single Wall S1, $e=0.0$

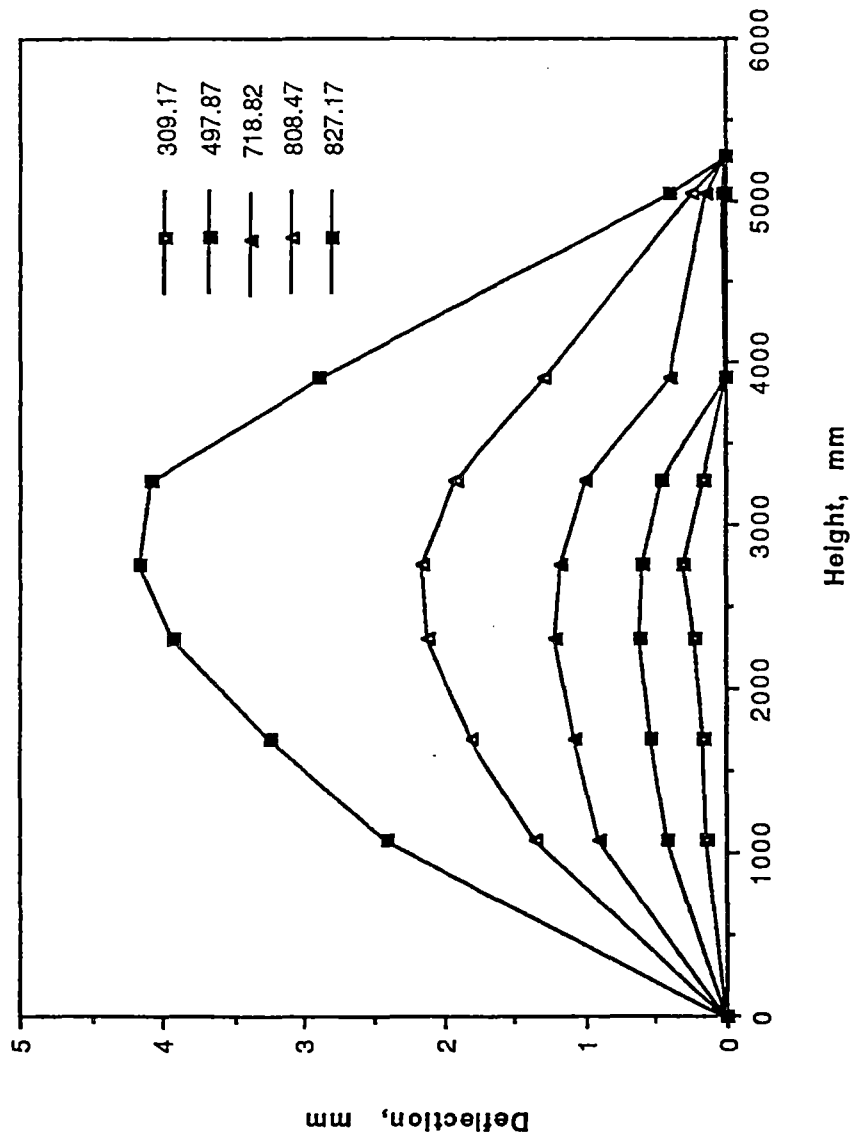


Figure 4.2 Deflected Shape of Unreinforced Single Wall S1, $e=0.0$

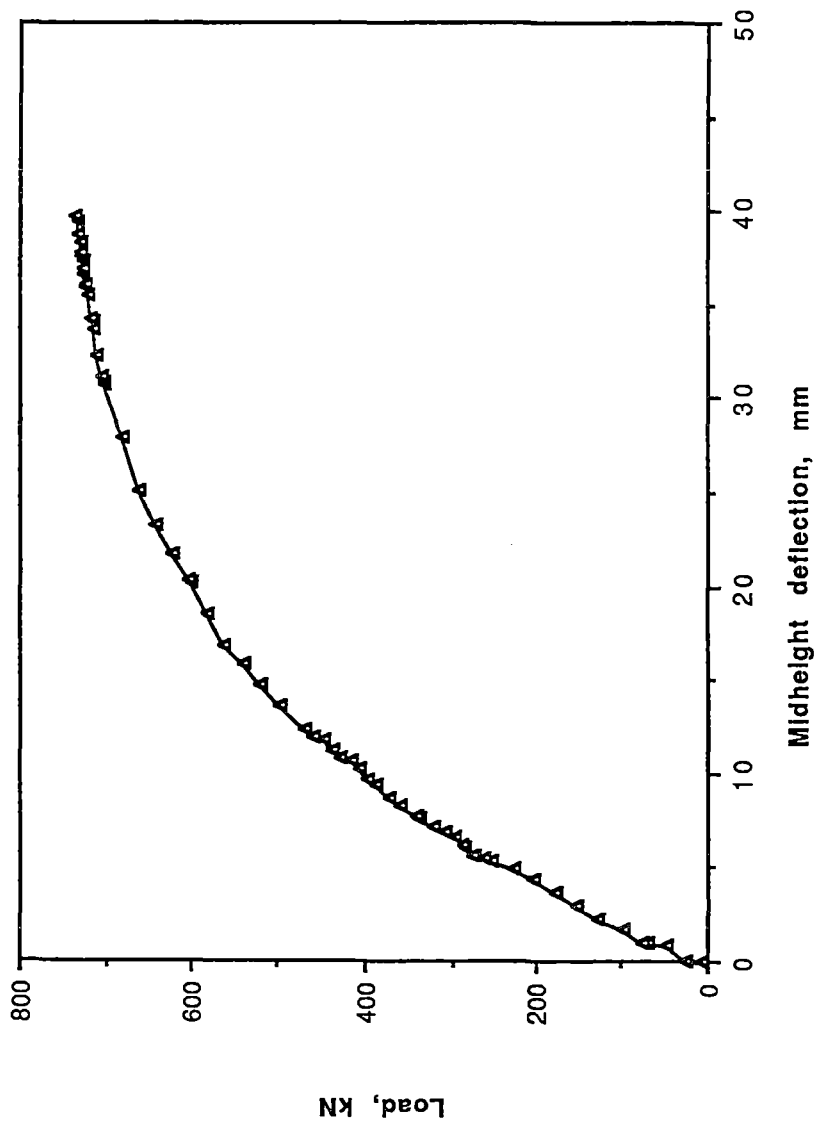


Figure 4.3 Unreinforced Single Wall S2, $e=t/6$

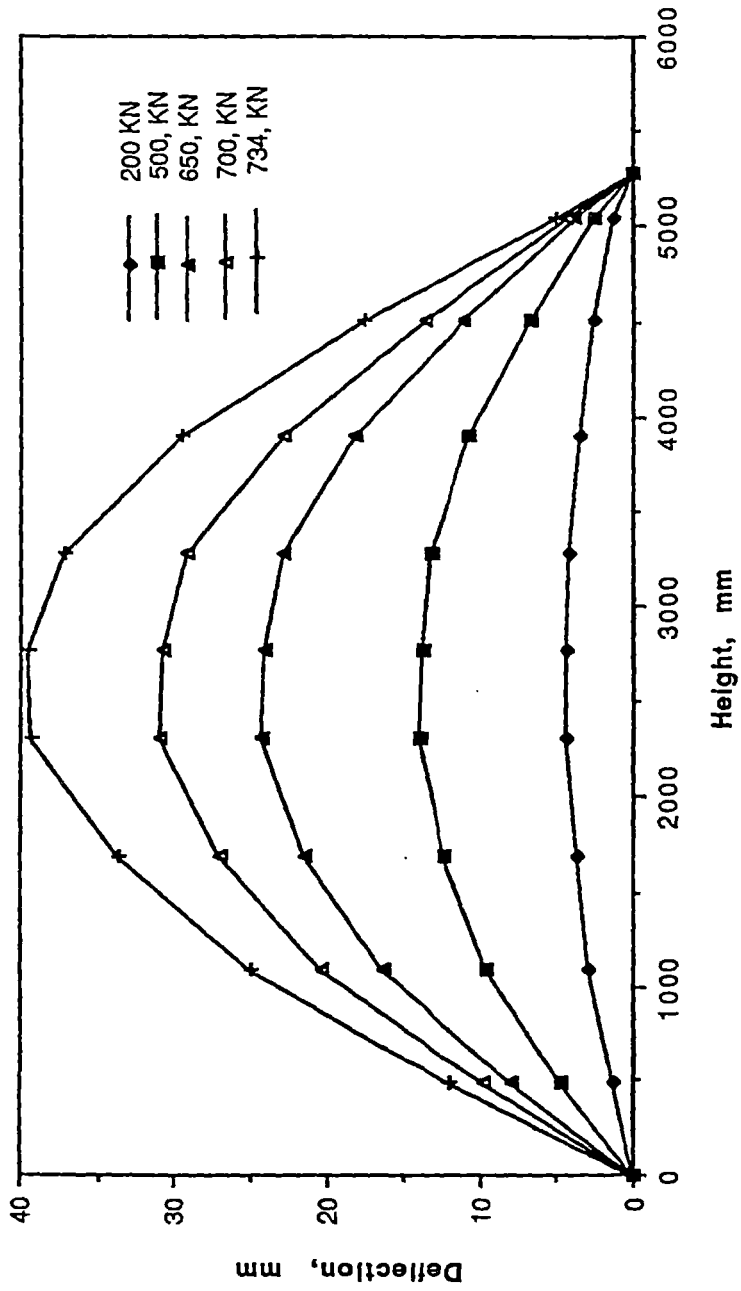


Figure 4.4 Deflected Shape of Unreinforced Single Wall S2, $e=t/6$

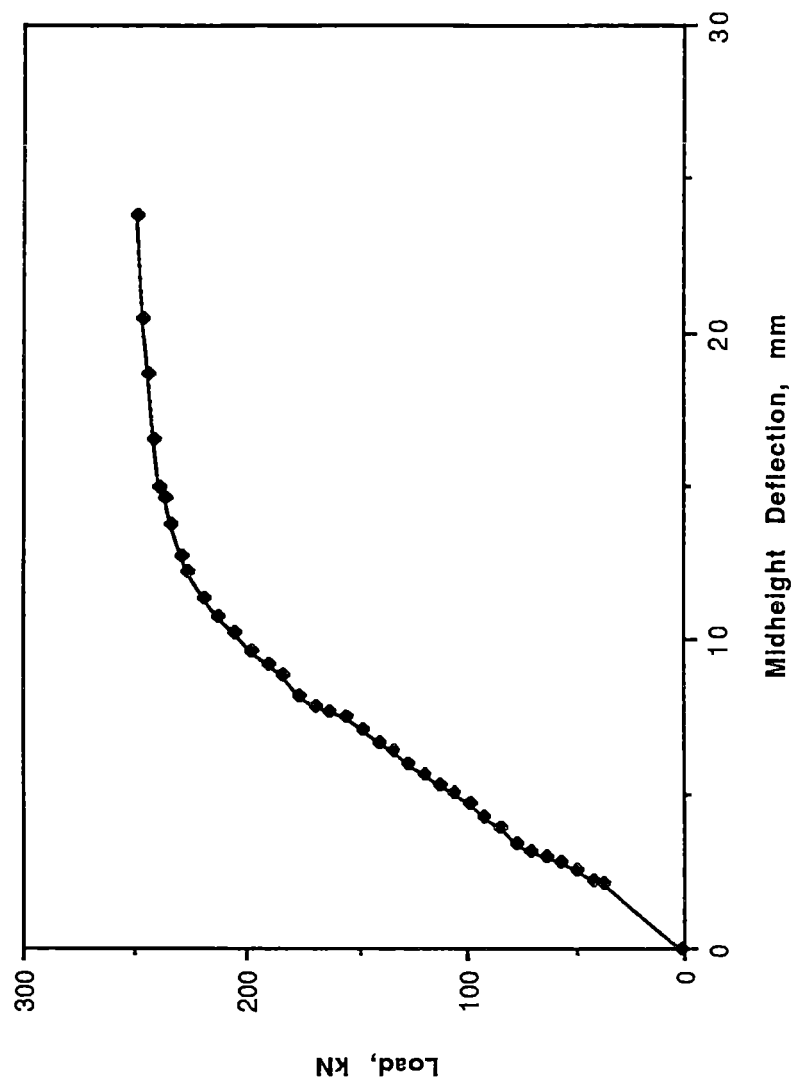


Figure 4.5 Unreinforced Single Wall S3, $e=t/3$

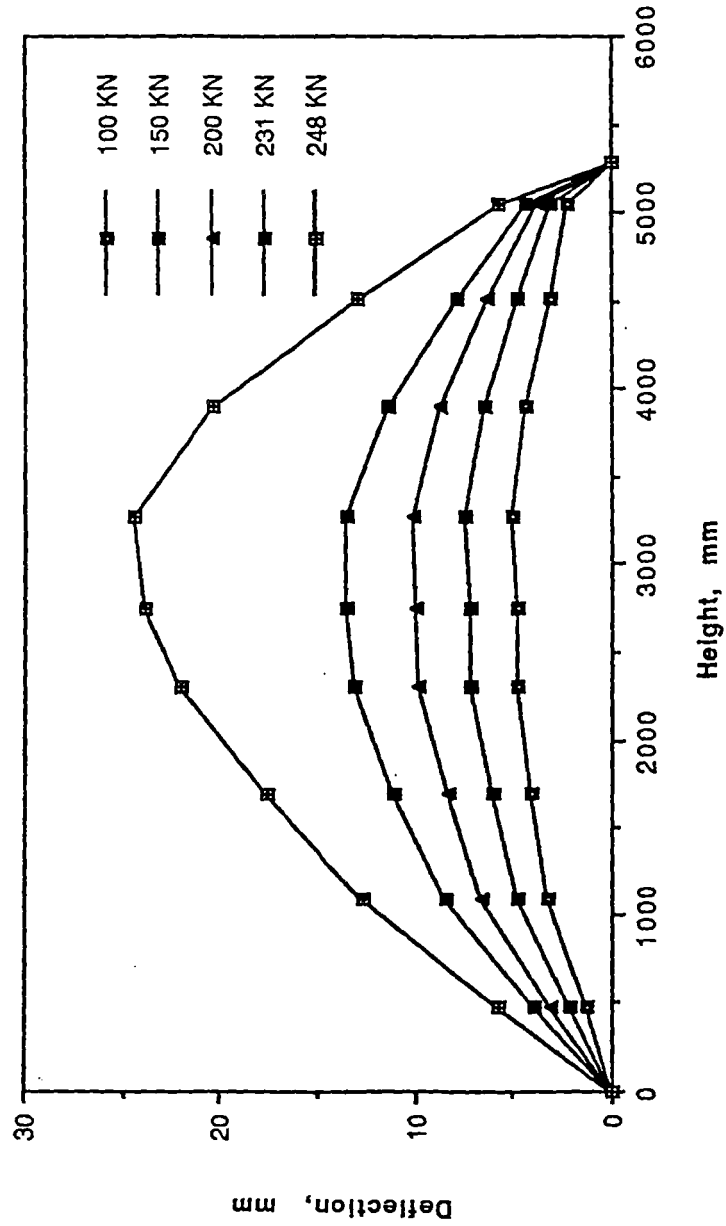


Figure 4.6 Deflected Shape of Unreinforced Single Wall S3, $e=t/3$

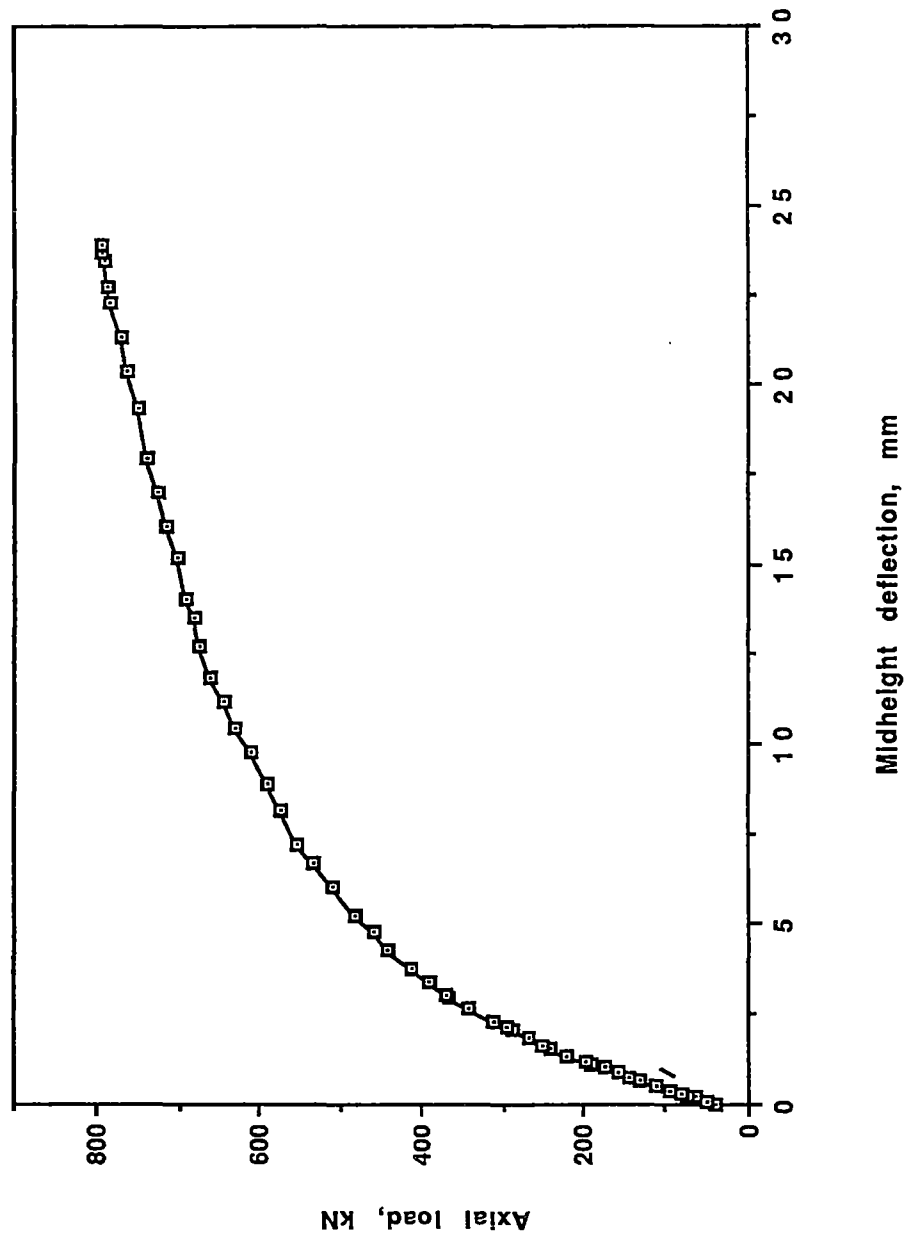


Figure 4.7 Cavity Wall C7, $e=0.0$

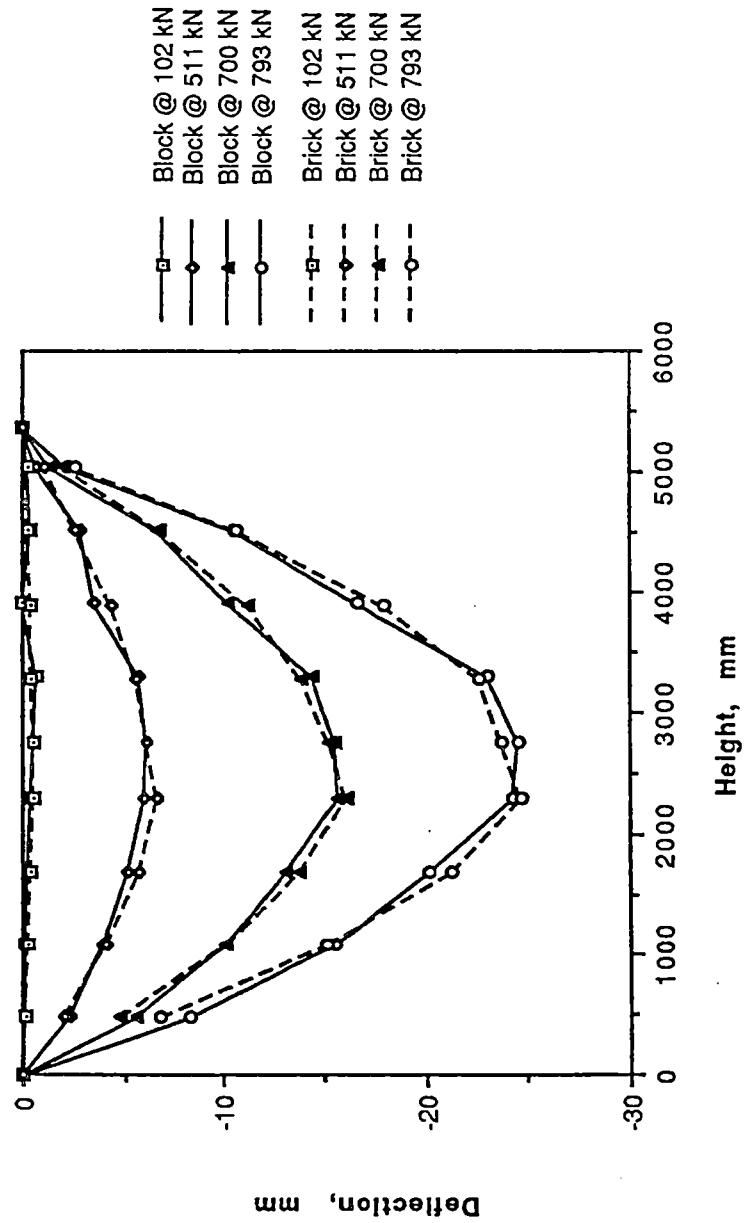


Figure 4.8 Deflected Shape of Cavity Wall C7, $e=0.0$

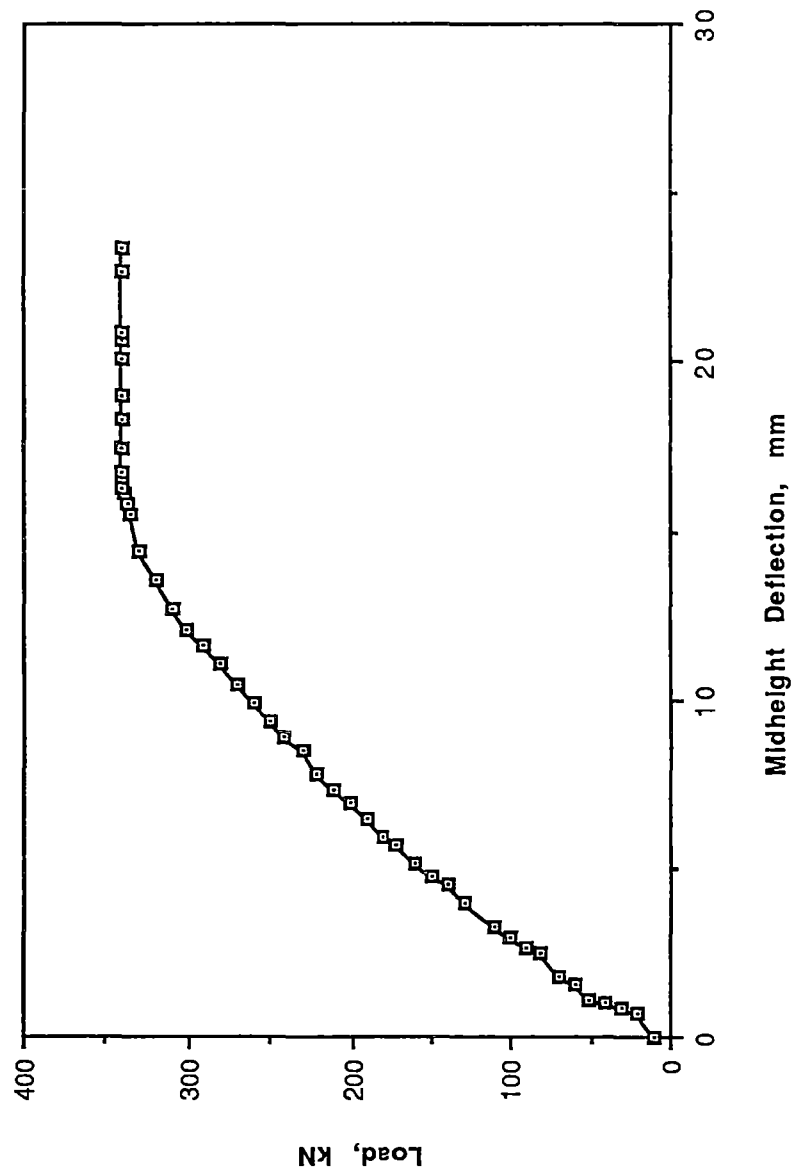


Figure 4.9 Cavity Wall C1, $e=t/3$

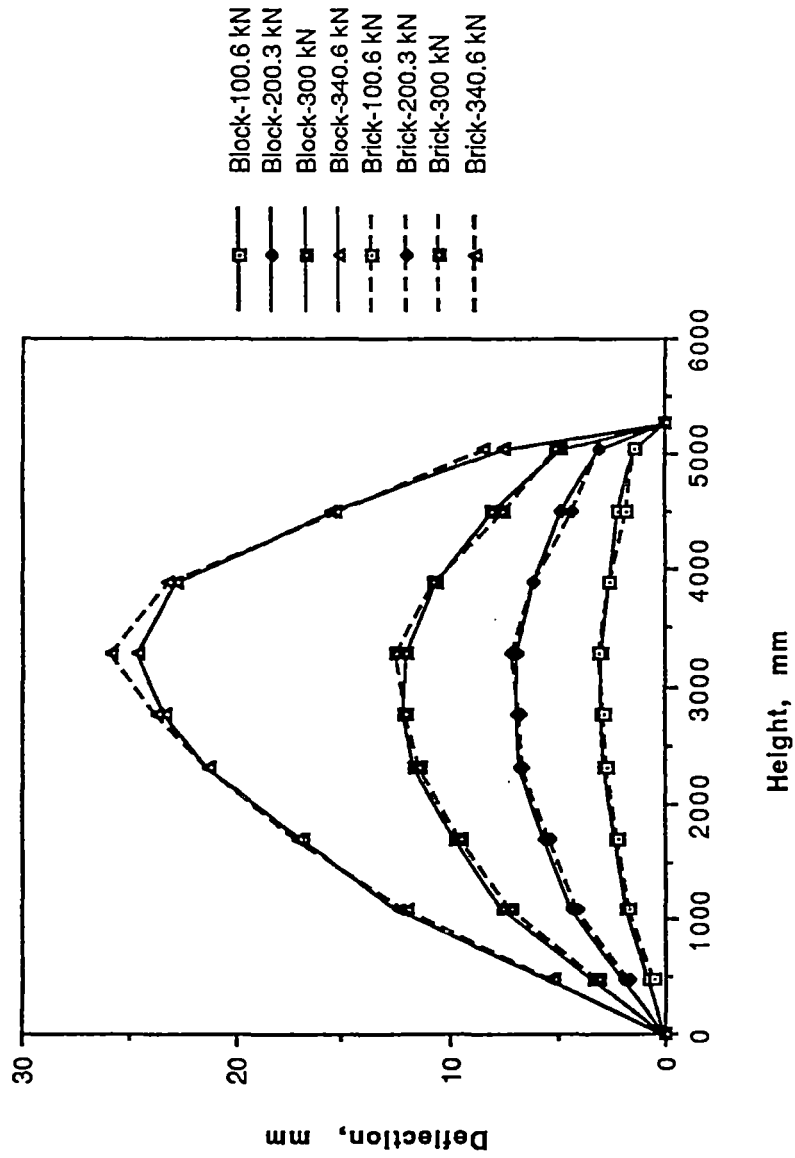


Figure 4.10 Deflected Shape of Cavity Wall C1, $e=t/3$

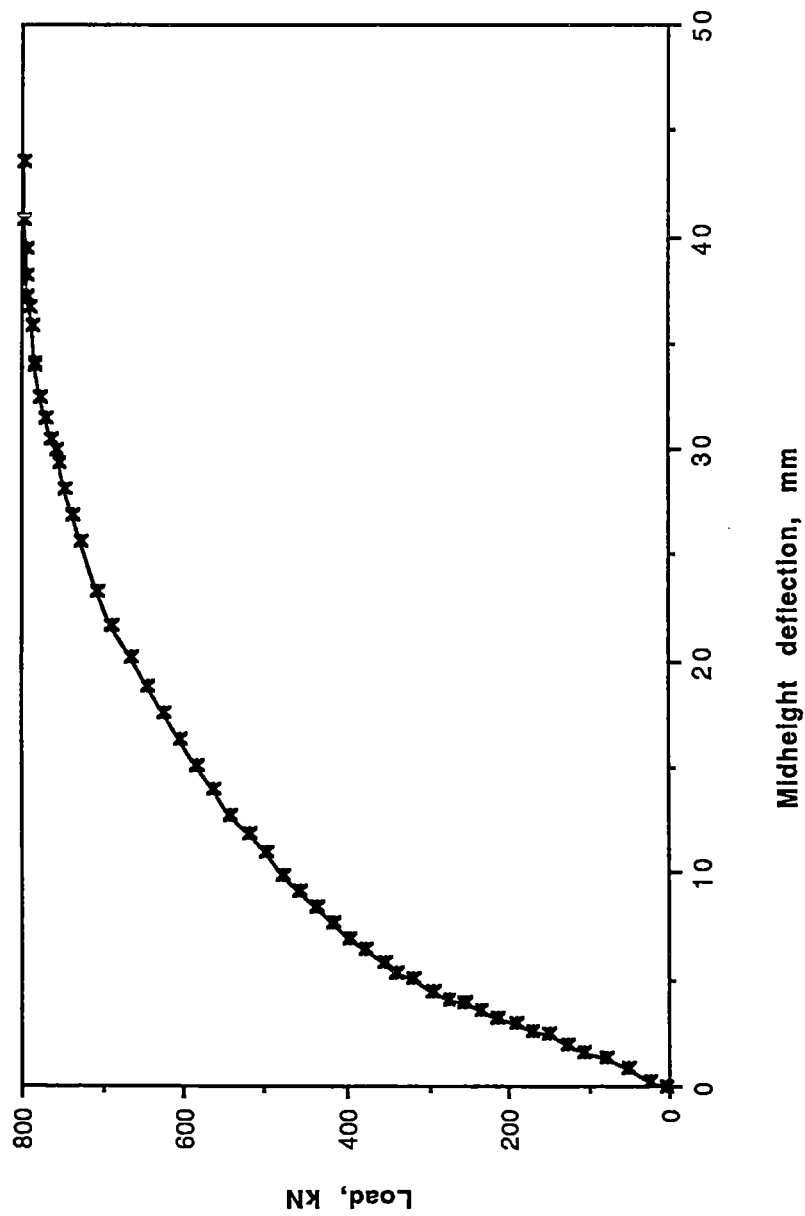


Figure 4.11 Cavity Wall C2, $e=t/6$ Towards Brick Veneer

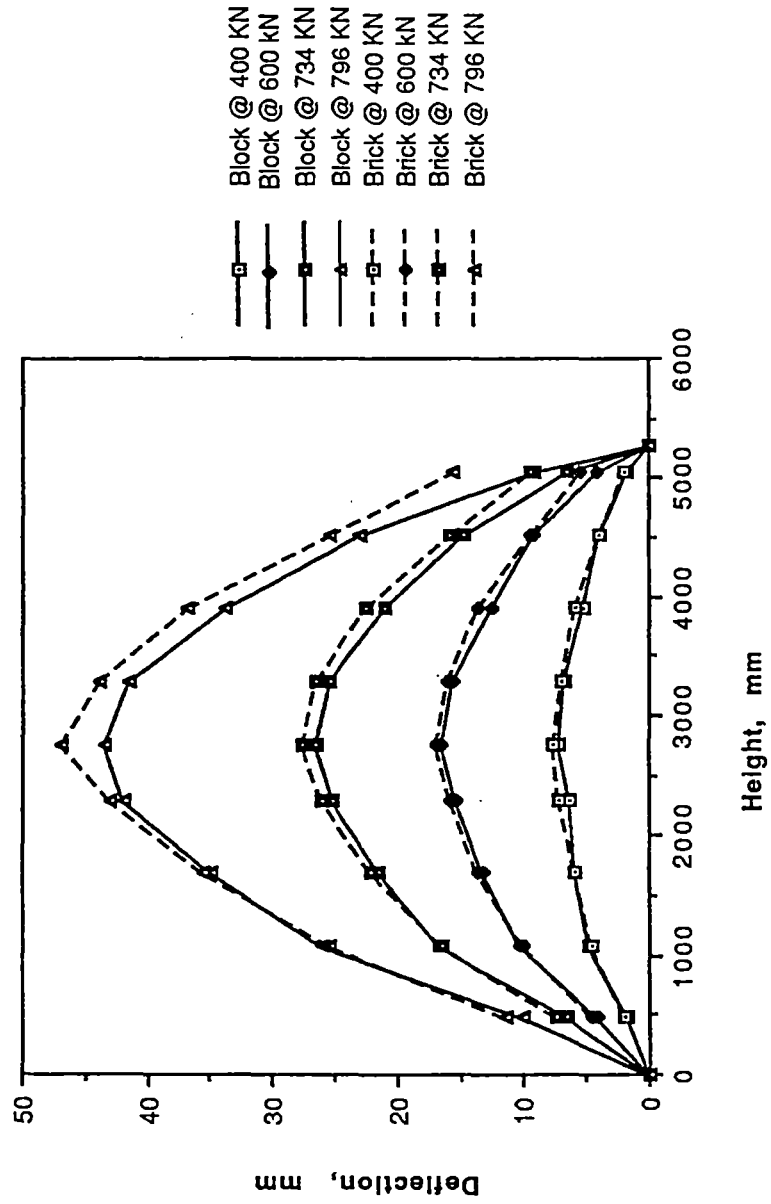


Figure 4.12 Deflected Shape of Cavity Wall C2, $e=t/6$ Towards Brick Veneer

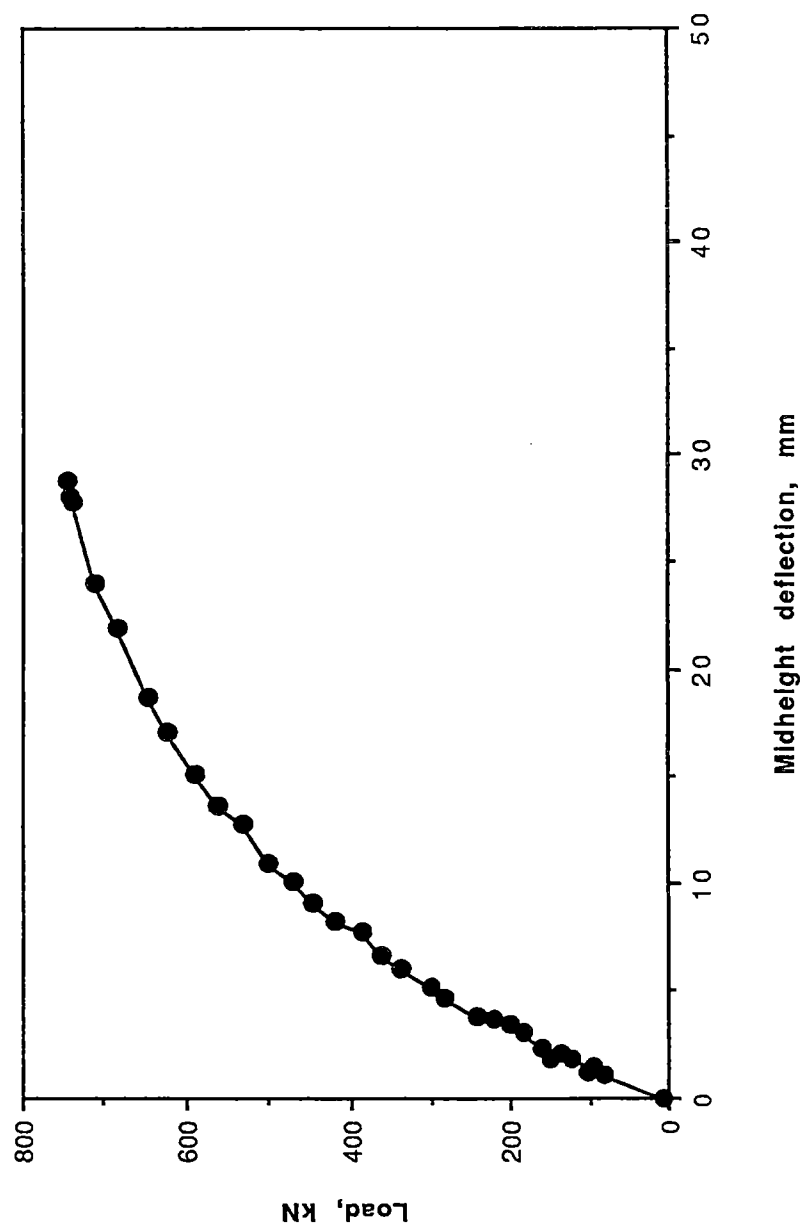


Figure 4.13 Cavity Wall C3, $e=t/6$ Away From Brick Veneer

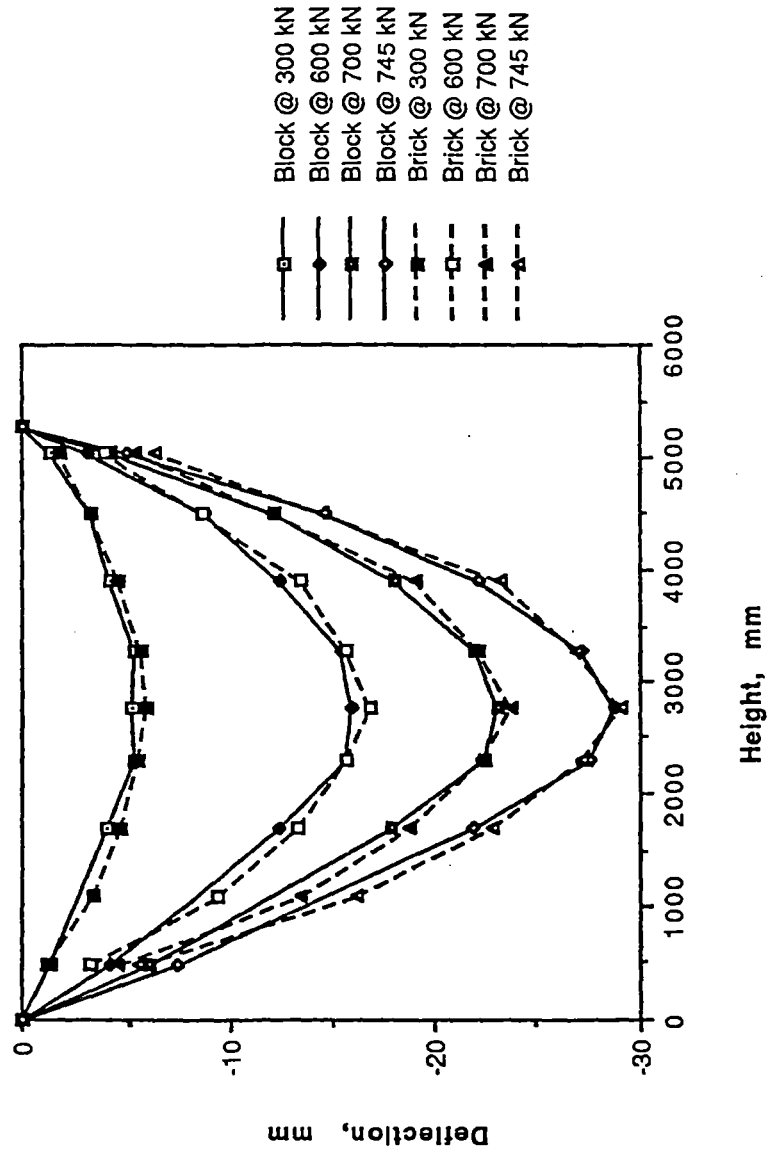


Figure 4.14 Deflected Shape of Cavity Wall C3, $e=t/6$ Away From Brick Veneer

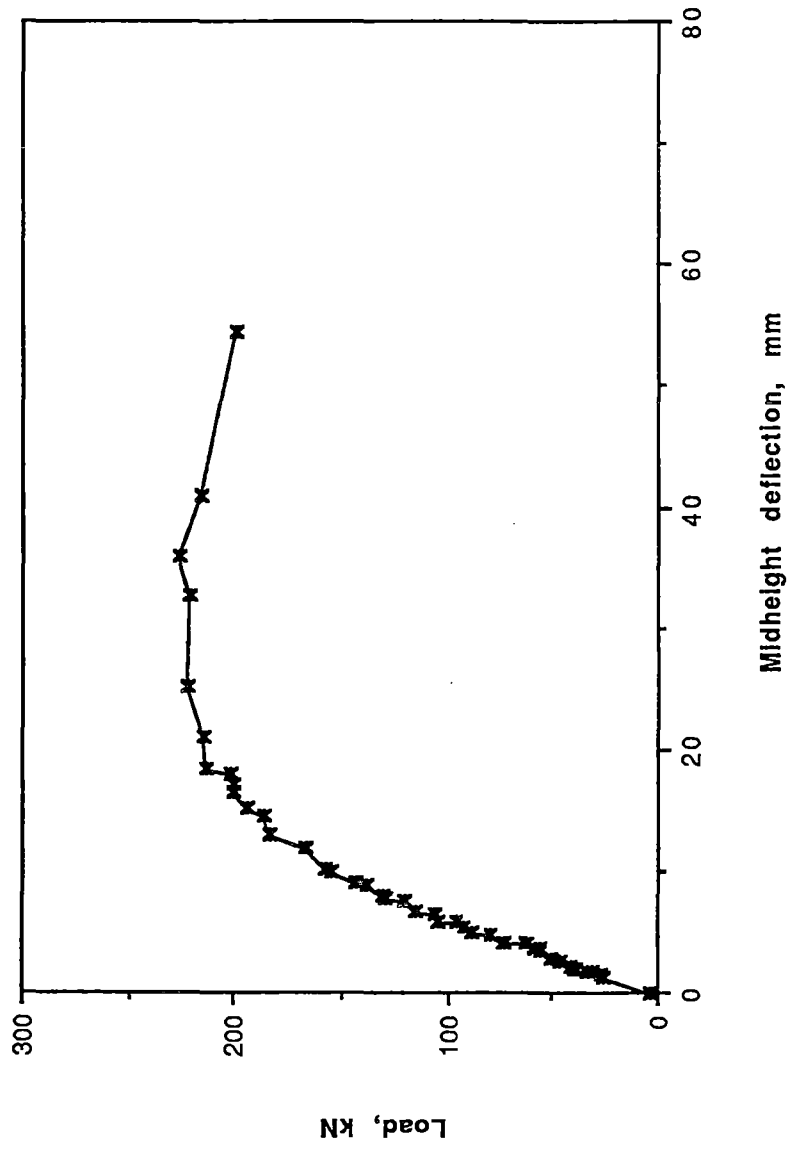


Figure 4.15 Reinforced Single Wall S4, $e=t/3$

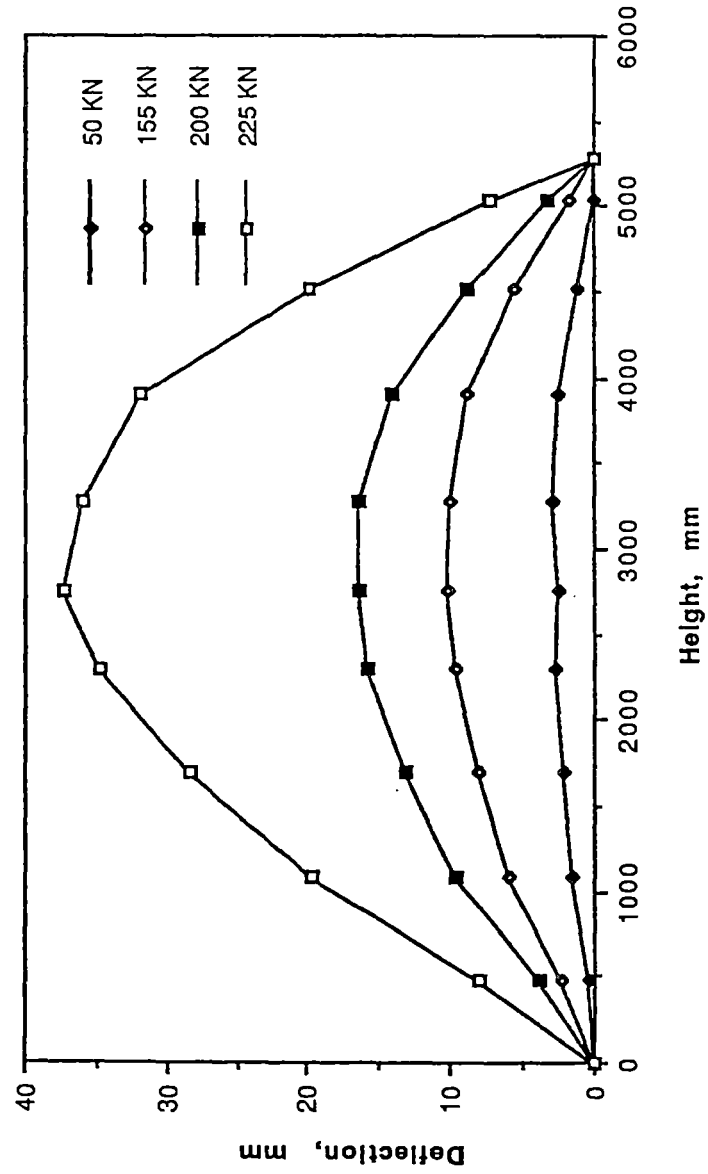


Figure 4.16 Deflected Shape of Reinforced Single Wall S4, $e=t/3$

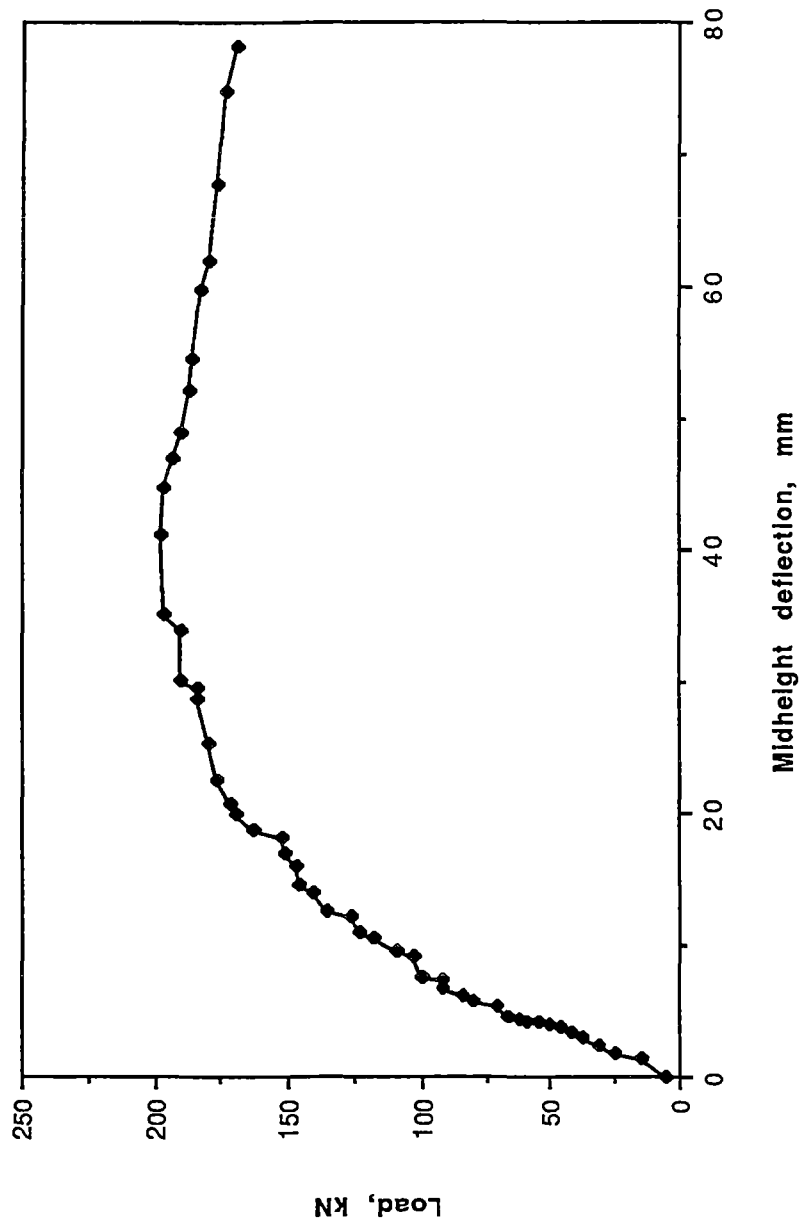


Figure 4.17 Reinforced Single Wall S5, $e=t/2.5$

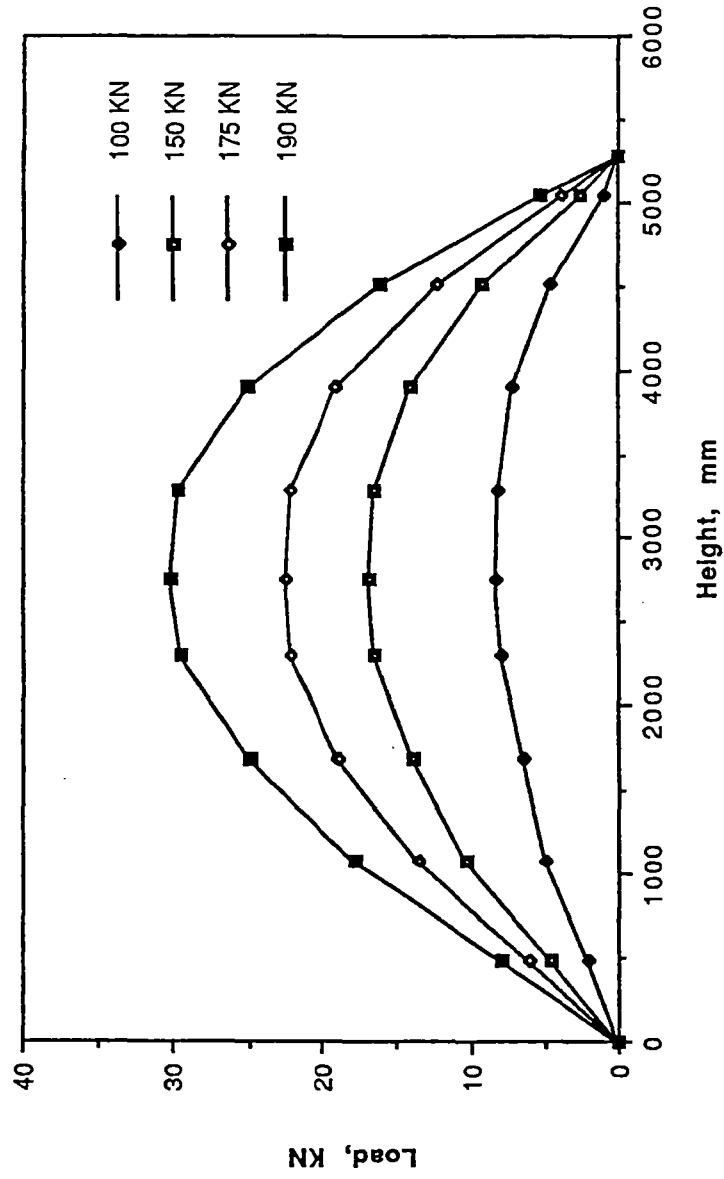


Figure 4.18 Deflected Shape of Reinforced Single Wall S5, $e=t/2.5$

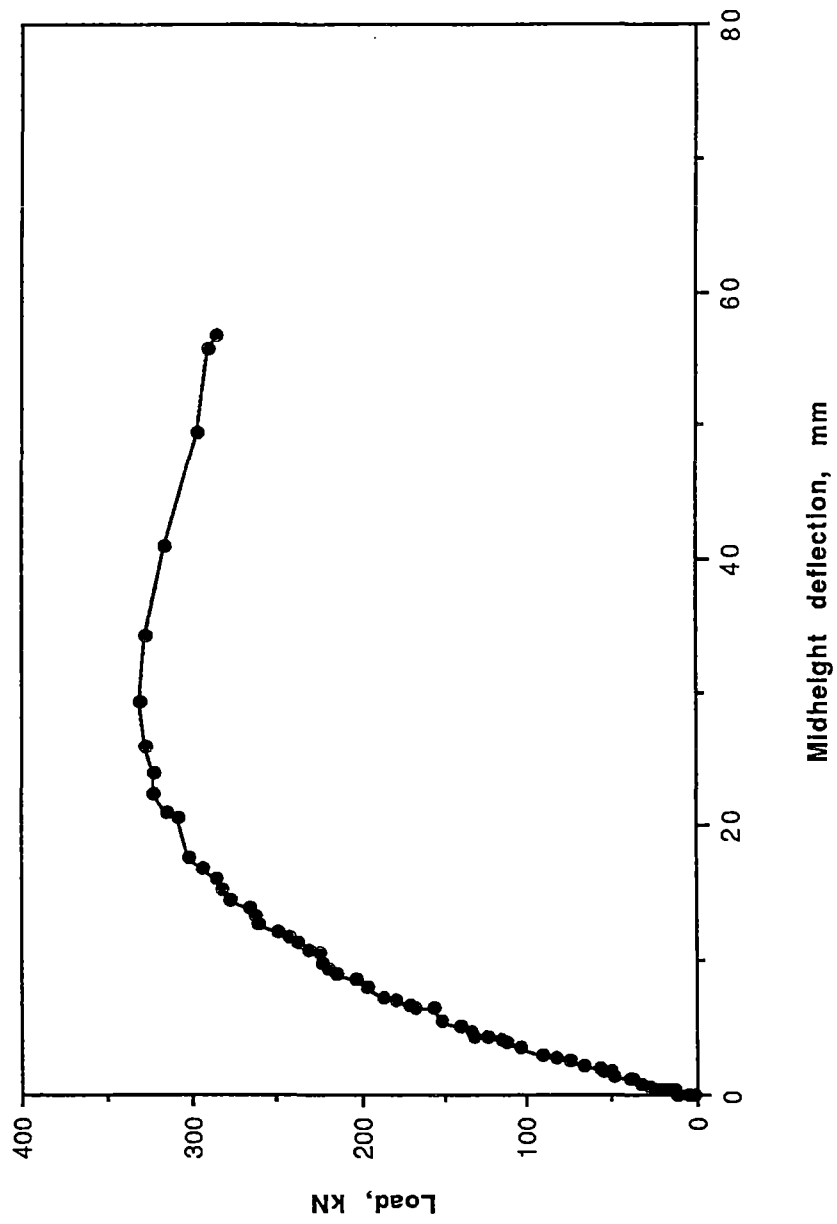


Figure 4.19 Cavity Wall C4, $e=t/3$, $c=100$ mm

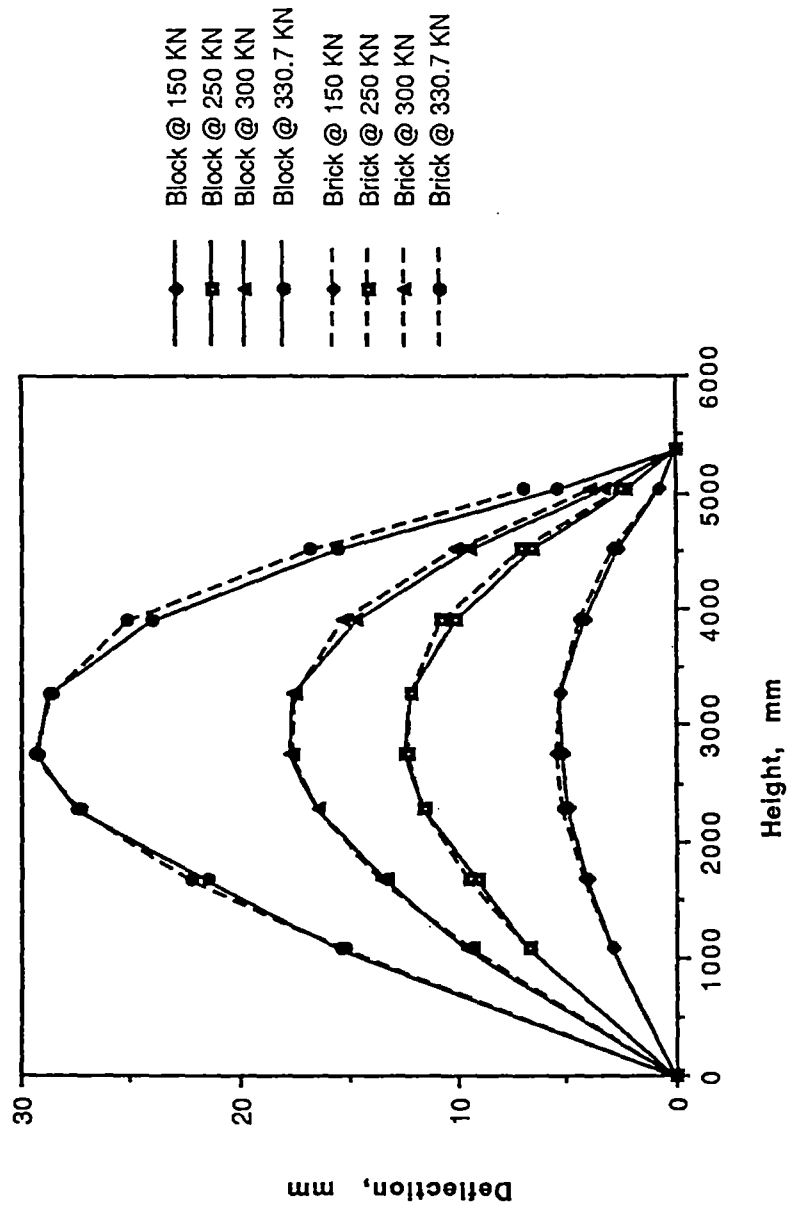


Figure 4.20 Deflected Shape of Cavity Wall C4, $e=t/3$, $c=100$ mm

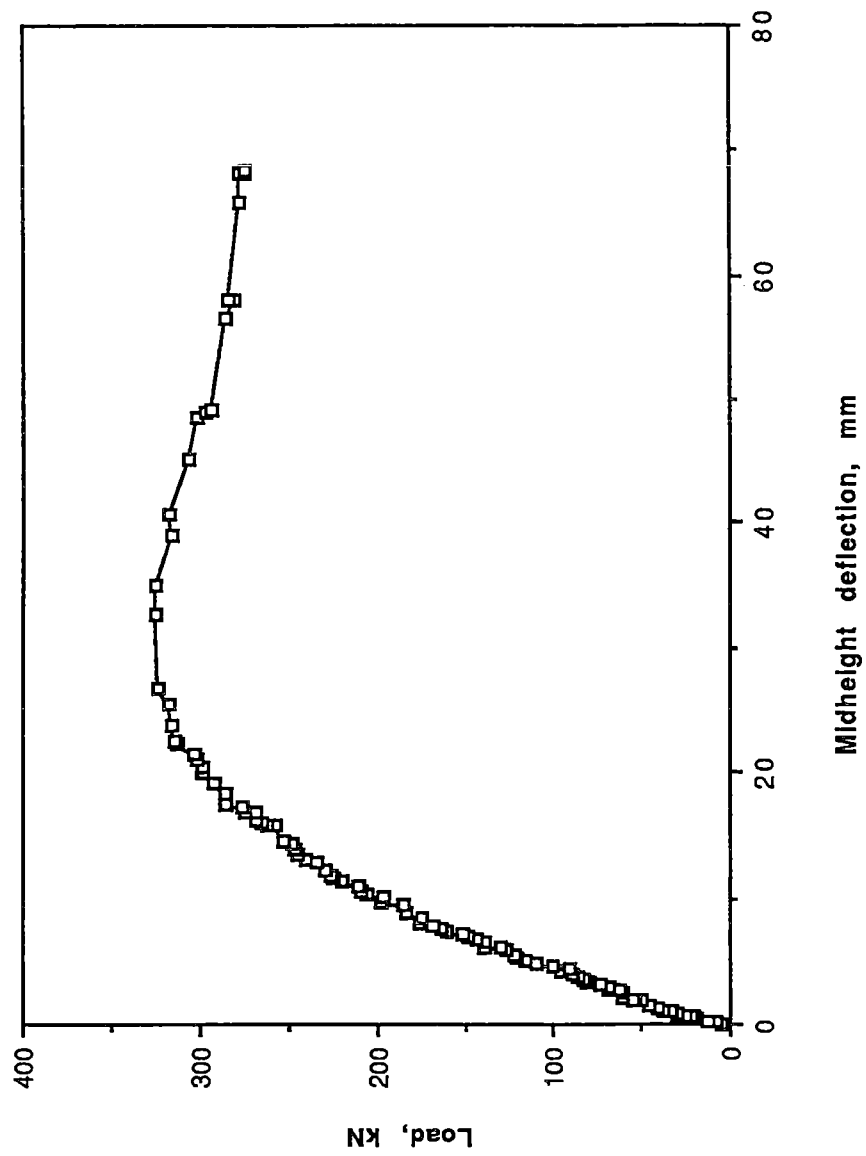


Figure 4.21 Cavity Wall C5, $e=t/3$, $c=75$ mm

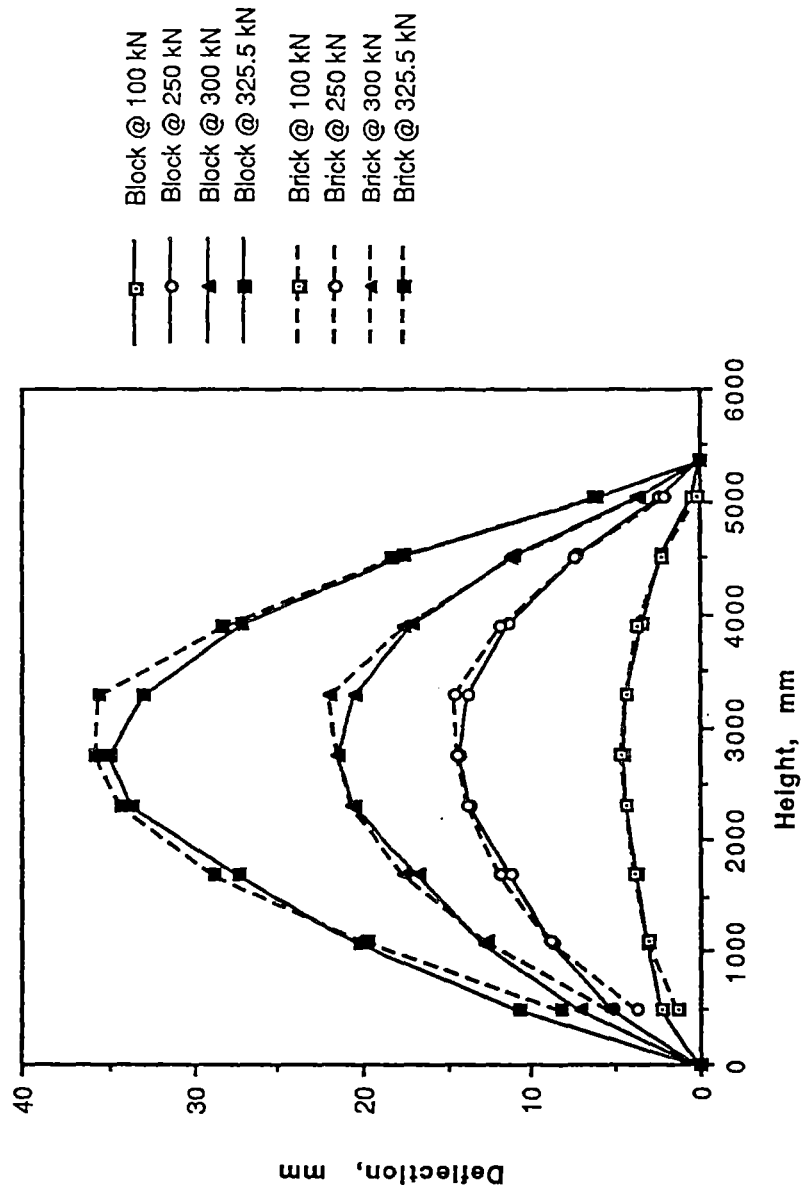


Figure 4.22 Deflected Shape of Cavity Wall C5, $e=t/3$, $c=75$ mm

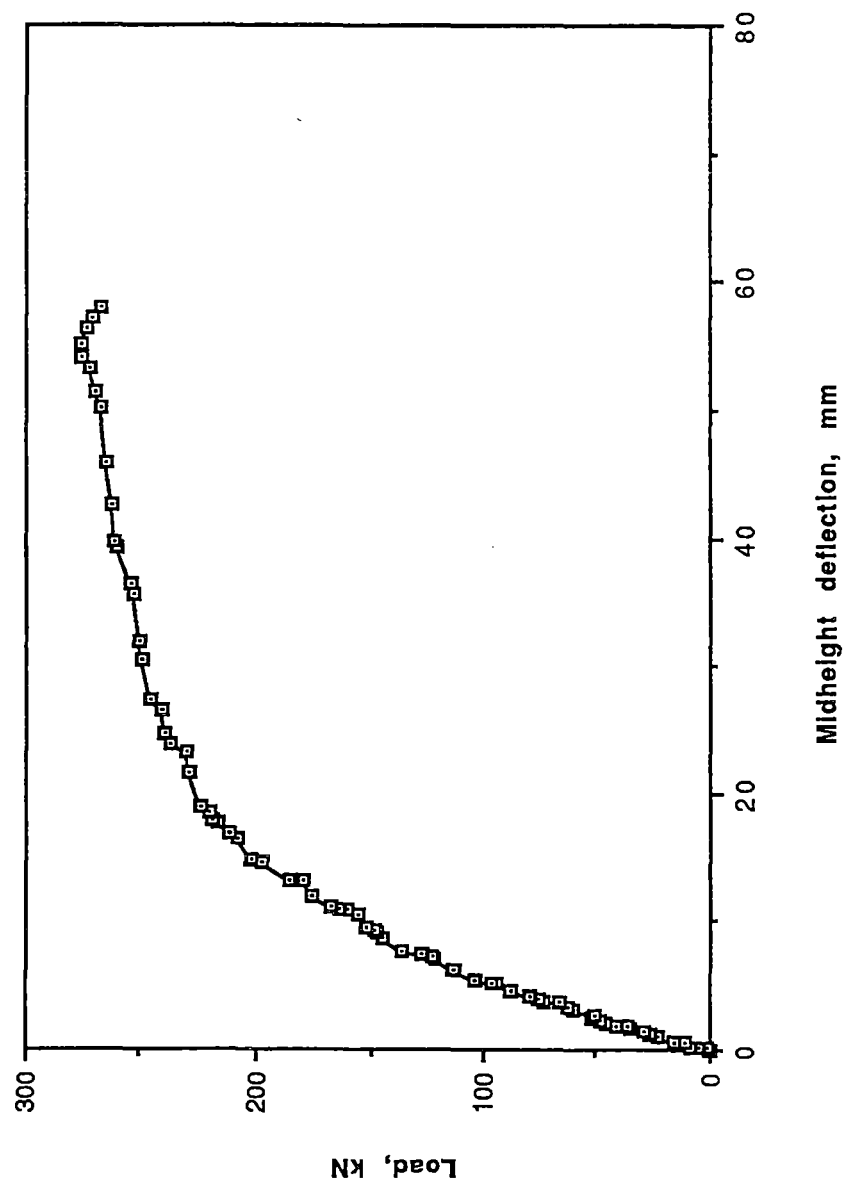


Figure 4.23 Cavity Wall C6, $e=t/2.5$

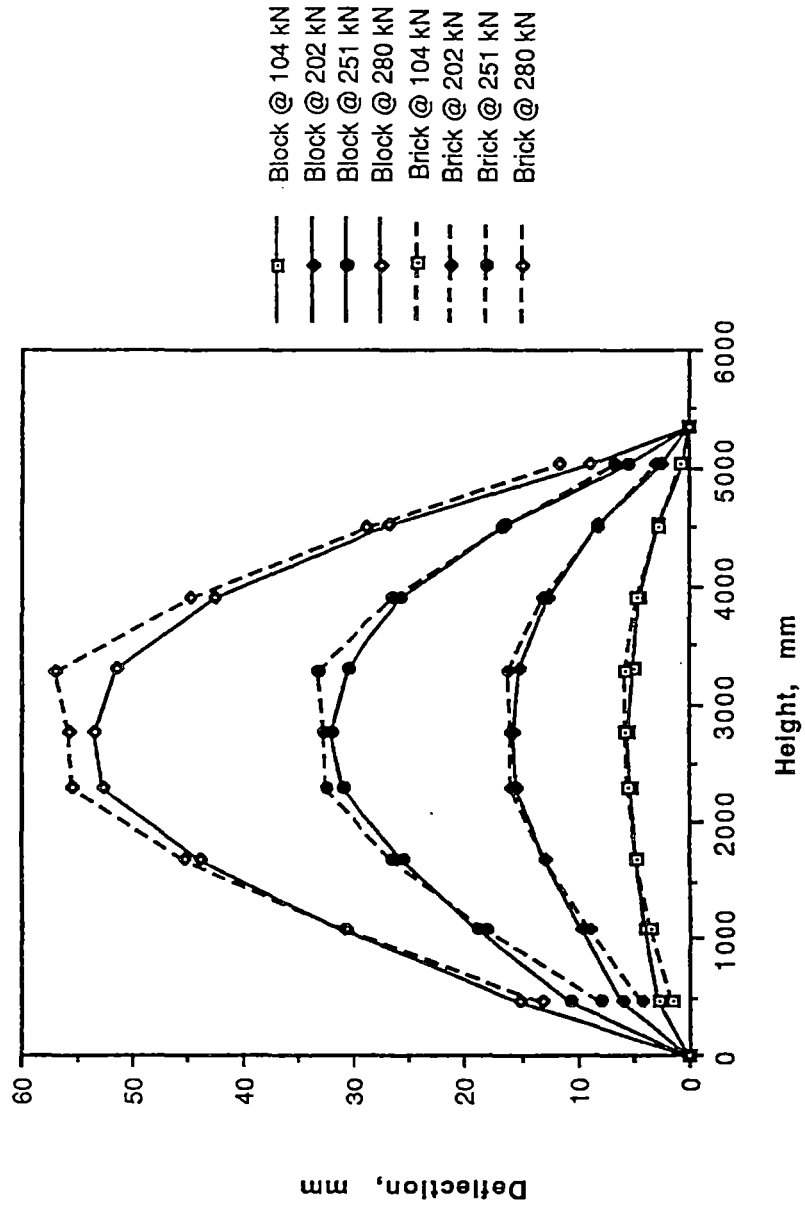


Figure 4.24 Deflected Shape of Cavity Wall C6, $e=t/2.5$



Plate 4.1 Typical Failure Pattern of Concrete Block Prism

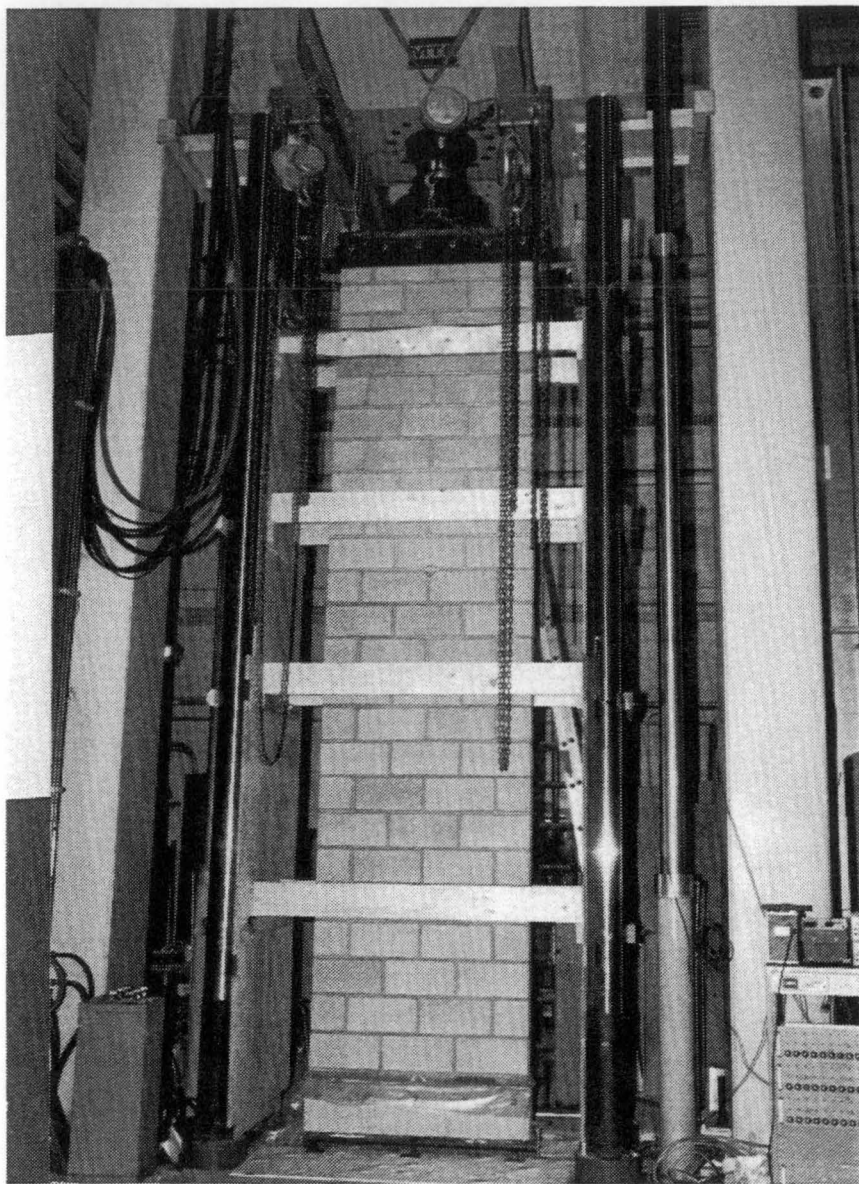


Plate 4.2 Wall S1 in the Testing Machine

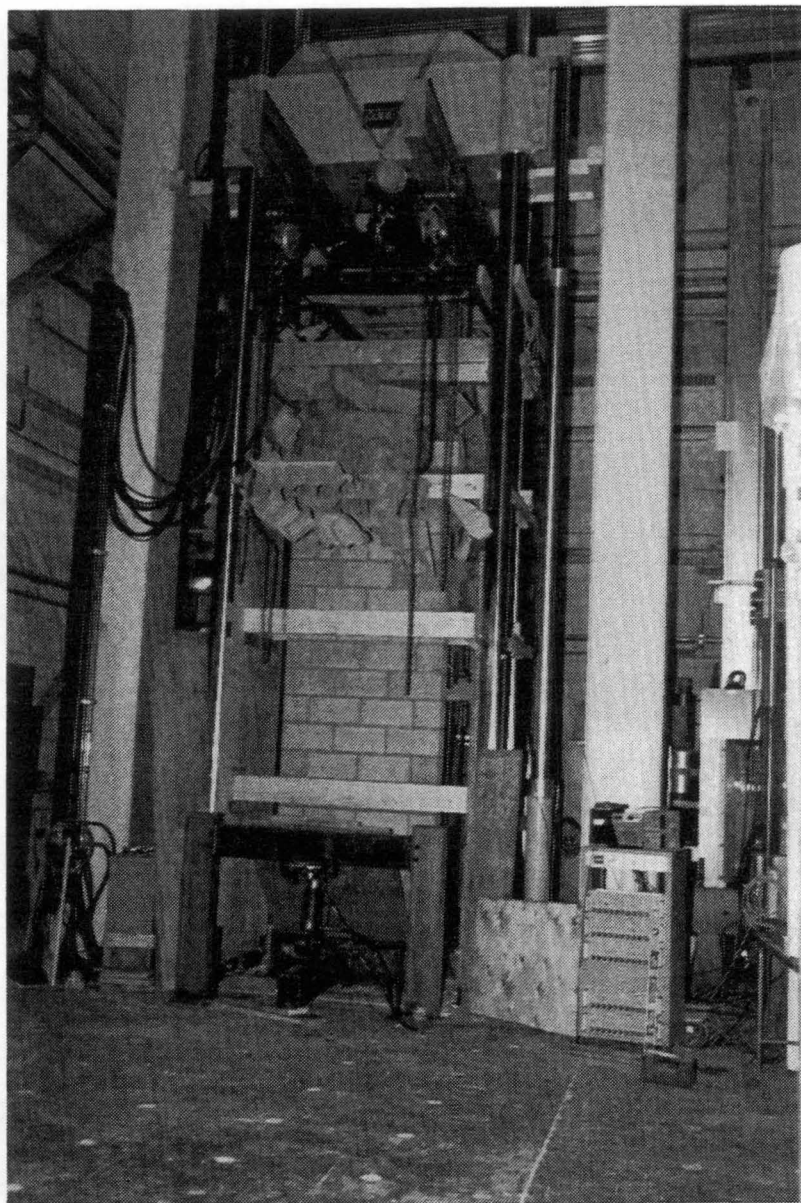


Plate 4.3 Wall S2 During Failure

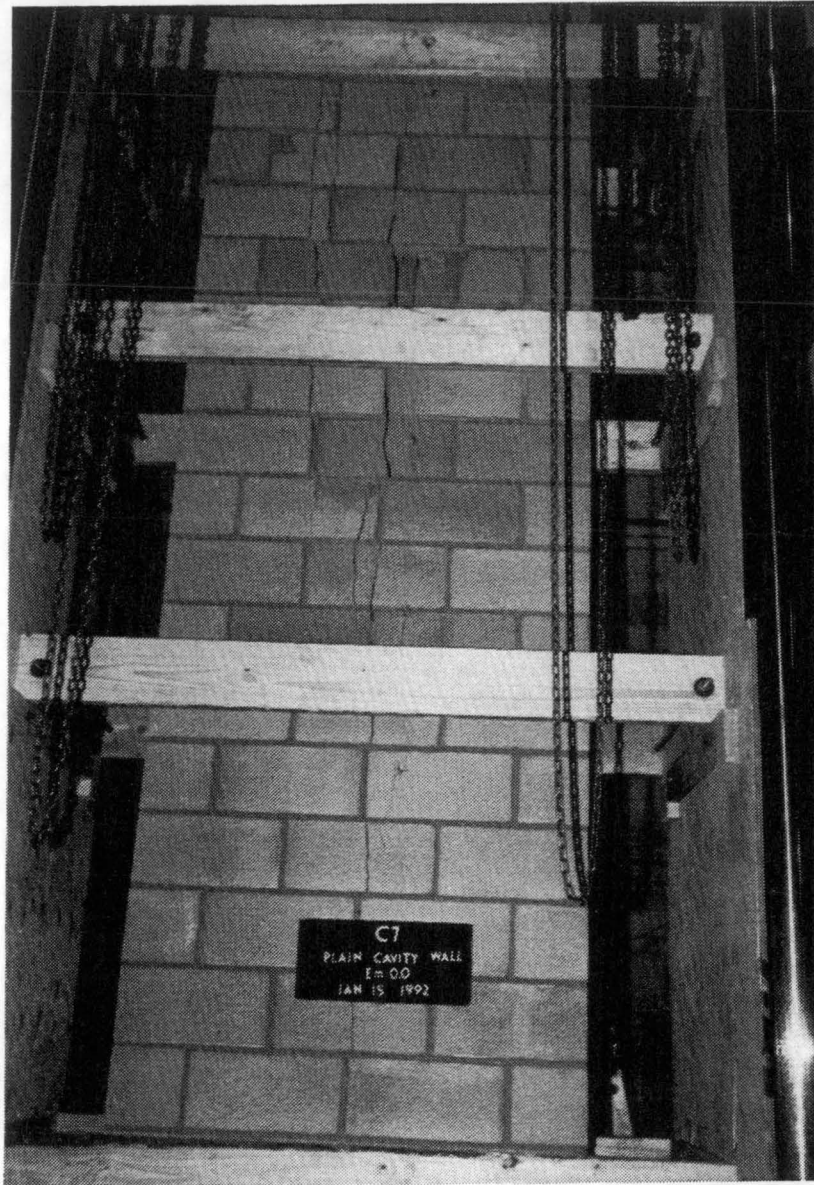


Plate 4.4 Wall C7 After Failure

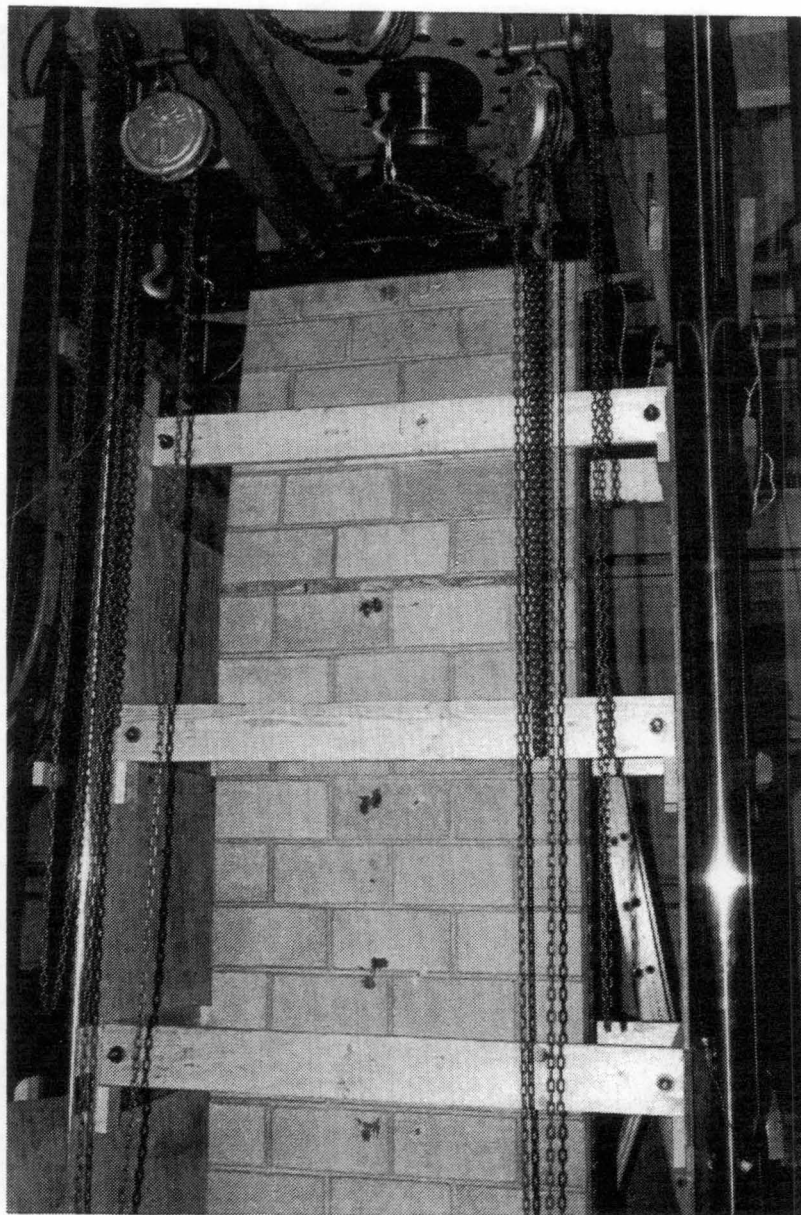


Plate 4.5 Wall C1 After Failure

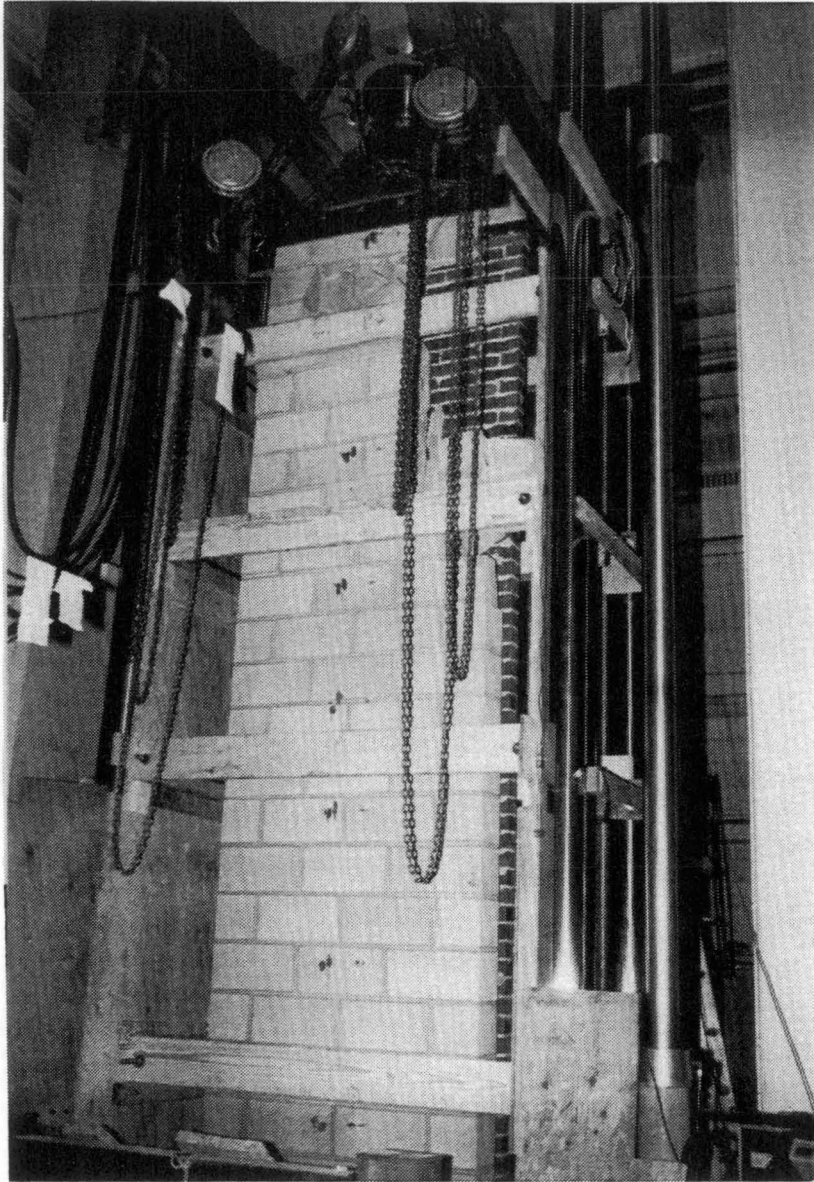


Plate 4.6 Wall C2 After Failure

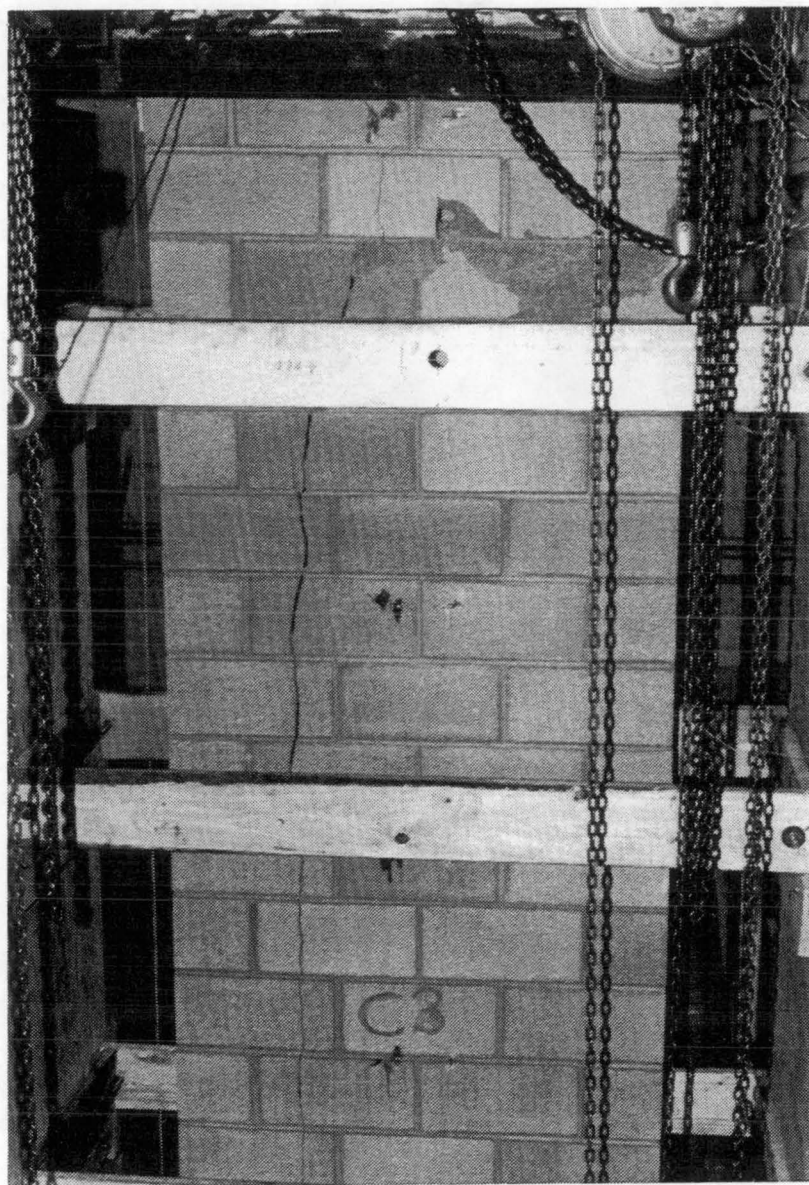


Plate 4.7 Wall C3 After Failure

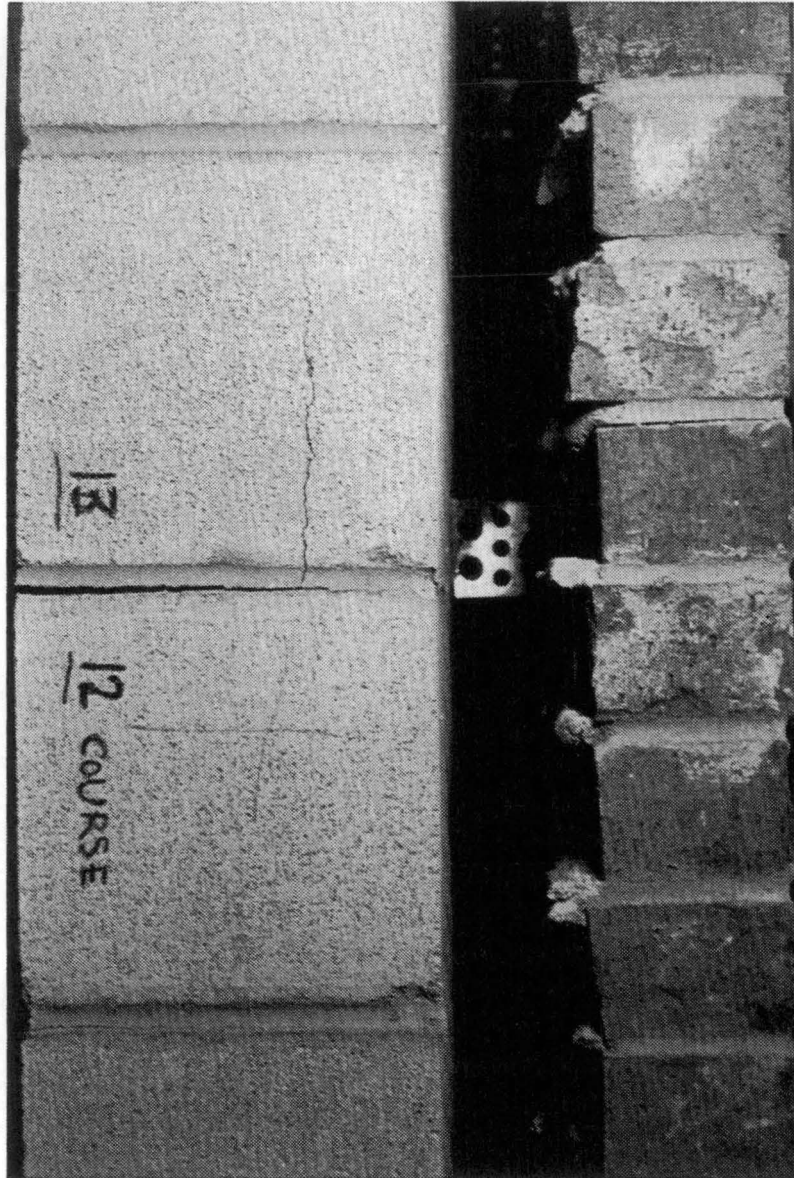


Plate 4.8 Crack in the Wall C5

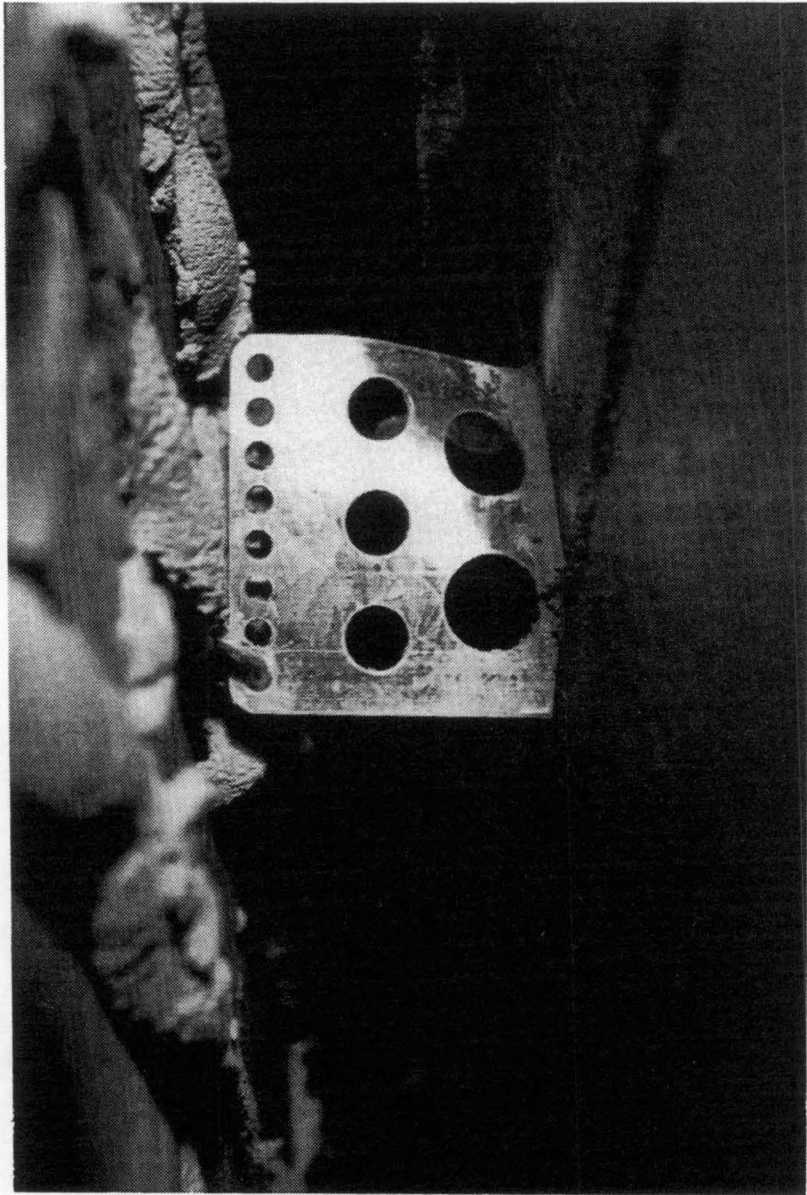


Plate 4.9 Topmost Connector in Wall C6

CHAPTER 5

DISCUSSION AND ANALYSIS OF TEST RESULTS

5.1 General Remarks

In this chapter, the experimental results of full scale walls are interpreted. The contribution of the veneer to the ability of the concrete block backup wythe to carry vertical load is examined. The flexural rigidity of the walls is evaluated from the experimental results and a comparison between single and cavity walls is made.

5.2 Discussion of Test Results

Fig. 5.1 and Fig. 5.2 illustrate the relationship between the rotation of the bottom end of the cavity walls and the load on the shelf angle. Here load on the shelf angle, is load in addition to the self weight of the brick veneer.

5.2.1 Behaviour of Axially Loaded Walls

The results obtained from specimens S1 and C7 (Fig 5.3), indicate that the cavity wall experienced a large deflection (24 mm), whereas the single wythe wall failed at a midheight deflection of

only 4 mm. The failure modes of both walls were similar, i.e. splitting of the webs. The large deflection of the cavity wall was caused by the influence of the veneer on the centre of rigidity of the assembly; i.e. cavity wall was in effect loaded eccentrically. At failure, the cavity wall was acted on by a vertical load of 793.1 kN and a moment of 18.8 kN-m [793.1×0.023] at midheight, while the single wythe wall was acted on by a vertical load of 845.5 kN and a moment of 3.5 kNm [845.5×0.00415]. This shows a considerable increase in moment capacity of the block wythe when a brick veneer is connected to it by shear connectors and subjected to axial load.

The failure mode of the loaded concrete block wythe was typical of that for masonry. At failure not one of the connectors was damaged. Because the wall deflected towards the brick veneer and the rigidity (EI) of the brick veneer is less than that of the block wythe, the connectors were most likely carrying a tensile load.

Fig 5.1 shows the relationship between the rotation of the bottom end of the wall and the load on the shelf angle. It indicates that a shear force was acting on the connectors. The same figure shows that, initially, the rotation is small and axial shortening of the block wall is such that it causes the connectors to transfer shear leading to a downward force on the shelf angle. Once the assembly deflects, the brick veneer shortens and the direction of the load on the shelf angle changes.

5.2.2 Influence of Direction of Eccentricity With Respect to Brick Veneer on the Ability of the Backup Wythe to Carry Vertical Load

The relation (based on eccentricity measured from the centroid of the block wythe) between the load and the midheight deflection of walls C2 and C3 is shown in Fig. 5.4.

The behaviour of both the walls was compared by taking into account the center of rigidity of the cavity wall. The center of rigidity was calculated using the flexural rigidity (EI) of the wythes and it was assumed that both the wythes are acting compositely. The modulus of elasticities of block and the brick masonry used in the calculation were 12075 MPa and 15000 MPa respectively and the moment of inertia of both the wythes was calculated using the gross section. The center of rigidity is located about 15 mm from the edge of block wythe (facing the cavity) away from the veneer. The wall when loaded with eccentricity of $t/6$ towards veneer (when measured from the center of the block wythe) deflected with the brick on the compression side. This was because initially the backup wythe behaved as an eccentricity loaded single wythe wall until the influence of brick veneer came into play. By the time the brick veneer influenced on the block wythe, the wall had already deflected enough towards the block wythe, which forced the wall to continue deflecting in the same direction.

Figures 5.1 and 5.5 show the rotation of the bottom end of the wall versus load on the shelf angle relationship and load on wall versus the rotation of the bottom end relationship respectively, for unreinforced cavity walls. In wall C2, with the rotation of the lower end of the wall, the load on the shelf angle is observed to increase. But in wall C3 the load on the shelf angle increases with rotation until about half of the ultimate load and later it becomes constant. From Fig 5.5 it is seen that the rotation increased with the increase in the load. In fact, in the case of wall C7 ($e=0.0$) the load on the shelf angle changes its direction from downwards to uplift with the rotation of the lower end of the wall. For wall C3 monitoring of load acting on the shelf angle didn't show the same cross over pattern (from downwards to upwards), it is speculated that initial imperfections reduced the effective eccentricity.

5.2.3 Influence of Cavity Width

Fig. 5.6 shows the load versus midheight deflection of specimens C4 and C5 and it shows- that the increase in cavity width from 75 mm to 100 mm increases the stiffness and decreases the deflection of the wall.

At failure wall C4 was acted upon by a load of 330.7 kN and a moment of 31.0 kNm $[330.7 \times (0.02921 + t/3)]$ at midheight, while wall C5 carried a load of 325.5 kN and a moment of 32.5 kNm $[325.5 \times (0.03499 + t/3)]$ at midheight. Wall C4 carried slightly more load and less moment than that of C5 and failed when the shear connector plates buckled. In wall C5 which had a cavity of 75 mm, failure occurred when the wue V-ties deformed. Furthermore, Fig. 5.6 indicates that the wall C4 had greater stiffness than wall C5.

It can be seen from Fig 5.2 and Fig 5.7 that the rotation of the bottom end of wall C4 ($c=100$ mm) was less than that of C5 ($c=75$ mm). That is with the increase in cavity width the deflection of the wall is reduced. From Fig. 5.7 it can be seen that at ultimate load, the load on the shelf angle was of the same order for both the walls, but the rotation of the bottom end of the wall C5 was more than that of C4. This is because the ultimate strength of the connectors was reached. Similar behaviour is seen for the wall C6 ($e=t/2.5$), in that wall also the V-ties were bent downwards.

5.2.4 Comparison Between Eccentrically Loaded Single And Cavity Wall ($c=75$ mm, Eccentricity Towards Brick Veneer).

5.2.4.1 Comparison Between Single Wall S2 And Cavity Walls C2, $e=t/6$.

Both single wythe and cavity walls failed in splitting of the webs. Fig. 5.8 illustrates the load versus mid-height deflection of both walls. At failure single wall S2 carried a load of 735.4 kN and a moment of 41.21 kNm $[735.4 \times (0.02438 + t/6)]$ at midheight, while cavity wall C2 carried a load of 798.0 kN and a moment of 60.0 kNm $[798.0 \times (0.04353 + t/6)]$ at midheight. It shows that when the block wythe is connected to the brick wythe by the shear connectors, the ultimate load carrying capacity and the stiffness of the block wythe are increased and the deflection is reduced.

It is seen from Fig 5.1 that with the rotation of the lower end of the wall, the load on the shelf angle increases. This shows that both the wythes were acting compositely and the shear connectors were subjected to shear stresses.

5.2.4.2 Comparison Between Single Wall S3 And Cavity Walls C1, $e=t/3$.

Both walls failed in cracking of horizontal mortar joint of the block wythe. Fig. 5.9 illustrates the load versus mid-height deflection for both walls. At failure single wall S3 was acted upon a load of 248.0 kN and a moment of 21.75 kNm $[248.0 \times (0.02438 + t/3)]$, while cavity wall C1 carried an ultimate load of 340 kN and a moment of 27.24 kNm $[340.0 \times (0.01681 + t/3)]$. This shows that by connecting the veneer to the block wythe, the eccentric load ($e=t/3$)

carrying capacity is increased by 37 % and the moment capacity is increased by 25 %. At a load of 205 kN and a midheight deflection of 10 mm, there is a sudden change in the slope of the single wall S3; at that load the midheight deflection of the cavity wall was 6.8 mm. This shows a 32% reduction in the deflection by using shear connected cavity walls.

From Fig 5.1 it is seen that with the increase in rotation of the bottom end of the wall, the load on the shelf angle increases. This shows the composite behaviour of the wythes.

5.2.4.3 Comparison Between Single Wall S4 And Cavity Walls C5, $e=t/3$.

Both walls failed in cracking of joints of the block wythe. Fig. 5.10 illustrates load versus midheight deflection of both walls. At failure single wall S4 was acted upon by a load of 225.8 kN and a moment of 22.69 kNm [$225.8 \times (0.03595 + t/3)$], while cavity wall C5 was acted upon by a load of 325.5 kN and a moment of 32.39 kNm [$325.5 \times (0.03498 + t/3)$]. This shows that there is 44 % increase in the ultimate load carrying capacity of the block wythe when a brick veneer is connected to it. From Fig 5.10 it can be seen that at the end of linear portion of the curve of single wall S4, at a load of 157 kN, the midheight deflection is of the order of 10.2 mm and at the same load the midheight deflection of the cavity wall is of the order

of 7.7 mm. This shows a considerable decrease in the deflection of the block wythe, when a brick veneer is connected to it by shear connectors.

From Fig 5.2 it is seen that with the increase in rotation of the bottom end of the wall, the load on the shelf angle increases. This shows the composite behaviour of the wythes.

5.2.4.4 Comparison Between Single Wall S5 And Cavity Walls C6, $e=t/2.5$.

Both walls failed by cracking of horizontal mortar joints in the block wythe. Fig. 5.11 shows the load versus midheight deflection relationship for both walls. At failure the single wall S5 carried a load of 197.1 kN and a moment of 23.39 kNm [$197.1 \times (0.04128 + t/2.5)$], while the cavity wall carried a load of 280.2 kN and a moment of 36.71 kNm. The ultimate load carrying capacity of the cavity wall was approximately 42 % higher than that of the single wythe wall. The deflection of the cavity wall is much less than that of the single wall.

From Fig 5.2 it can be seen that with the increase in rotation of the bottom end of the wall, the load on the shelf angle increases. This shows the composite behaviour of the wythes.

5.3 Flexural Rigidity of Walls

Slenderness effects on masonry walls, are at present accounted for by reduction factors in which axial capacity is reduced by factors dependent on the wall slenderness and eccentricity of load. Recently, the Moment Magnifier method¹⁴ in which approximate effective rigidity is assumed has become popular. The Moment Magnifier method is applied to the experimental results and the effective flexural rigidity of the walls is calculated.

For walls with both ends hinged and subjected to equal end eccentricity under single curvature bending, the maximum moment occurs at mid-height. The moment along the wall is magnified [$M=P(e+\Delta)$] with the deflection of the wall. The magnified moment is estimated using the- well known relation :

$$M_m = \frac{P e}{1 - \frac{P}{P_E}} \quad (1)$$

$$\text{Where } P_E = \pi^2 EI / l^2 \quad (2)$$

is the Euler buckling load.

P= vertical load

e= eccentricity of the load.

The apparent rigidity at a certain deflected shape can be obtained by substituting relation 2 into 1 and solving for EI.

$$EI = \frac{Pl^2(e+\Delta)}{\pi^2 \Delta} \quad (3)$$

Using Eq. 3, the apparent flexural rigidity (EI) is calculated for a number of load levels for the wall tested. The results are plotted in figures 5.12, 5.13, 5.14 and 5.15.

Fig. 5.12 shows the EI versus load relationship for unreinforced walls S2, C2 and C3. It is observed that the flexural rigidity (EI) of the cavity walls C2 and C3 is considerably greater than that of the single wall S2. For certain portion of the loading, the flexural rigidity of cavity wall C2 is little bit more than that of the wall C3, this is because here the flexural rigidity (EI) is calculated without taking into account the centre of rigidity of the assembly.

Fig. 5.13 shows the EI versus load relationship for unreinforced walls S1 and C3. A significant increase in the flexural rigidity of the wall is observed. It is also observed that for both the walls the flexural rigidity is constant for approximately 80% of the load carrying capacity.

Fig. 5.14 shows the EI versus load relationship for reinforced walls S4, C4, C5 (subjected to $e=t/3$). Cavity walls C4, C5 have higher EI values as compared to that for single wall S4. The flexural rigidity of wall C4 is greater than that of wall C5. This shows that the

flexural rigidity of the wall with 100 mm cavity is more than that of the wall with a cavity of 75 mm.

Fig. 5.15 shows the EI versus load relationship for reinforced walls C6 and S5 (subjected to $e=t/2.5$). It is seen that the flexural rigidity of the cavity wall C6 is almost twice that of the single wall S5. When comparing Figs. 5.14 and 5.15, it is noticed that the contribution of veneer towards the flexural rigidity increases with the increase in the eccentricity of load. For all walls tested the flexural rigidity (EI) is almost constant to 3/4th of their load carrying capacity.

The stiffness of a wall is a function of the elastic modulus (E_m) of the material in the wall, and the effective moment of inertia (I_{eff}) of the cross-section of the wall. An increase in either of these two variables will increase the stiffness of the wall. CSA Standard S304-M84¹ recommends that E_m , be assumed equal to $1000 f'_m$. It is known that the value of I_{eff} is a fraction of the uncracked moment of inertia, I_o . Due to tension cracking the moment of inertia also varies along the height of the wall. An equivalent moment of inertia for the whole wall is required to estimate the stiffness of the wall.

Hatzinikolas (1978) developed an equation for the equivalent stiffness of an unreinforced or reinforced wall to be used for design calculations. The equation is

$$I_{eff} = 2 \left(\frac{1}{2} - \frac{e}{t} \right) I_o \quad (4)$$

This equation yields a straight line plot of I_{eff} versus e/t with intercepts at $I_{eff}=I_o$ (where $e/t=1/2$). For small values of e/t this relation was found to give satisfactory results for I_{eff} , while for larger values of e/t the equation greatly underestimated I_{eff} when compared to experimental results.

Eq. 4 was modified to include the influence of shear connected brick veneer on the backup wythe. The following empirical relation is proposed for the calculation of effective rigidity of cavity walls.

$$(EI)_{eff} = E \left\{ \frac{1}{2} - \frac{e}{t} + \left(\frac{e}{t} \right)^2 \right\} \alpha \beta \quad (5)$$

where $\alpha = 9/5 I_o$ for unreinforced backup wythe.

$= 2/3 (I_o + 2 I_{cr})$ for reinforced backup wythe.

$$\beta = \left\{ 1 + \frac{e}{t} + \gamma \left(\frac{I_c - 2.3 I}{I} \right) \right\}$$

Here I_o is the uncracked moment of inertia of the block wythe and I_{cr} is the moment of inertia of the cracked section. I_e is the moment of inertia of the cavity wall with respect to the axis passing through the centroid of the block wythe and I is the moment of inertia of the cavity wall with zero cavity, about the same axis. The

coefficient of connectivity γ , depends on the shear connector arrangement and it is taken as 1.0 for the present arrangement.

The EI values obtained from the experimental results corresponding to one third of the ultimate load were compared with the EI values calculated using the proposed relation. The comparison is presented in Table 5.1. It is seen that for all the walls the theoretical EI value is less than the experimental EI value. More experimental data is required to test the validity of proposed equation.

Table 5.1 Comparison of Experimental and Theoretical EI values

Wall No.	Eccentricity, Cavity (mm)	1/3 (Ult. load) kN	Experimental EI x 10 ¹² (N-mm ²)	Theoretical EI x 10 ¹² (N-mm ²)
C1(unreinforced)	t/3, c=75	113	62	52
C2(unreinforced)	t/6 towards veneer, c=75	266	6.6	59
C3(unreinforced)	t/6 away from veneer, c=75	248	62	59
C4(reinforced)	t/3, c=100	110	59	59
C5(reinforced)	t/3, c=75	108	45	4.1
C6(reinforced)	t/2.5, c=75	93	4.6	4.0

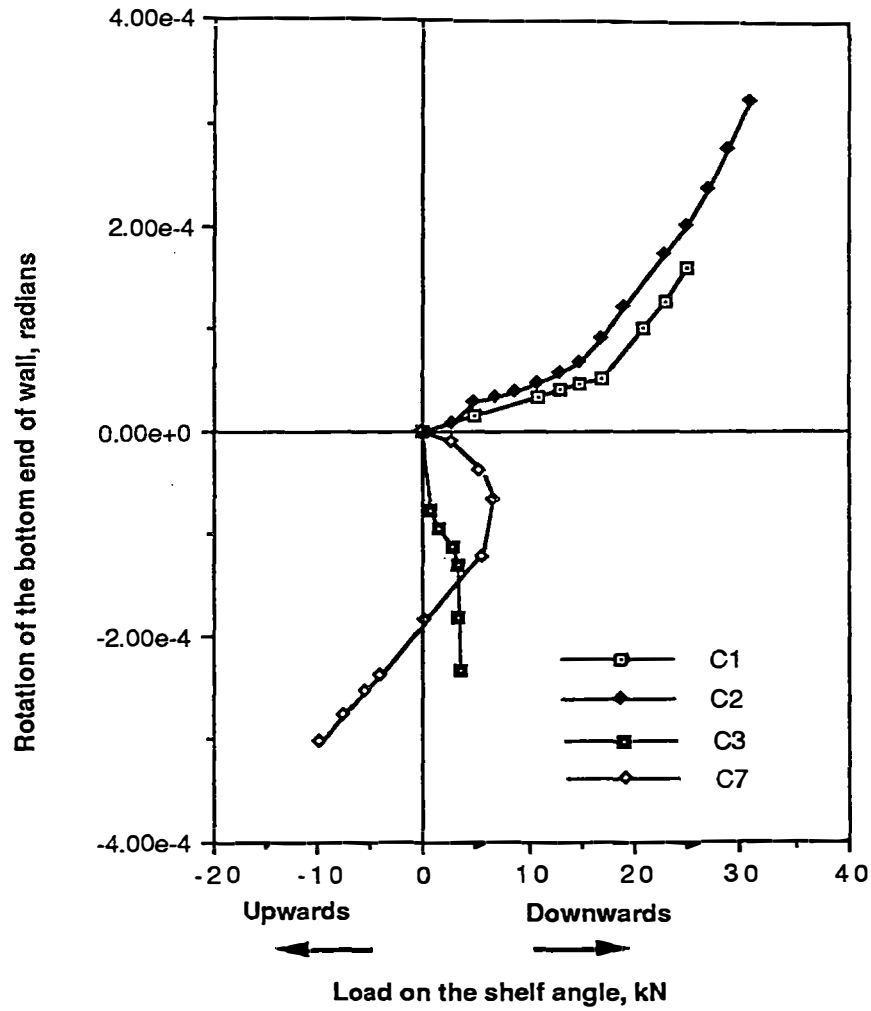


Figure 5.1 Rotation Versus Load on Shelf Angle Unreinforced Cavity Walls

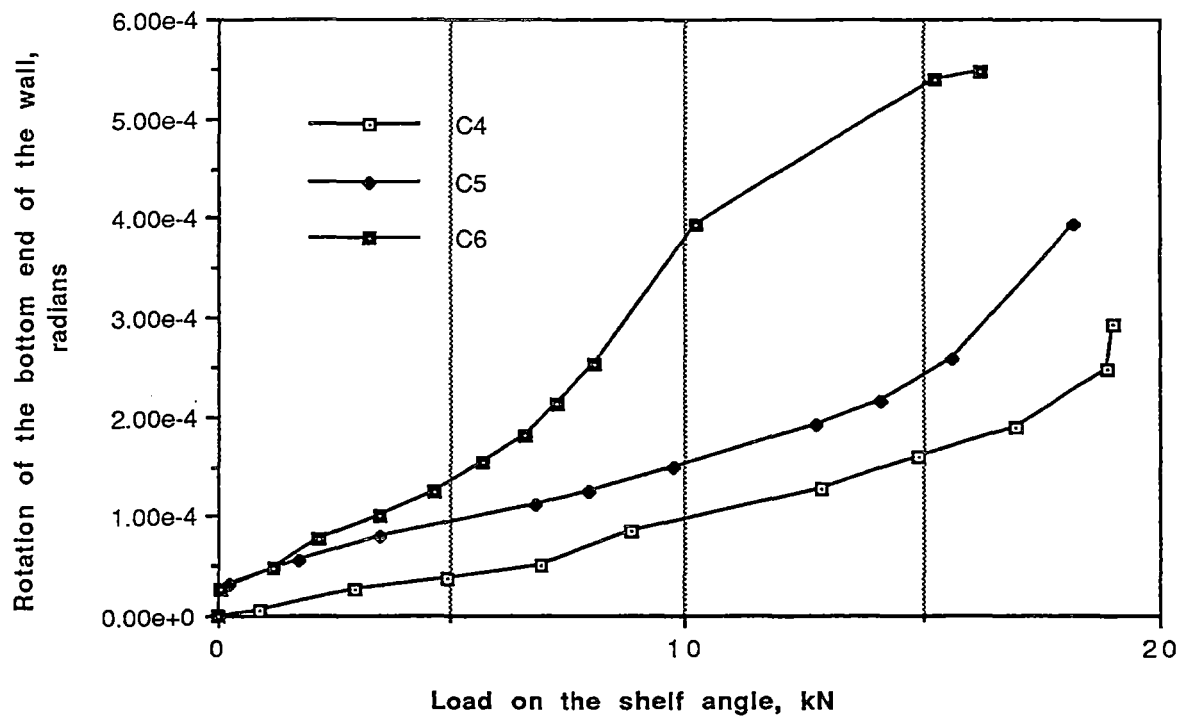


Figure 5.2 Rotation Versus Load on Shelf Angle for Reinforced Cavity Walls

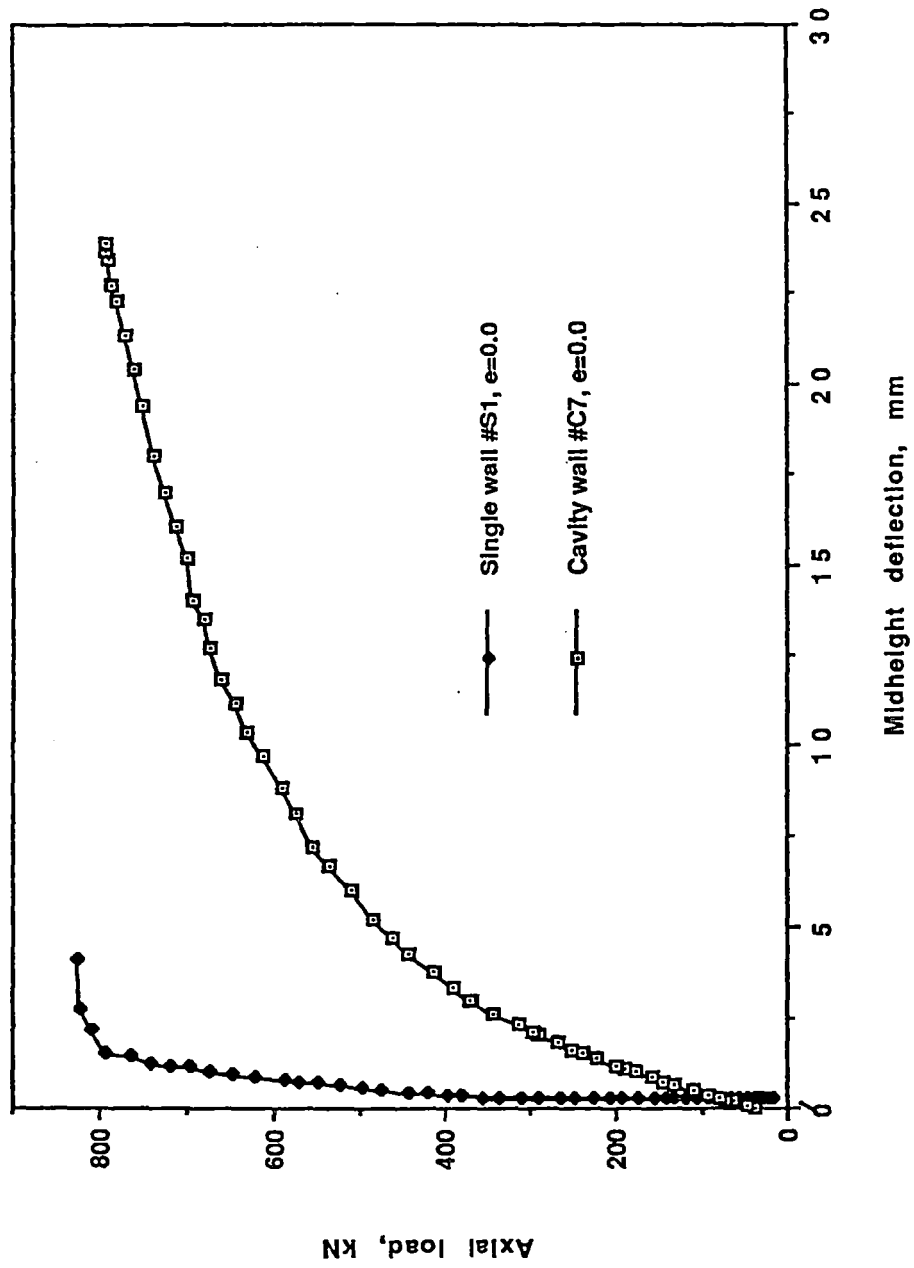


Figure 5.3 Single Wall S1 and Cavity Wall C7

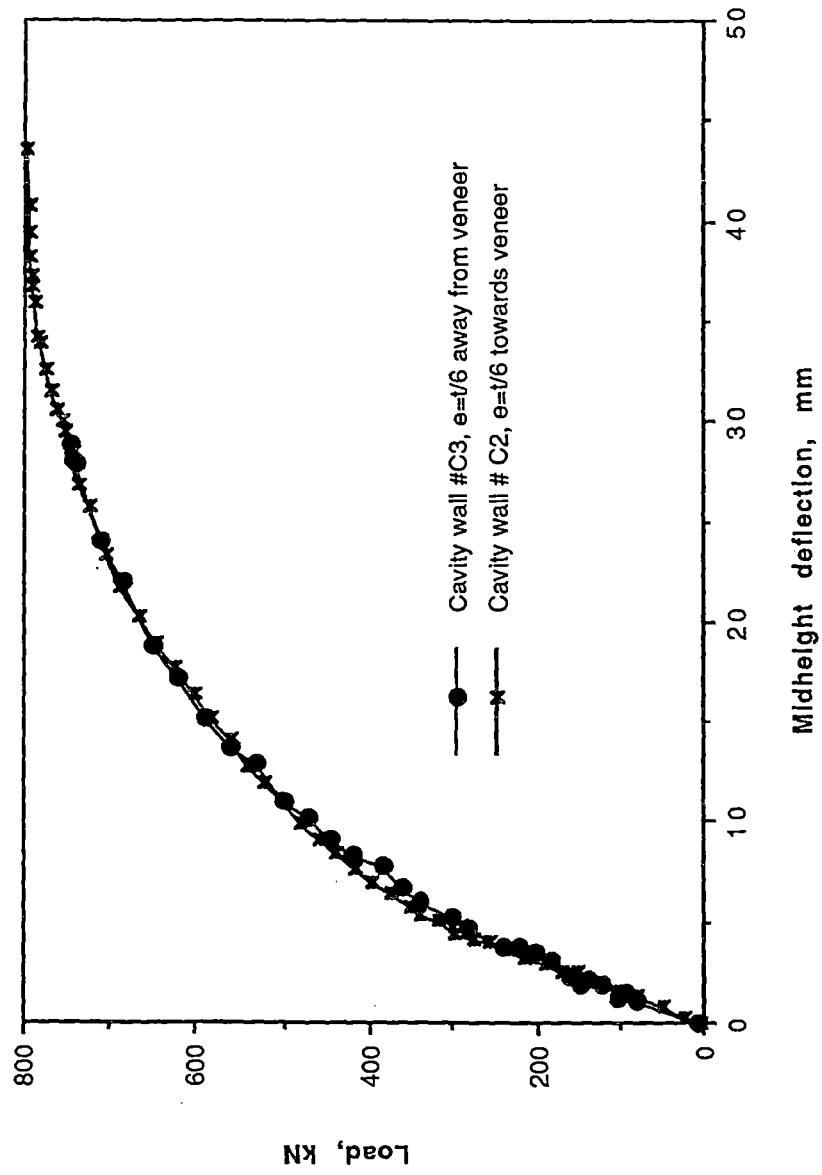


Figure 5.4 Cavity Walls C2 and C3

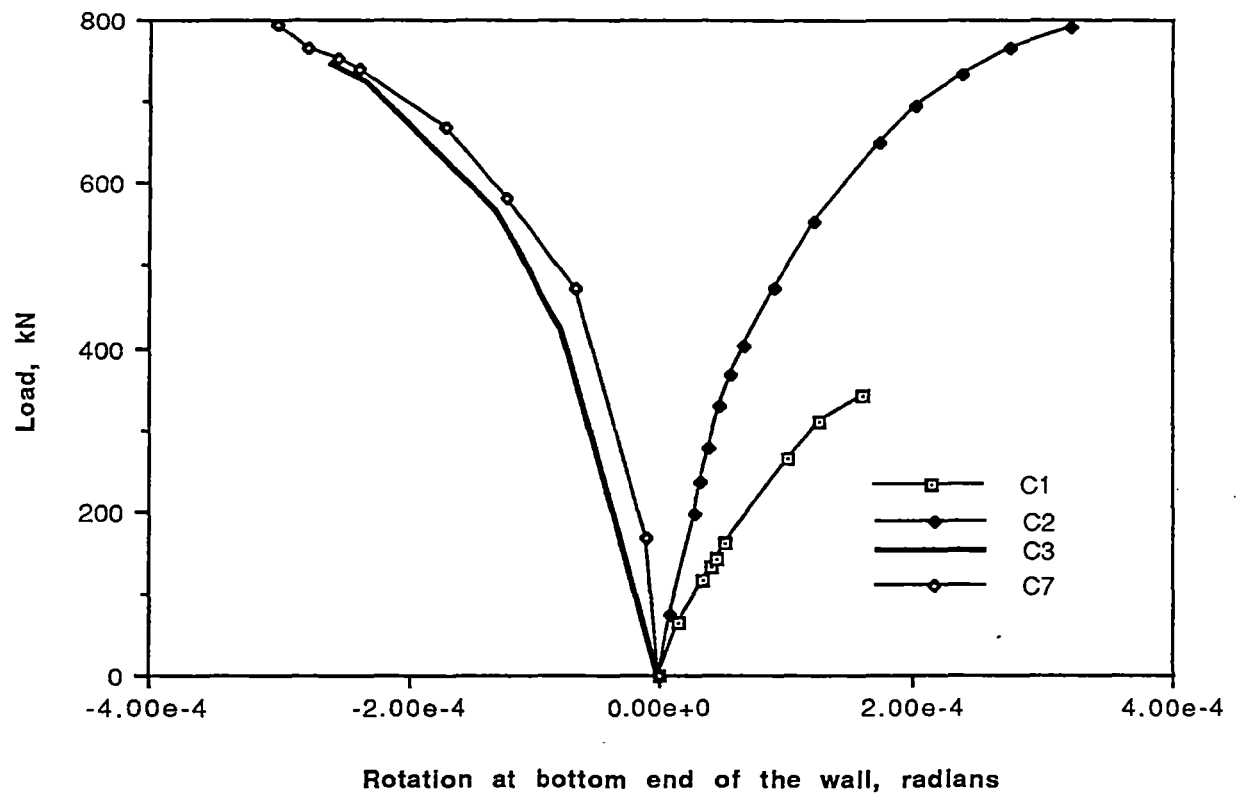


Figure 5.5 Load Versus Rotation for Unreinforced Cavity Walls

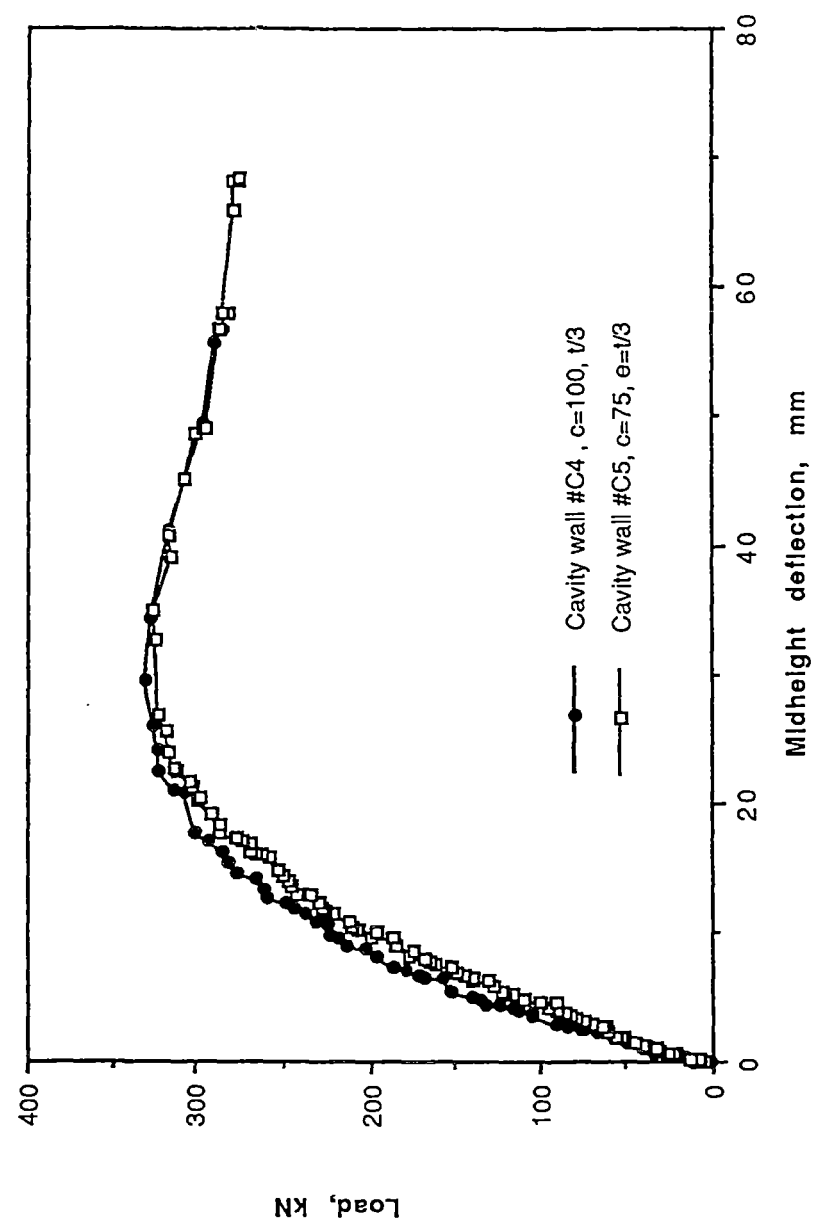


Figure 5.6 Cavity Walls C4 and C5

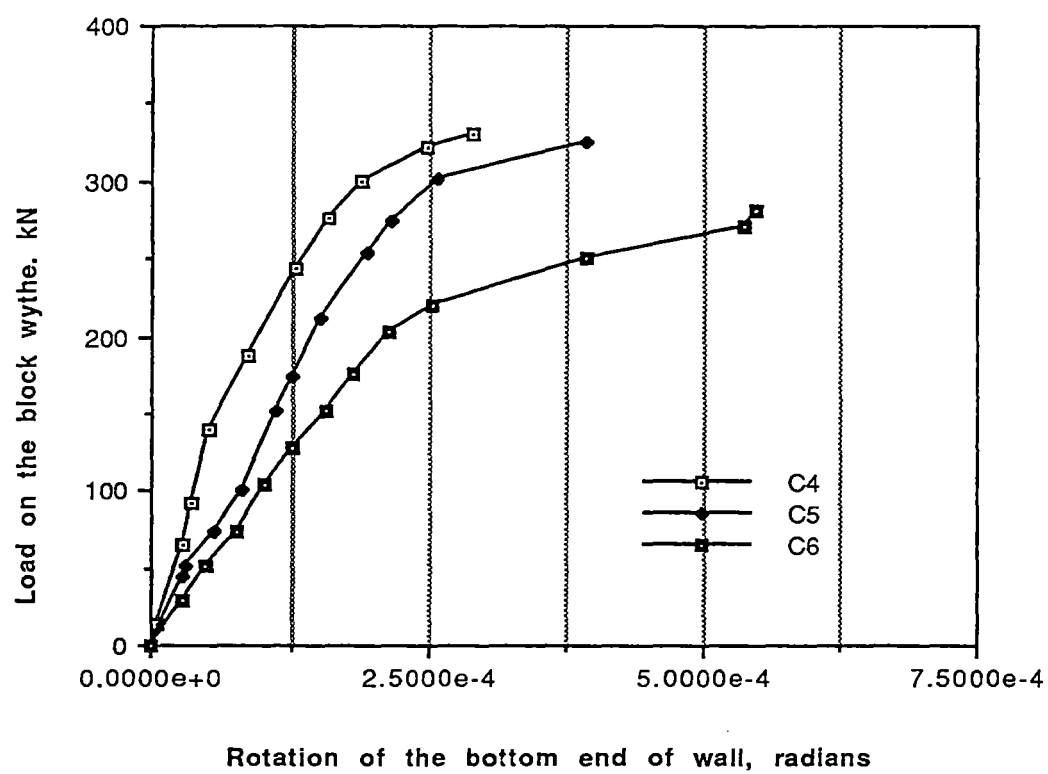


Figure 5.7 Load Versus Rotation for Reinforced Cavity Walls

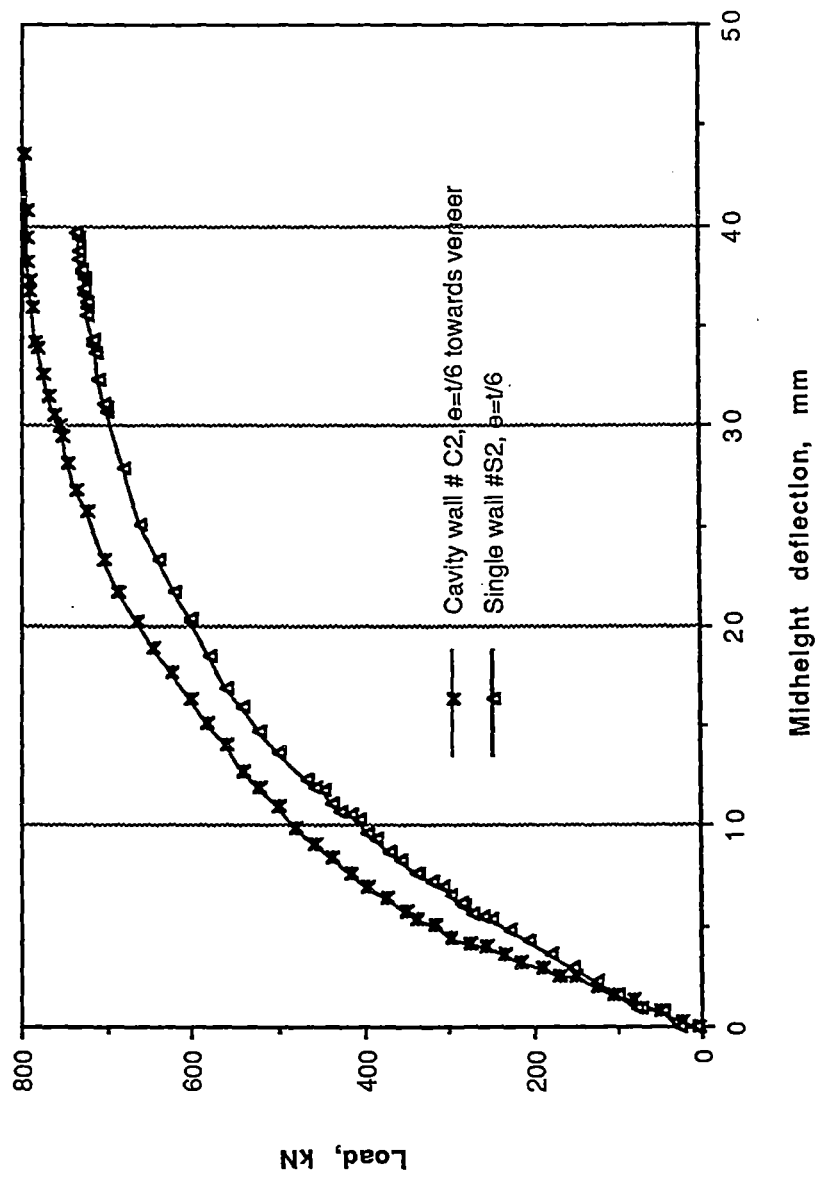


Figure 5.8 Single Wall S2 and Cavity Wall C2

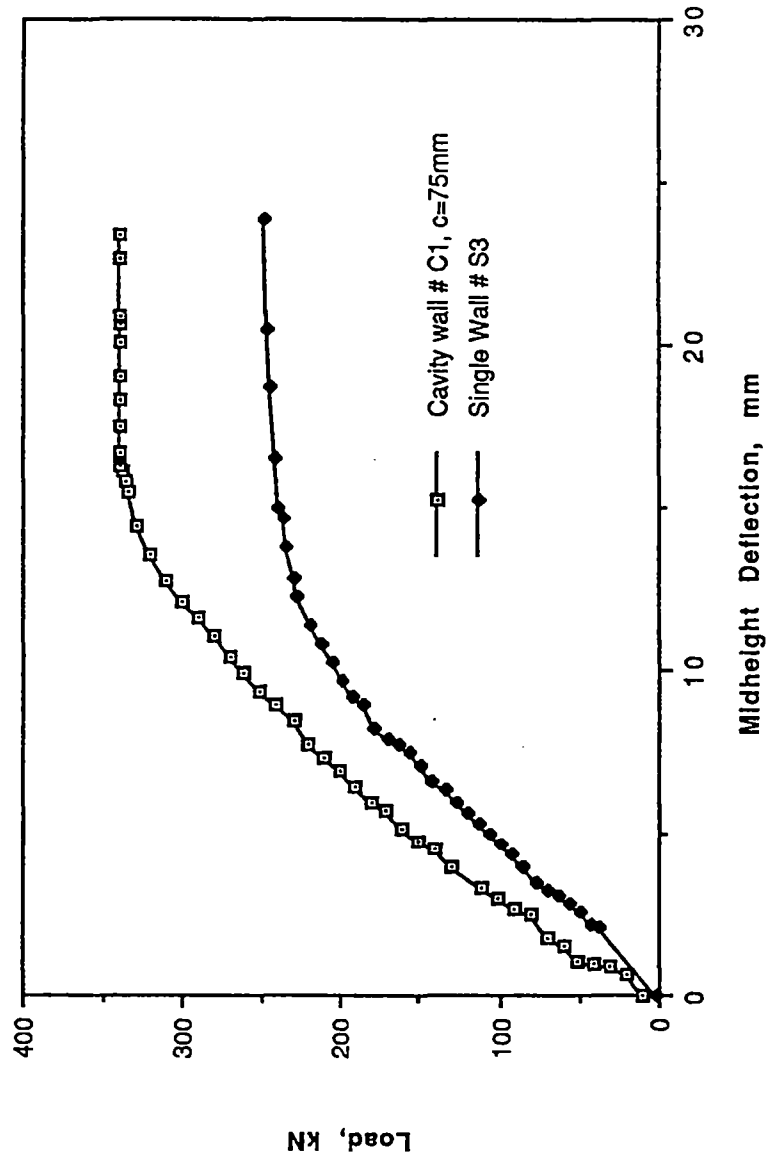


Figure 5.9 Single Wall S3 and Cavity Wall C1

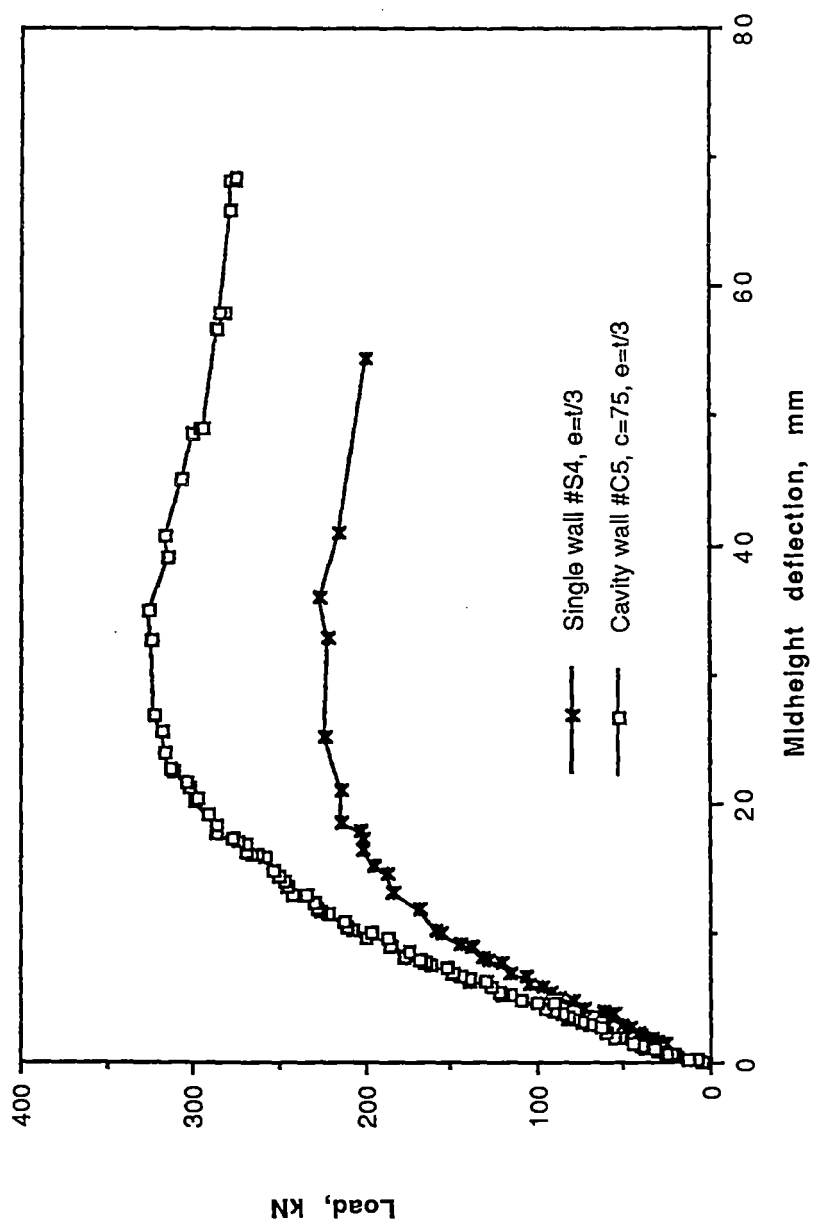


Figure 5.10 Single Wall S4 and Cavity Wall C5

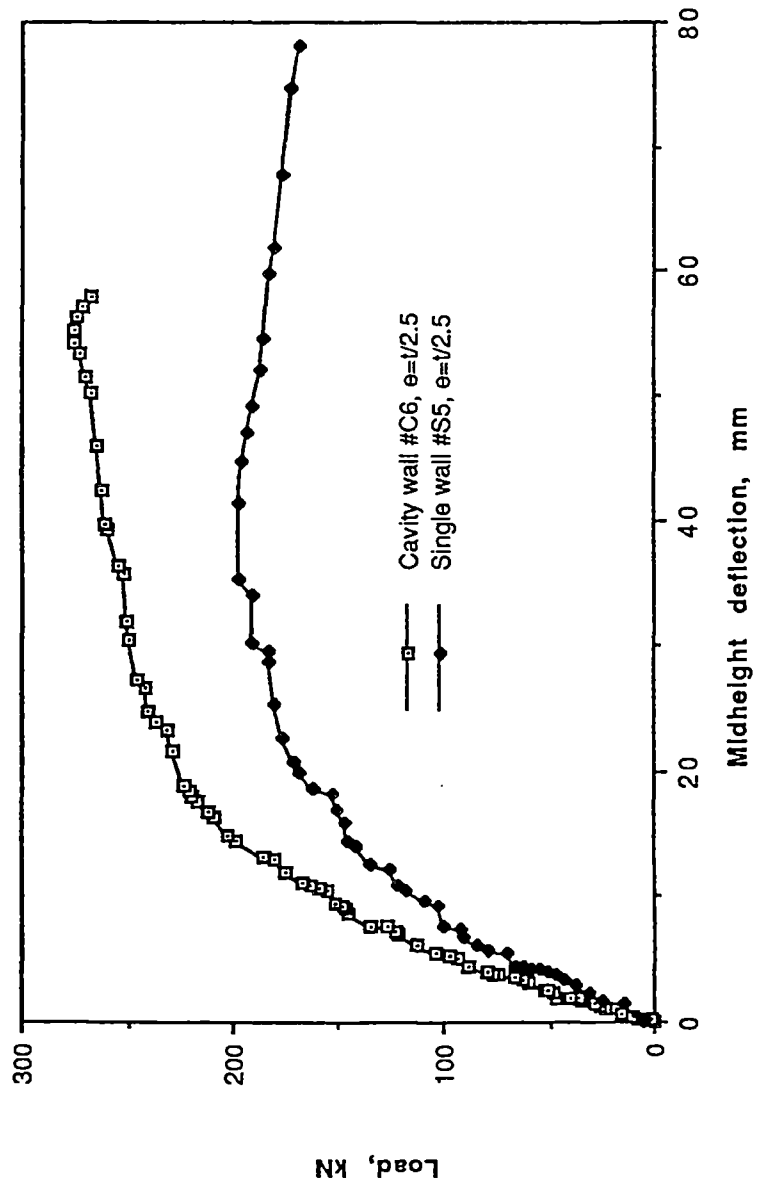


Figure 5.1.1 Single Wall S5 and Cavity Wall C6

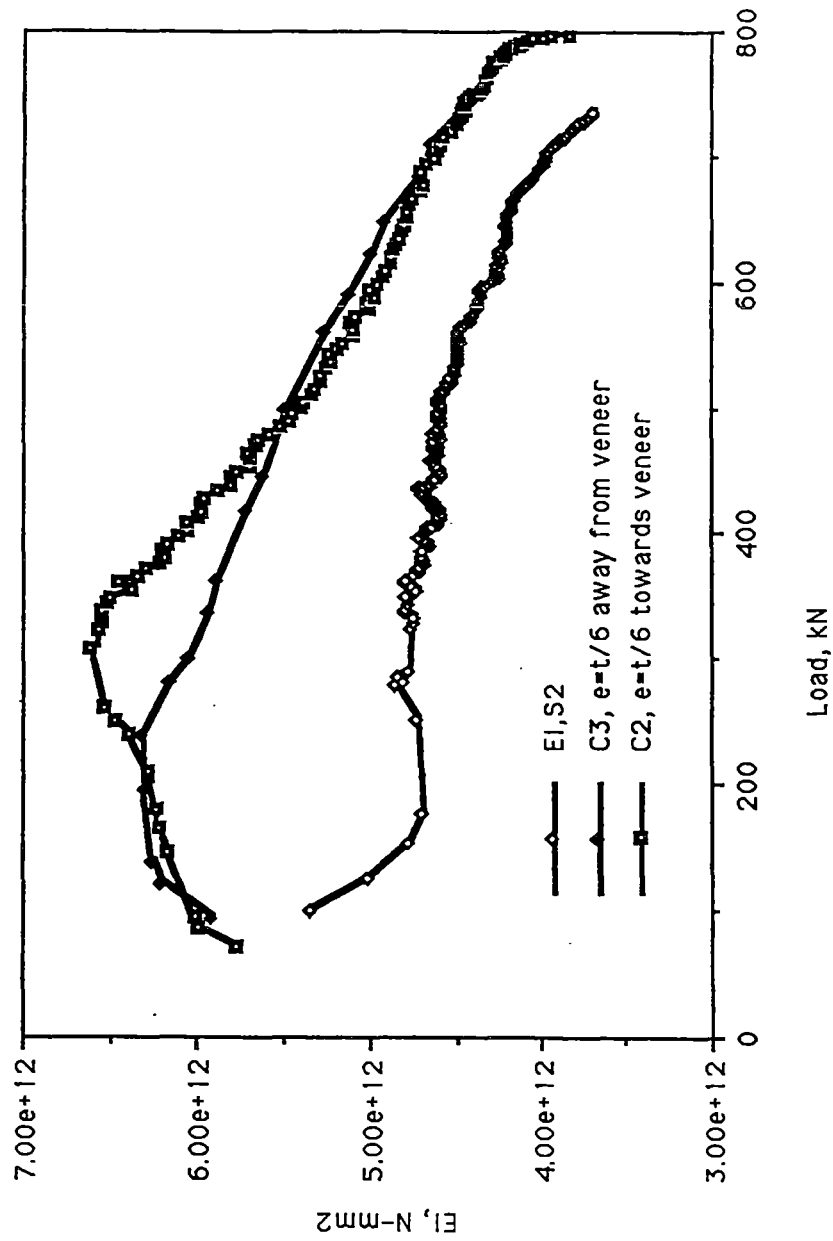


Figure 5.12 Flexural Rigidity of Unreinforced Walls S2, C2, C3

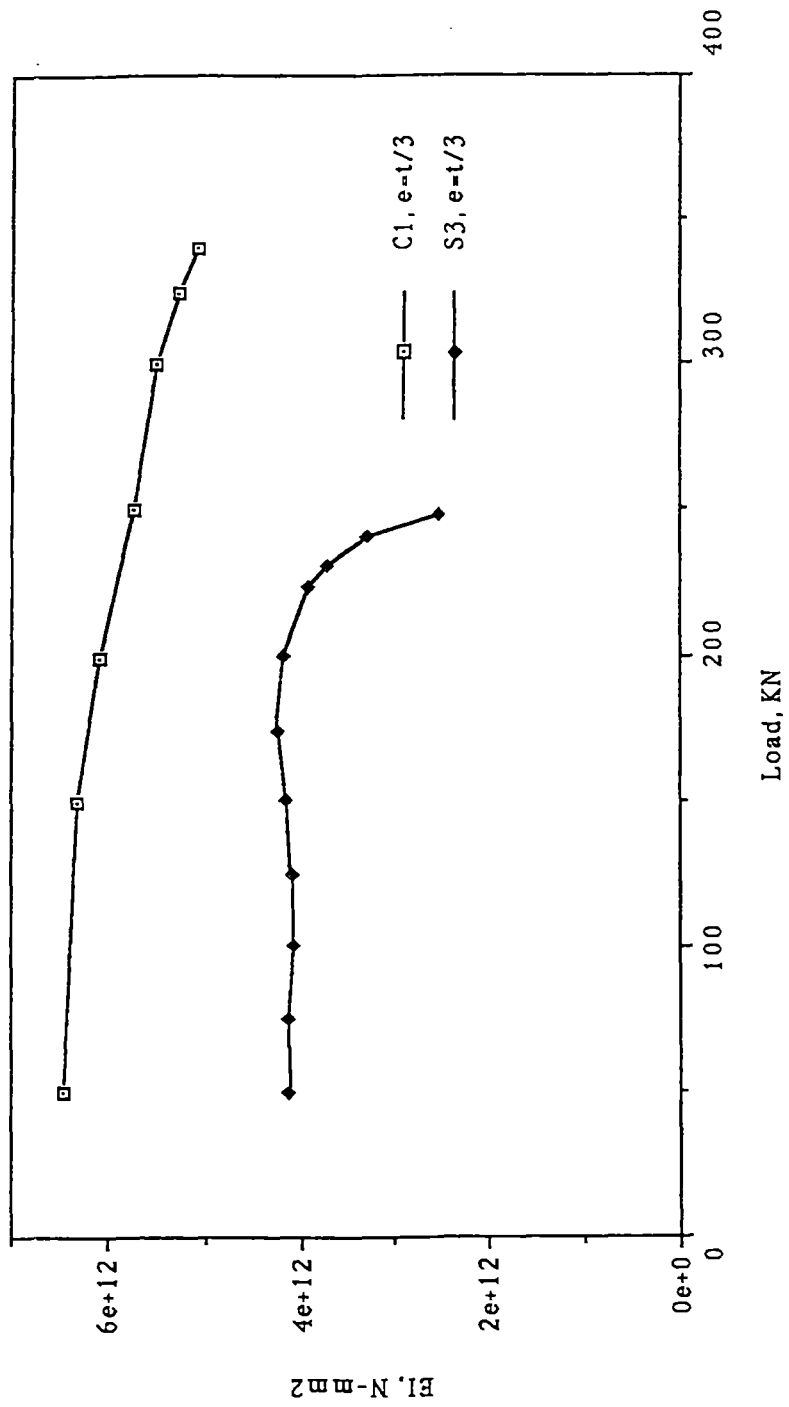


Figure 5.13 Flexural Rigidity of Unreinforced Walls S1 and C3

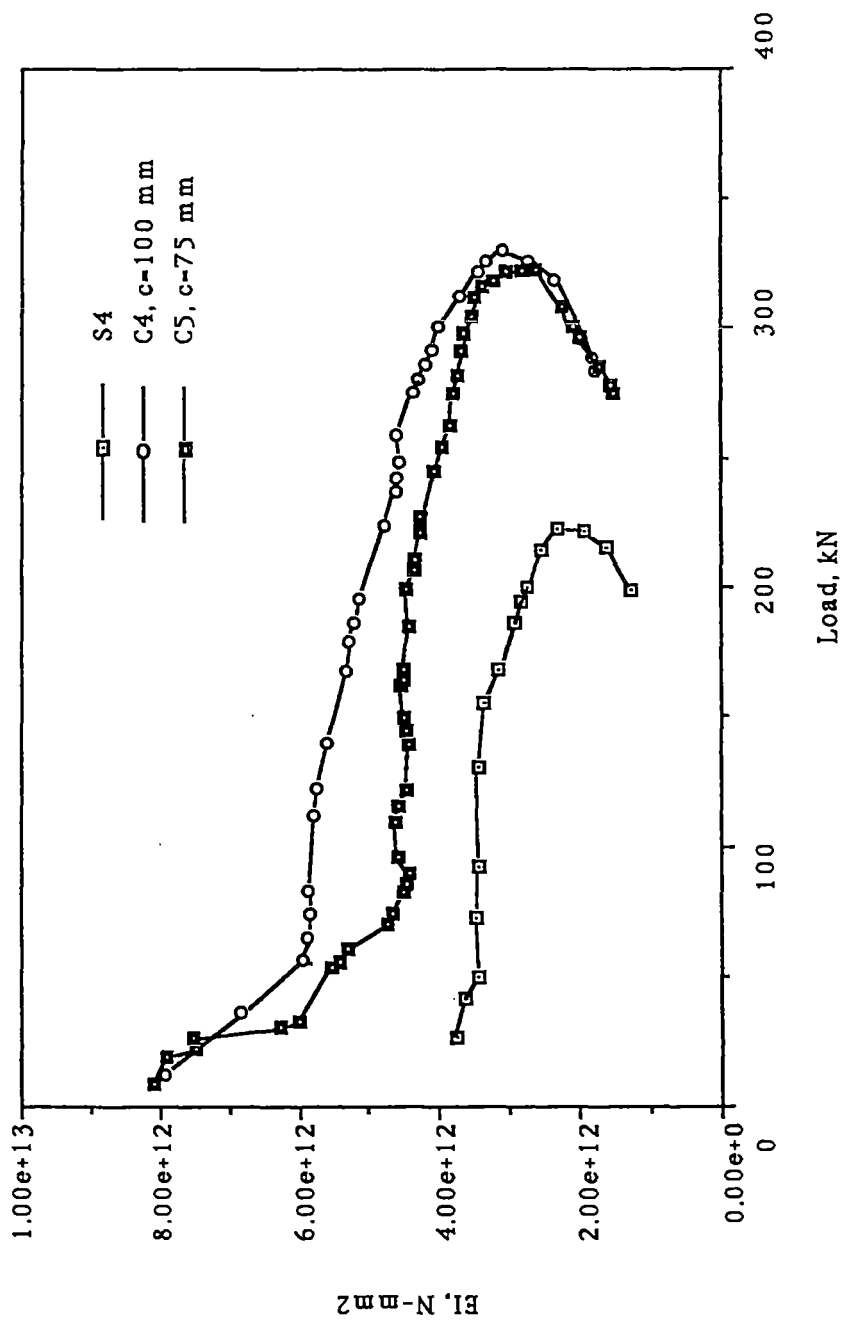


Figure 5.14 Flexural Rigidity of Reinforced Walls S4, C4, C5

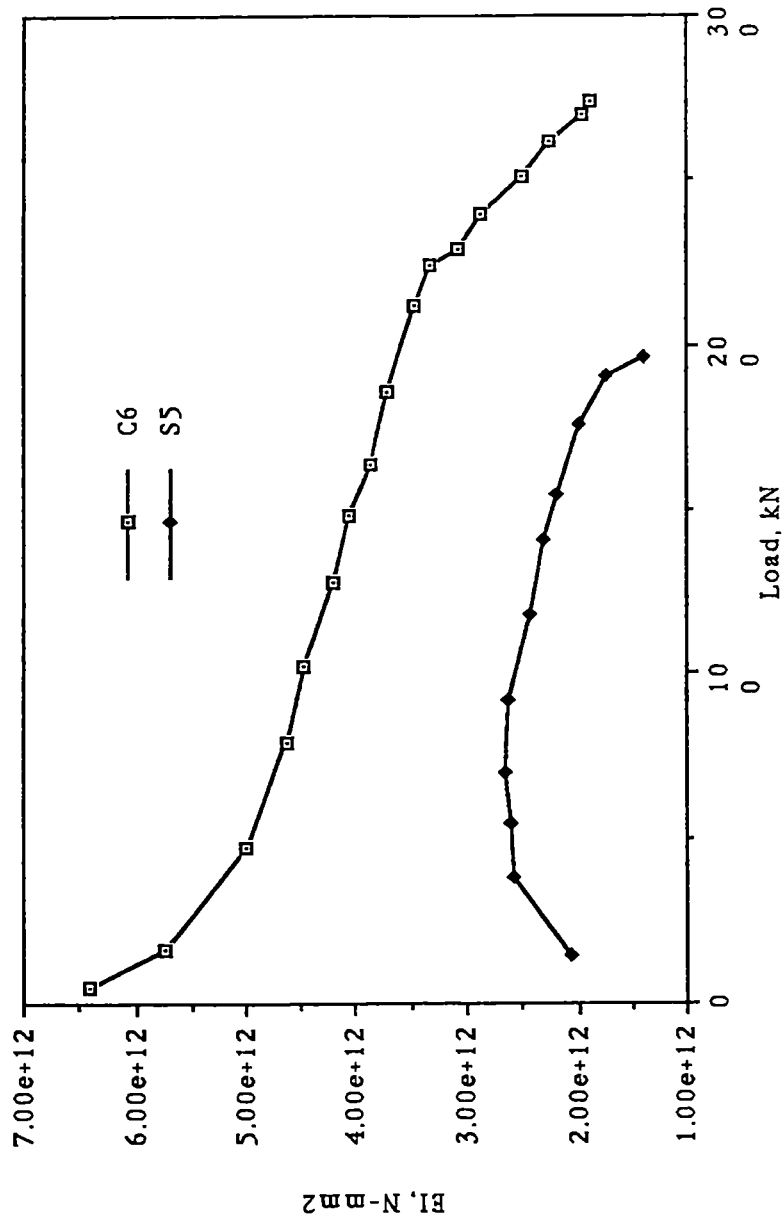


Figure 5.15 Flexural Rigidity of Reinforced Walls S5 and C6

CHAPTER 6

SUMMARY, CONCLUSIONS AND RECOMMENDATIONS

6.1 Summary

The test program undertaken is considered preliminary and it has shown that the concept of shear connecting load bearing cavity walls has considerable merits and it enhances the performance of these assemblies. Based on the limited test data from this program the following conclusions and recommendations are made.

6.2 Conclusions

1. Slender block walls with shear connected brick veneer when subjected to vertically eccentric loads, with eccentricity towards the brick veneer, the stiffness, and the ultimate load carrying capacity of the block wall is increased while deflection is reduced considerably. Thus, in designing slender shear connected cavity walls, the brick veneer may also be considered as a structural component.
2. Since all the shear connectors in all the unreinforced walls were undeformed, it can be concluded that these shear

connectors had enough strength and the selected shear connector arrangement was satisfactory. In reinforced walls, as the connectors were deformed, either the spacing of the shear connectors needs to be reduced or their strength increased for more wall strength and stiffness.

3. The stiffness of the shear connected cavity walls subjected to eccentric load increases with increase in cavity width.
4. The contribution of brick veneer to the ability of concrete backup wythe increases with the increase in eccentricity of the load.
5. The flexural rigidity of shear connected cavity walls is more than that of single wythe walls and it is dependent on the eccentricity of loading.
6. More experimental results are required to check the validity of the proposed relation.

6.3 Recommendations

1. From this testing program it is observed that the center of rigidity of the wall for the tested cavity walls with cavity of 75 mm lies between the center of the block wythe and $t/6$

towards the veneer from the center. More tests need to be carried out on cavity walls loaded with eccentricities below $t/6$ towards the veneer and also on walls with of different cavity widths to determine the center of rigidity of the cavity wall.

2. Reinforced cavity walls loaded with eccentricity less than $t/3$ should be tested to see if the connector has enough strength. If not the connector for reinforced wall should be made stiffer.
3. Similar tests should be carried out on wall loaded with unequal end eccentricities and eccentricities subjecting wall to double curvature bending.
4. Further tests should be carried out incorporating variables such as cavity width, block sizes, brick sizes, mortar strength and reinforcement, direction of eccentricity and wall height so as to be able to come up with an analytical basis and design rules.

CHAPTER 7

REFERENCES

1. CSA Standard, CAN3-S304-M84, "Masonry Design for Buildings", Canadian Standards Association, Ontario, Canada.
2. Yokel, F. Y., Mathey, R. G. and Dikkers, R. D., "Strength of Masonry Walls Under Compressive and Transverse Loads", Building Science Series 34, March 1971, U.S. National Bureau of Standards.
3. Kumar, S. and De Vekey, R. C., 1982, "Narrow Lightweight Block Walls: Performance Under Vertical Load", International Journal of Masonry Construction: Vol 2., No.3, 1982, pp 91-102.
4. Neis, V. V., Ghosh, S. and Hatzinikolas, M., "Strength Tests on Slender Plain Block Masonry Walls with Veneer Wythes", Can. J. Civ. Eng. 18, 738-748 (1991).
5. Adnan F. Alani, M. Tarik El-Katib, Roy A. Ovanessian, and Iqbal N. Korkees, "Cavity Load Bearing Brick Walls with Steel and Brick Ties", Journal of Structural Engineering (Madras), Vol 16, No. 4, January 1990, pp 101-108.

6. Adnan F. Alani, M. Tarik El-Katib, Roy A. Ovanessian, and Iqbal N. Korkees, "Structural Evaluation of Load Bearing Brick Cavity Walls with Brick Ties", Journal of Structural Engineering (Madras), Vol 16, No. 3, January 1989, pp 85-93.
7. Mullin, P. and O'Connor, O., "The Use of Steel Reinforcement Systems to Improve the Strength and Stiffness of Laterally Loaded Cavity Brick Walls", Journal of Structural Engineering, ASCE, Vol. 113, No.2, February 1987. pp 334-348.
8. Pacholok, K. W., "Shear Connectors in Masonry Cavity Walls", M.Sc. Thesis, University of Alberta, Department of Civil Engineering, September 1988.
9. Papanikolas, P. K., Hatzinikolas, M., Warwaruk, J., "Behaviour of Shear Connected Cavity Walls", Structural Engineering Report No. 169, Department of Civil Engineering, University of Alberta, September 1990.
10. CSA Standard, CAN3-A165.1-M85, "Concrete Masonry Units", Canadian Standards Association, Ontario, Canada.
11. CSA Standard, CAN3-A370-M84, "Connectors for Masonry", Canadian Standards Association, Ontario, Canada.

12. CSA Standard, CAN/CSA-A82.1-M87, "Burned Clay Brick (Solid Masonry Units Made from Clay or Shale), Canadian Standards Association, Ontario, Canada.
13. CSA Standard A179-1975, "Mortar and Grout for Unit Masonry", Canadian Standards Association, Ontario, Canada.
14. Hatzinikolas, M.A., Longworth, J. and Warwaruk, J. "Concrete Masonry Walls". Structural Engineering Report No. 70, Department of Civil Engineering, University of Alberta, Edmonton, September 1978.